5-2-2007

Kinetic and Crystallographic Studies of Drug-Resistant Mutants of HIV-1 Protease: Insights into the Drug Resistance Mechanisms

Fengling Liu

KINETIC AND CRYSTALLOGRAPHIC STUDIES OF DRUG-RESISTANT MUTANTS OF HIV-1 PROTEASE: INSIGHTS INTO THE DRUG RESISTANCE MECHANISMS

by

Fengling Liu

Under the Direction of Irene T. Weber

ABSTRACT

HIV-1 protease (PR) inhibitors (PIs) are important anti-HIV drugs for the treatment of AIDS and have shown great success in reducing mortality and prolonging the life of HIV-infected individuals. However, the rapid development of drug resistance is one of the major factors causing the reduced effectiveness of PIs. Consequently, various drug resistant mutants of HIV-1 PR have been extensively studied to gain insight into the mechanisms of drug resistance. In this study, the crystal structures, dimer stabilities, and kinetics data have been analyzed for wild type PR and over 10 resistant mutants including PR_{L24I}, PR_{I32V}, PR_{M46L}, PR_{G48V}, PR_{I50V}, PR_{F53L}, PR_{I54V}, PR_{I54M}, PR_{G73S} and PR_{L90M}. These mutations lie in varied structural regions of PR: adjacent to the active site, in the inhibitor binding site, the flap or at protein surface. The enzymatic activity and inhibition were altered in mutant PR to various degrees.

Crystal structures of the mutants complexed with a substrate analog inhibitor or drugs indinavir, saquinavir and darunavir were determined at resolutions of 0.84 – 1.50 Å. Each mutant revealed distinct structural changes, which are usually located at the mutated residue, the flap and inhibitor binding sites. Moreover, darunavir was shown to bind to PR at a new site on the flap surface in PR_{I32V} and PR_{M46L}. The existence of this additional inhibitor binding site may explain the high effectiveness of darunavir on drug resistant mutants. Moreover, the unliganded structure PR_{F53L} had a wider separation at the tips of the flaps than in unliganded wild type PR. The absence of flap interactions in PR_{F53L} suggests a novel mechanism for drug resistance. Therefore, this study enhanced our understanding of the role of individual residues in the development of drug resistance and the structural basis of drug resistance mechanisms. Atomic resolution crystal structures are valuable for the design of more potent protease inhibitors to overcome the drug resistance problem.

INDEX WORDS: protease inhibitor, substrate analog inhibitor, indinavir, saquinavir, darunavir, TMC114, active site mutation, flap mutation, distal mutation.

KINETIC AND CRYSTALLOGRAPHIC STUDIES OF DRUG-RESISTANT MUTANTS OF HIV-1 PROTEASE: INSIGHTS INTO THE DRUG RESISTANCE MECHANISMS

by

FENGLING LIU

A Dissertation Submitted in Partial Fulfillment of Requirements for the Degree of

Doctor of Philosophy

In the College of Arts and Sciences

Georgia State University

2006

KINETIC AND CRYSTALLOGRAPHIC STUDIES OF DRUG-RESISTANT MUTANTS OF HIV-1 PROTEASE: INSIGHTS INTO THE DRUG RESISTANCE MECHANISMS

by

FENGLING LIU

Major Professor: Irene Weber

Committee: Giovanni Gadda

John Houghton

Electronic Version Approved:

Office of Graduate Studies

College of Arts and Sciences

Georgia State University

May 2007

ACKNOWLEGEMENTS

I would like to sincerely thank my advisor Dr. Irene Weber for her guidance, encouragement, and patience throughout my graduate study at Georgia State University. She taught me protein crystallography and innumerable lessons and insights into research. Her technical and editorial advice was essential for the completion of my dissertation. She always respects my interest and put my needs as her top priority. Importantly she provides me a pleasant laboratory environment for my study and research. In all, I am very blessed to have her as my mentor who has set a great example for me to follow.

My sincere thanks also go to my committee members Dr. Giovanni Gadda and Dr. John Houghton. They have provided lots of valuable advices at my annual meetings and defense.

I give special thanks to Dr. Andrey Kovalevsky and Dr. Peter Boross for fruitful collaborations. They educated me crystallography and kinetics, respectively. Andrey helped me solve a couple of crystal structures and also critiqued my writing. Thanks also go to Yuan-Fang Wang for teaching me using various programs for solving crystal structures. The friendship of Yunfeng Tie, Ping Liu and Bin Fang is much appreciated and has led to many interesting and good-spirited discussions relating to my research. I am also grateful to my colleagues Tingyi Chiu, Johnson Agniswamy, Alexander Chumanevich.

My thanks go to Dr. Robert Harrison for his insightful questions and inspiriting suggestions at our lab meetings. His students Hao Wang, Patra Volarath, Xianfeng Chen also provided help with computer programs.

I am gratitude to Dr. Arun Ghosh and Merck for providing protease inhibitors and Dr. John Louis for providing HIV protease constructs. I also thank the staff at the SER-CAT (ID-22 beamline) at the Advanced Photon Source, Argonne National Laboratory for assistance during X-ray data collection. My research was supported in part by the Georgia Research Alliance, the Georgia Cancer Coalition, the National Institute of Health grants and Molecular Basis of Disease Program at Georgia State University.

Finally, I would like to express my whole-heart thankfulness to my parents (Guangxin Liu and Siai Lin) for their unconditional love. Without their great support and encouragement, I could not make it for today. I am deeply indebted them.

TABLE OF CONTENTS

LIST OF TABLES

LIST OF FIGURES

LIST OF ABBREVIATIONS

Å	Angstrom
ALA	alanine
AMMP	Another Molecular Mechanics/Modeling Program
ARG	arginine
AS	ammonium sulfate
ASP	aspartic acid
ASN	asparagine
C	carbon
CYS	cysteine
DMSO	dimethylsulfoxide
GEL	1-O-octyl-2-heptylphosphonyl-SN-glycero-3-phosphoethanolamine
GLU	glutamic acid
GLN	glutamine
GLY	glycine
DRV (TMC114)	darunavir (3R,3AS,6AR)-hexahydrofuro [2,3-B]furan-3-yl(1S,2R)-3-[[(4-aminophenyl)sulfonyl](isobutyl) amino]-1-benzyl-2-hydroxypropylcarbamate
HIS	histidine
HIV-1	Human Immunodeficiency Virus 1
ILE	Isoleucine

IPTG	isopropyl-D-thio-galactopyranoside
LB	Luria-Bertani
LEU	leucine
LYS	lysine
M	molar
MET	methionine
MR	molecular replacement
Na^+	sodium ion
PDB	Protein Data Bank
PEG	polyethylene glycol
PHE	phenylalanine
PO_4^{3-}	phosphate ion
PR	wild type HIV-1 protease
PR_{L24I}	PR with L24I mutation
PR_{D25N}	PR with D25N mutation
PR_{M46L}	PR with M46L mutation
PR_{I50V}	PR with I50V mutation
PR_{F53L}	PR with F53L mutation
PR_{I54V}	PR with I54V mutation
PR_{I54M}	PR with I54M mutation
PR_{G73S}	PR with G73S mutation
PR_{I84V}	PR with I84V mutation

PR_{V82A}	PR with V82A mutation
PR_{L90M}	PR with L90M mutation
PRO	proline
RMS	root mean square
SER	serine
SO_4^{2-}	sulfate ion
SQV	saquinavir cis-N-tert-butyl-decahydro-2-[2(R)-hydroxy-4-phenyl-3(S)-[[N-2-quinolylcarbonyl-L-asparaginyl]amino]butyl]-(4AS)-isoquinoline-3(S)-carboxamide
THR	threonine
TRP	tryptophan
TYR	tyrosine
µl	microliter
VAL	Valine

GENERAL INTRODUCTION

1. AIDS and HIV

It has been over two decades since HIV (Human Immunodeficiency Virus) was first recognized as the pathogenic/causative agent for AIDS (Acquired Immunodeficiency Deficiency Syndrome) (Barre-Sinoussi 1983; Gallo 1984; Popovic 1984). Since then, the pathogenesis and treatment of AIDS has been extensively studied and great progress has been made. However, the pandemic of AIDS is still globally expanding and the fight against this dreaded disease is long-lasting. According to the UNAIDS report, over 40 million people worldwide are living with HIV, of which a half million are in the United States. In 2005 alone, 5 million individuals were newly infected with HIV and more than 3 million died of AIDS (UNAIDS/WHO 2005). It means that every 6 seconds a person is newly infected with HIV and that every 10 seconds a person dies of AIDS or AIDS-associated infection (Greene 2004). The global spending on AIDS treatment and care is huge, US $300 million in 1996 and US $5 billion in 2003. Nevertheless, the budget is far below the need especially in the south of Africa, where the pandemic hits hardest.

1.1 HIV Life Cycle

The infection of HIV begins with the recognition of viral envelope glycoprotein to the cell surface receptors CD4 and other coreceptors on the host cells (Maddon 1986; Deng 1996). The binding of CD4 to envelope glycoprotein gp120 induces conformational changes in gp120 and causes enhanced binding affinity for

other coreceptors (Wu 1996). After the virus fuses with the host cell membrane, HIV releases the viral genetic material into the cytoplasm of the host cell. HIV belongs to the retrovirus family, which possesses two copies of single-strand RNA in its viral particle. The viral RNA is first reverse transcribed into DNA; the DNA replicates into double strands, and then inserts into the genome of the human host cell. So the viral genome is replicated with the host cell genome. The viral genome is translated into three primary polyproteins (Figure 1): Gag, Gag-pol and Env. Gag (group antigen) encodes internal structural components of the virion: matrix, capsid, and nucleocapsid proteins. Pol (polymerase) contains reverse transcriptase and integrase, two key enzymes in the viral replication. Another important enzyme, the protease, is located at the upstream of Pol in Gag-pol polyprotein. Env encodes two exterior proteins SU (surface unit glycoprotein) and TM (transmembrane envelope). These exterior proteins recognize the surface receptors on the target cells in the early stage of infection (Coffin 1997). The HIV particle packing is a self-assembly course under the direction of the Gag precursor polyproteins (Gheysen 1989; Luban 1993). When the uncleaved viral precursor polyproteins, viral RNA and other elements are packed into the viral particles and released from the infected cells, they are immature or have no infectious ability. The virus only becomes infectious after the PR cleaves the Gag and Gag-pol into functional proteins (Emini 2002). Besides these primary proteins, HIV also encodes some accessory proteins, which regulate the viral infection, replication and maturation. All the retroviruses follow a similar life cycle, including fusion, reverse transcription, integration, translation, assembly and budding (Figure 2).

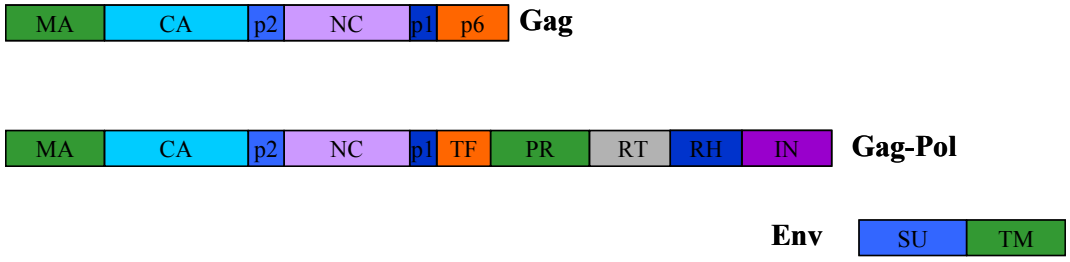

Figure 1: Genetic organization of HIV-1 and the cleavage sites of HIV PR at Gag and Gag-pol polyproteins. Some of accessory proteins are omitted for clarity. MA for matrix, CA for capsid, NC for nucleocapsid, TF for transframe, RT for reverse transcriptase, RH for RNase H, IN for integrase, p1 and p2 are spacer peptides. p6 is peptide at 3' region of the Gag precursor and negatively regulates the PR activity. SU for surface unit glycoprotein and TM for transmembrane envelope.

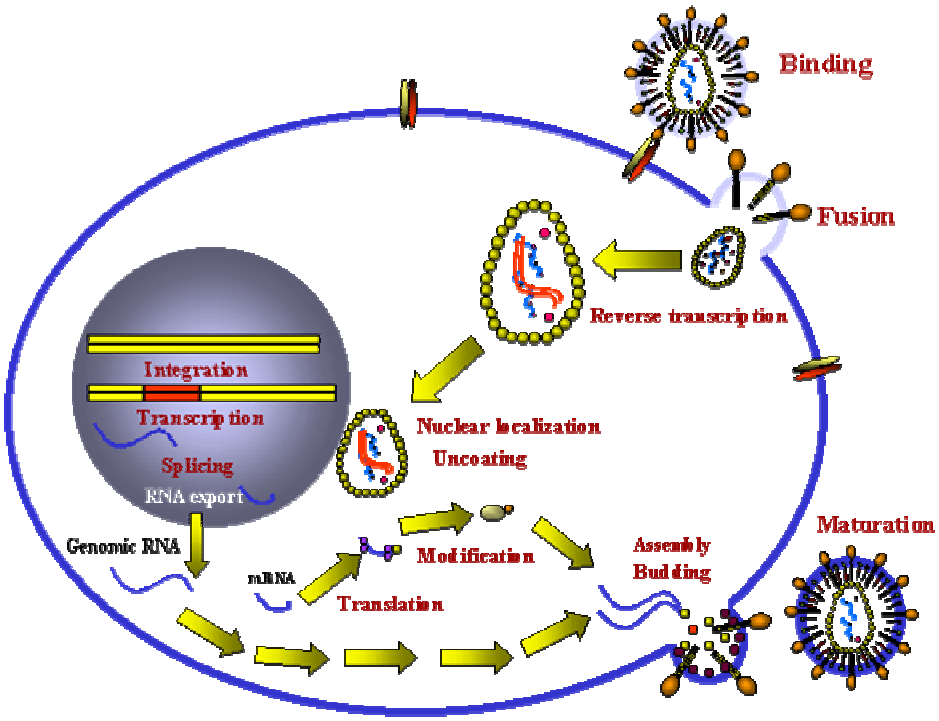

Figure 2: The life cycle of HIV includes fusion, reverse transcription, integration, and assembly (from the website: pathmicro.med.sc.edu/lecture/hivstage.gif).

Most of the key steps in the life cycle of HIV can be employed as targets to design anti-HIV drugs.

1.2 The Role of HIV PR

HIV protease (PR) is an endopeptidase that catalyzes the cleavage of Gag and Gag-pol polyproteins into mature proteins. The active form of the PR is a homodimer with 99 amino acid residues in each subunit. For convenience, the residues in one subunit are numbered 1-99 and those from the other subunit are numbered 1'-99'. The two subunits form an active site cavity, in which the substrate binds and is hydrolyzed. Most of PR inhibitors are designed to bind in the active site cavity of PR and competitively exclude the binding and cleavage of natural substrates. When the PR is inactivated by inhibitor or mutation of key residues, the cleavage of Gag and Gag-pol polyproteins is interrupted; as a result, the budding viral particles become noninfectious (Kohl 1988; Seelmeier 1988).

Besides the function in hydrolysis of viral polyproteins, PR has also been detected to cleave cellular proteins, such as NF-κB precursor, cytoskeleton and sarcomeric proteins. The cleavage of those cellular proteins has been speculated to play a role in viral replication and infection (Riviere 1991; Shoeman 1993).

2. HIV-1 PR Structure

After recognizing the indispensable role of PR in virus maturation, intensive efforts have been made to determine the three dimensional structures of PR, which are crucial for the design of anti-viral drugs. The three dimensional structures of HIV-1 PR were one of the first retroviral PR structures solved by X-ray crystallography (Lapatto 1989; Miller 1989; Navia 1989; Wlodawer 1989). Since 1989, more than

200 HIV PR structures unliganded or complexed with various inhibitors or substrates have been deposited in the Protein Data Bank (Berman 2000) and HIV Protease Database (Wlodawer 1993; Vondrasek 1997). Meanwhile, many other retroviral PR structures have been solved by X-ray crystallography, including those of ASLV (Avian Sarcoma-Leukosis Virus) (Miller 1989), RSV (Rous Sarcoma Virus) (Jaskolski 1990), HIV-2 (Mulichak 1993; Tong 1993), SIV (Simian Immunodeficiency Virus) (Rose 1993; Zhao 1993), FLV (Feline Leukemia Virus) (Wlodawer 1995), EIAV (Equine Infectious Anemia Virus) (Gustchina 1996), and recently HTLV-1 (Human T-cell Leukemia Virus) (Li 2005). As can be seen in Figure 3, the retroviral PRs share some common features in amino acid sequence and tertiary structure. Among the structures of known retroviral PRs, the sequence similarity is low and only about 20 residues are highly conserved (Figure 3A), most of which are located around the active site and substrate binding site (Rao 1991 ; Coffin 1997). Despite the diversity of the amino acid sequences, the overall three dimensional structures of PR are extremely similar in the central region (Figure 3B). They share conserved structural motifs at the conserved triplet (Asp-Thr-Gly) at the active site, the flap region, the dimer interface and a conserved water molecule.

2.1 The Catalytic Site and Proposed Catalytic Mechanisms of HIV-1 PR

Like other aspartic PRs, the HIV-1 PR contains a conserved triad, Asp-Thr-Gly, at residues 25-27 (Cairns 1988). The mutation of Asp25 causes the HIV-1 PR to be completely inactive and thus the Asp25 plays an irreplaceable role in the reaction of hydrolysis of peptide bonds (Kohl 1988; Seelmeier 1988).

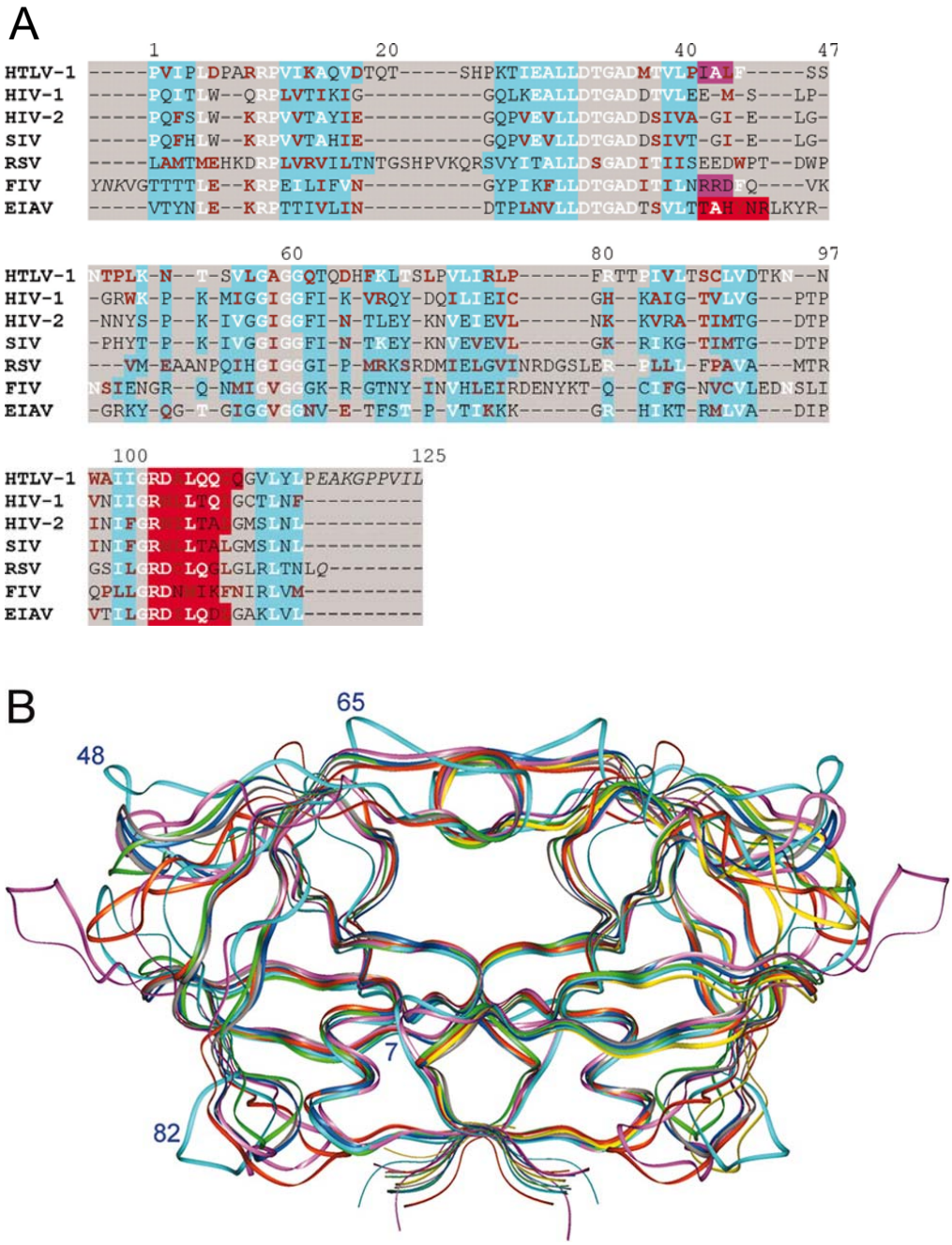

Figure 3A: Alignment of retroviral PR sequences of known structure; 3B: Structural superposition of retroviral PR. HIV-1 PR is colored in green; HIV-2 PR in dark blue; HTLV-1 PR in blue; SIV PR in gray; RSV PR in magenta; EIAV PR in yellow; and FIV PR in red (Li, 2005)

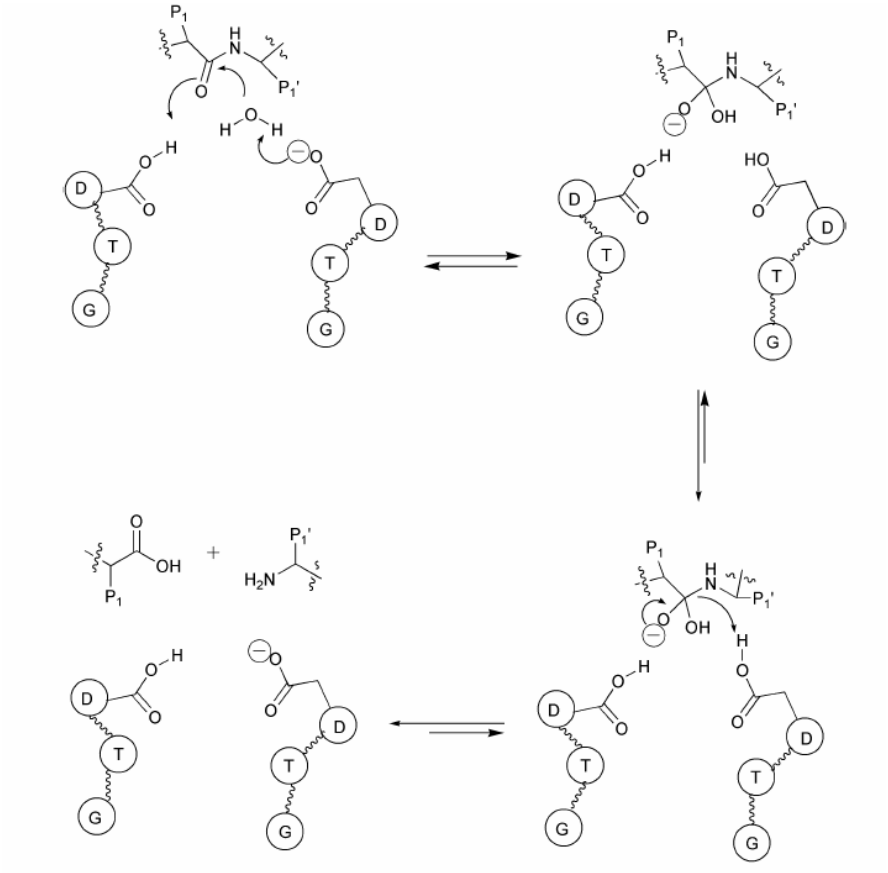

Figure 4A: The proposed “the general-base mechanism” for aspartic PR (Brik, 2003)

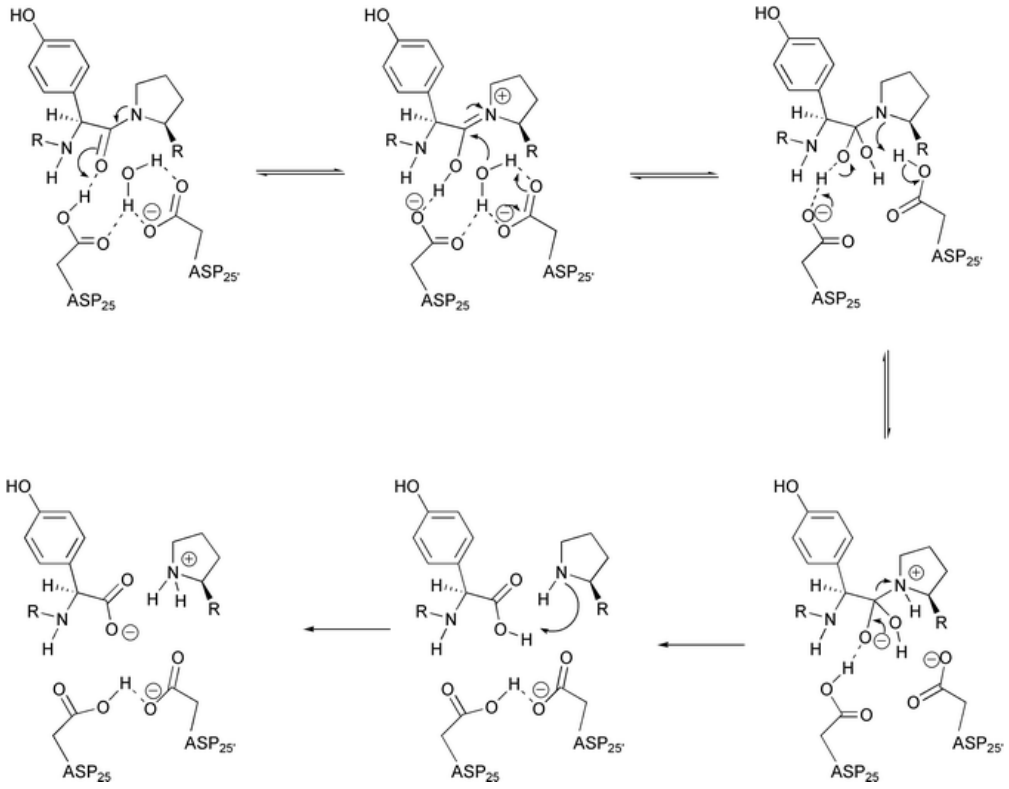

Figure 4B: The proposed catalytic mechanism of HIV PR by Hyland (Brik, 2003)

Several catalytic mechanisms of HIV PR have been proposed although the detailed catalytic mechanisms remain unclear. The catalytic mechanism of aspartic PR has been extensively studied in nonviral aspartic PR before focusing on HIV PR (Pearl 1984; Fruton 1987; Suguna 1987). Despite some disagreement about the details among the various proposed mechanisms, the general acid-base mechanism is commonly accepted for aspartic PR. Suguna (1987) proposed a mechanism based on a crystal structure of *Rhizopys chinensis* PR complexed with a substrate analog inhibitor. In this mechanism, one of the carboxylate of the aspartate in an unprotonated state acts as a base to attack the water in the active site, as illustrated in Figure 4A. The activated water in turn attacks the carbonyl C of substrate at the scissile bond to form a tetrahedral intermediate. The other carboxylate of aspartate in protonated state acts as an acid to polarize the carbonyl bond. The intermediate is broken into carboxylic acid and amine products as a result of the protonation of the scissile amide N and unstable bonds.

Some catalytic mechanisms have been proposed specifically for HIV PR. Based on solvent isotope effects and structure data, Hyland proposed the mechanism as shown in Figure 4B (Hyland 1991; Hyland 1991; Brik 2003). In this mechanism, the proton of one of the carboxylate O of Asp25 attacks the carbonyl C of the substrate, and nucleophilic water attacks the unprotoned Asp25 and the photon is transferred to the Asp25 and the hydroxyl is transferred to the carbonyl C. The newly gained proton of Asp25 then is transferred to the amide N of the substrate; simultaneously (Hyland 1991; Silva 1996) or subsequently (Okimoto 1999) a proton from hydroxyl group of the carbonyl C donates to the amide N (Piana 2002). A

concerted mechanism has also been proposed (Antonov 1981; Jaskolski 1991) and the major standpoint is that the nucleophilic water and acidic unprotonated Asp25 simultaneously attack the scissile bond.

Based on those proposed mechanisms, the nucleophilic water is indispensable and should be located between the two active site aspartates. In unliganded crystal structures of HIV PR, a uranyl ion has been found to bind between the two active site aspartates (Wlodawer 1989) but no water molecule has been observed at this position. In the crystal structures of HIV PR complexed with inhibitors, there is no space to accommodate a water molecule or other atoms bigger than a proton at this position. Nevertheless, a conserved water molecule that bridges two C=O groups of the substrate at the scissile bond and NH groups of the main chain of Ile50 and Ile50' has been consistently observed in most of inhibitor-bound HIV PR structures. This water has been proposed to be involved in the catalytic reaction (Gustchina 1990; Harrison 1994). According to the molecular dynamic simulations of HIV PR by Harrison (1994), this conserved water molecule is likely to attack the scissile bond along with two aspartates from the opposite side of the substrate. The flexibility of the flap of HIV allows this water to enter the right position for the reaction. In summary, the understanding of the HIV PR catalytic mechanism remains incomplete. However, the various proposed mechanisms share some similarity and generally agree with the involvement of the nucleophilic water and the function of the two aspartic residues.

2.2 The Dimer Interface

Since the active form of PR is composed of two subunits, the dimer stability has significant effects on the enzyme activity. The dimer stability of PR is maintained

through noncovalent interactions of the four strands of ß-sheet comprising residues 1-4 (N-terminus) and 96-99 (C-terminus) and the residues 24-29 at the active site region. In addition, the interactions between residues from two subunits Ile50 and Gly51', Asp29, Arg87 and Arg8' also influence the dimerization significantly (Weber 1990; Louis 2003). Finally, the binding of substrates or inhibitors greatly enhances the dimer stability.

2.3 The Flap Region

A glycine-rich loop from residues 45-55, known as the flap, folds into an extended anti-parallel β strand. Unlike the pepsin-like PR, which has only a single flap (James 1982), the active HIV-1 PR possesses two flap regions, one from each monomer (Figure 5). The flap clinches a substrate into its active site cavity and releases products out of the active site, so it has to be fairly flexible. The analysis by molecular dynamic simulations and NMR experiments suggests that the flap is in the dynamic equilibrium of fully open (allowing the entry of substrate), semi-open (as in the structures without binding of inhibitor) and closed conformations (as in the inhibitor-bound structures); and the semi-open is anticipated to be the major conformation for unliganded PR (Nicholson 1995; Freedberg 2002; Hornak 2006). The comparison of crystal structures of the unliganded PR and PR/inhibitor complexes has shown that the tips of the flaps (near residue 50) shift 7 Å (Miller 1989). It has been predicted that the flaps must swing about 15 Å from their position in the inhibitor-complexed PR to allow the polyprotein substrate to enter the active site (Gustchina 1990).

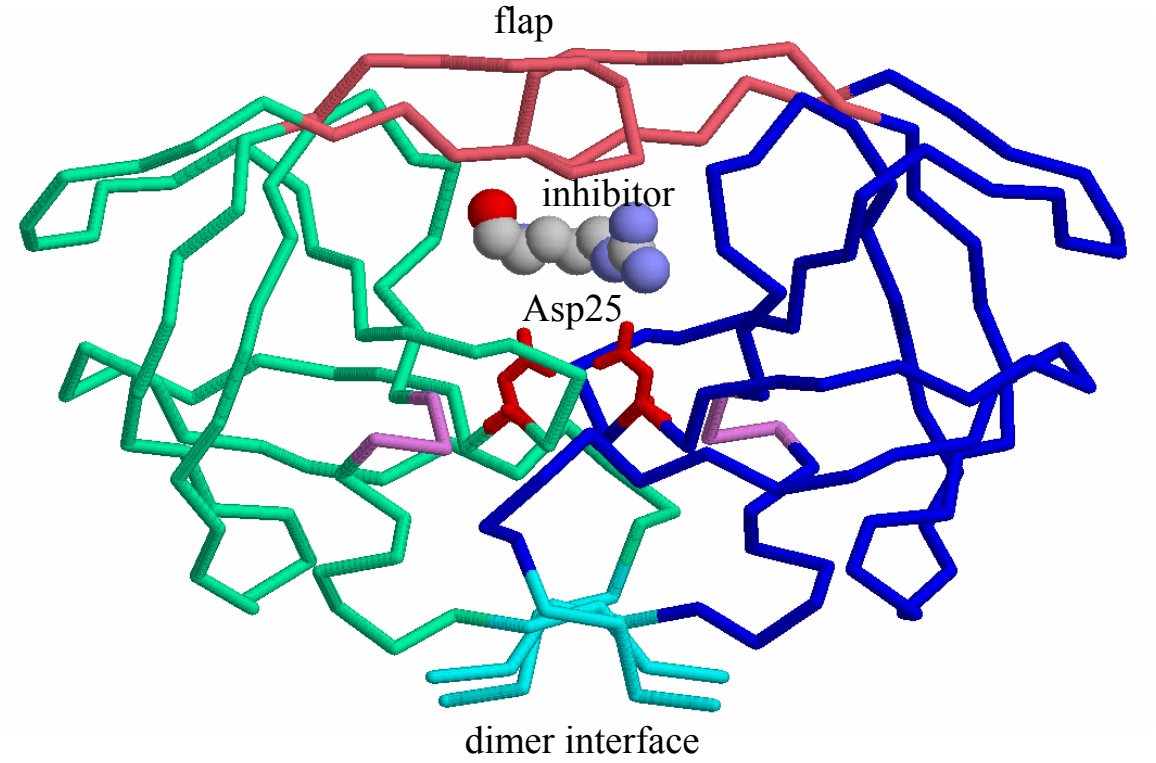

Figure 5: The overall structure of HIV PR/inhibitor complex. The flap region is indicated in pink; the dimer interface at the N and C terminus regions in cyan; Active site Asp25 in red; the inhibitor as spheres.

Large scale mutagenesis has been done to identify the side chains required for PR activity at each residue in the flap region (Shao 1997). Three groups of residues were defined, including the side chains (Met46, Phe53 and Lys55) that are directed outward toward solvent, which are the most tolerant to substitutions, side chains (Ile47, Ile50, Ile54 and Val56) directed inward, which only tolerate a few conservative substitutions, and the Gly-rich region (Gly48, Gly49, Gly51, Gly52), which is the most sensitive region to substitutions (Shao 1997). Therefore, the conformation of the flaps and residues in that region greatly contribute to the PR activity and the substrate or inhibitor binding affinity.

3. HIV PR Substrate Specificity

Understanding the substrate specificity of HIV PR is important for studying the molecular basis of drug resistance and development of new drugs. For the optimal catalysis, the minimal length of substrates is 7 amino acids (Darke 1988; Tozser 1991; Tomasselli 1994; Coffin 1997). The substrate of HIV PR binds to the dimer in an asymmetric way, as illustrated in Figure 6. The residues of substrate at carboxyl terminus of the scissile bond are defined as P1, P2, P3 and P4, and correspondingly P1', P2', P3' and P4' in the amino terminus (Schechter 1967). The residues of PR that accommodate the side chains P4'-P4 of substrate are correspondingly defined as subsites S4'-S4.

The substrate specificity is determined by the overall shape and chemistry of the side chains of peptide substrates rather than the specific sequences (Konvalinka 1990; Tozser 1991; Griffiths 1992; Tozser 1992; Prabu-Jeyabalan 2002; Ozer 2006).

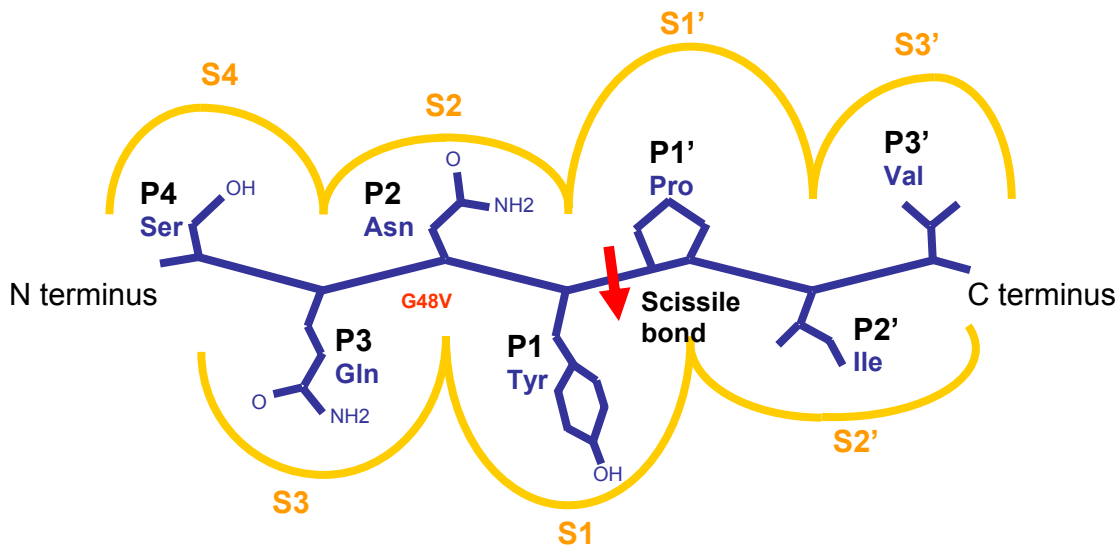

Figure 6: the schematic diagram of a substrate (P4-P3') bound to HIV-1 PR (S4-S3') subsites. The scissile bond is indicated by an arrow.

Substrate sequences cleaved by protease are relatively diverse. Despite this diversity, some common features can be deduced from the analysis of natural viral sequences, enzyme kinetic and mutagenesis studies (Pettit 1991; Poorman 1991; Tozser 1992; Coffin 1997; Louis 2000; Beck 2002). P1 and P1' favor large hydrophobic amino acids; P2 and P2' are typically occupied by hydrophobic and small polar residues. P3 is glutamine or basic amino acids; P4 is normally a small amino acid.

4. Viral Mutation Mechanisms

The HIV genome-wide natural polymorphisms have been observed up to 30% among various viral subtypes and the polymorphisms of PR exist in over 49 out of 99 residues (Boden 1998; Hertogs 2000; Velazquez-Campoy 2001). Besides the natural polymorphisms, the emergence of drug resistance is very severe. And it is probably the main factor leading to the failure of current treatment of HIV. It is estimated that over 70% of HIV-1 infected individuals harbor drug resistant virus and nearly 5-10% of them reveal resistance to all of the current RT and PR inhibitors (Yu 2005). What makes it even worse is that virus strains carrying drug resistant mutations are transmitted directly to newly infected individuals, which corresponds to about 10-15% of the total newly infected (Hirsch 1998; Wainberg 1998).

Multiple factors contribute to the rapid development of mutations in the virus. First, the virus is intrinsically prone to mutate because HIV RT has no 3'-5' exonuclease proofreading function. During the reverse transcription, the error rate of RT is approximately 1 in 4000-10,000 base pairs (Preston 1988; Mansky 1995; Mansky 1998). That means roughly one base mutation is introduced in each viral life

cycle. Second, the viral turnover is extremely high, approximately 10 billion new viral particles per day in an untreated HIV-infected individual (Ho 1995; Wei 1995; Perelson 1996). Third, genetic diversity of HIV can be amplified through recombination when two viruses with different genetic makeup simultaneously infect the same host cell (Robertson 1995; Kuwata 1997). Fourth, the APOBEC3G system, an RNA editor and DNA mutator, speeds up the mutation rates. The APOBEC3G is packed into HIV virions, binds to proviral DNA and yields dC to dU mutations in the viral minus-strand DNA. If the minus-strand DNA is not degraded or repaired, it serves as a template to replicate the plus-strand DNA, with dG to dA mutations (Chiu 2006). Fifth, drug pressure causes the rapid selection of drug resistant strains. In the presence of antiretroviral drugs, resistant strains remain as the dominant species after other strains are killed (Drake 1993). In cell culture in the presence of drugs, the wild-type virus is almost completely replaced by drug-resistant mutants after fourteen days (Wei 1995).

5. Anti-HIV Drugs

The extraordinary efforts to develop effective therapeutics have resulted in the discovery of drugs for the treatment of AIDS. Over 20 drugs have been approved by the FDA (Food and Drugs Administration) for the treatment of AIDS patients. Those drugs have shown great success by providing to HIV-infected individuals a longer life span and improved quality of life. The current drugs mainly inhibit the biological function of two key retroviral enzymes: reverse transcriptase (RT) and protease (PR).

5.1 HIV Reverse Transcriptase Inhibitors

As one of the major enzymes, the HIV reverse transcriptase (RT) converts the HIV single strand RNA into DNA, which is integrated into the host genome for viral replication. The crystal structures of RT in the presence or absence of DNA have been determined (Kohlstaedt 1992; Jacobo-Molina 1993). The active RT is comprised of a heterodimer, with molecular weight 66 and 51 kDa for each subunit. Both of the subunits (p66 and p55) are folded into a hand configuration with four subdomains known as "fingers", "palm", "thumb" and "connection", as illustrated in Figure 7.

Two distinct classes of HIV-1 RT inhibitors have been applied in the clinic, namely nucleoside/nucleotide analogs (NRTIs, 11 drugs) and non-nucleoside inhibitors (NNRTIs, 3 drugs) (examples in Figure 8). NRTIs are in the form of prodrugs which need to be activated by cellular kinases through two phosphorylation steps. Phosphorylated NRTIs compete with natural dNTPs to incorporate into the elongating DNA chains. The difference between NRTIs and natural dNTPs is that the former do not have the 3'-OH group, required for DNA chain elongation. After binding to the dNTP site, NRTIs terminate the growth of the DNA chain. The other class of RT inhibitors, NNRTIs, bind to the hydrophobic pocket close to the active site of the RT and prevent the conformational changes of RT required for DNA elongation, thus terminating the DNA replication. Importantly, all of these inhibitors bind to allosteric sites (non active sites) of RT (Erickson 1996).

5.2 HIV Protease Inhibitors (PIs)

Since their introduction in the market, the PIs have shown great success in the treatment of HIV infection (Wlodawer 1998). The currently approved PIs by FDA include amprenavir, indinavir, lopinavir, nelfinavir, ritonavir, saquinavir, atazanavir,

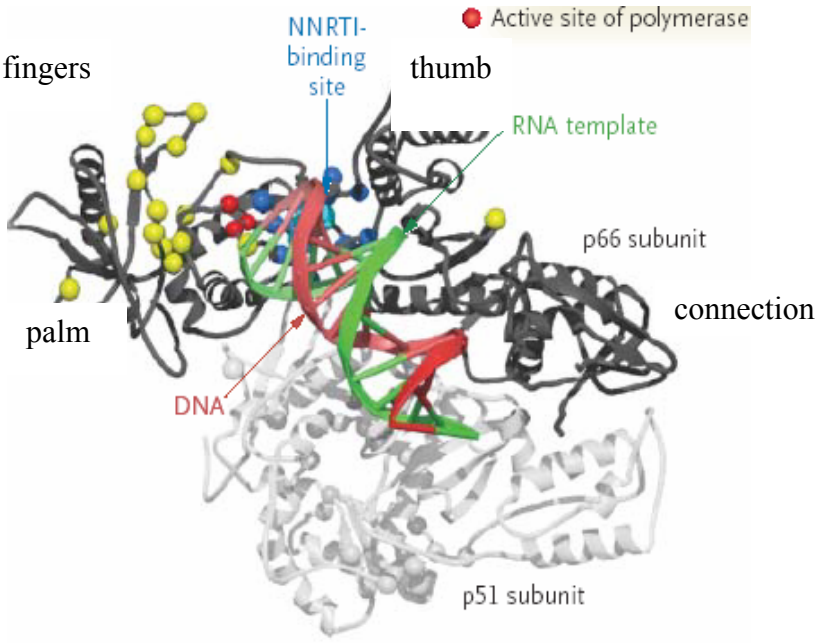

Figure 7: The complex of HIV reverse transcriptase with an RNA-DNA Duplex. RT comprises two subunits p51 and p66, which have fingers, palm, thumb and connection. Yellow sphere indicates the mutations conferring resistance to NRTI and blue sphere indicate the mutations conferring NNRTIs (Clavel 2004).

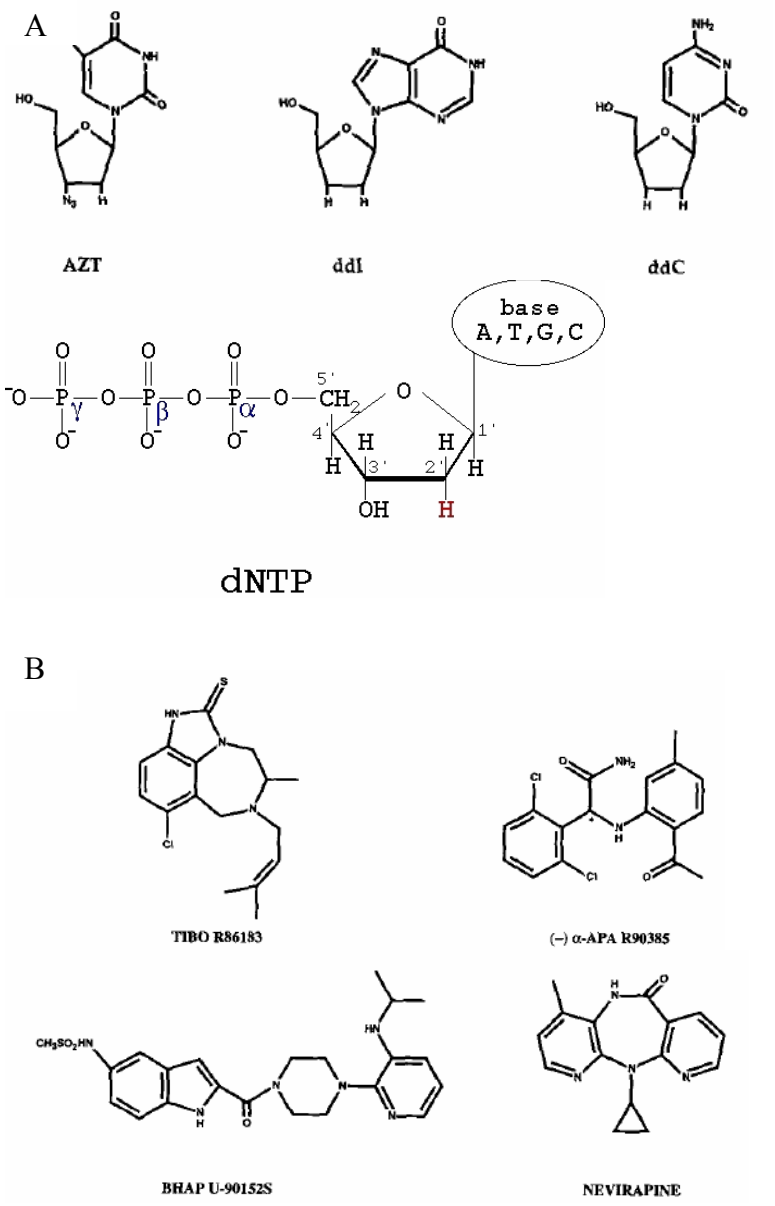

Figure 8A: the chemical structures of NRTIs; 8B: the chemical structures of NNRTIs (Erickson 1996).

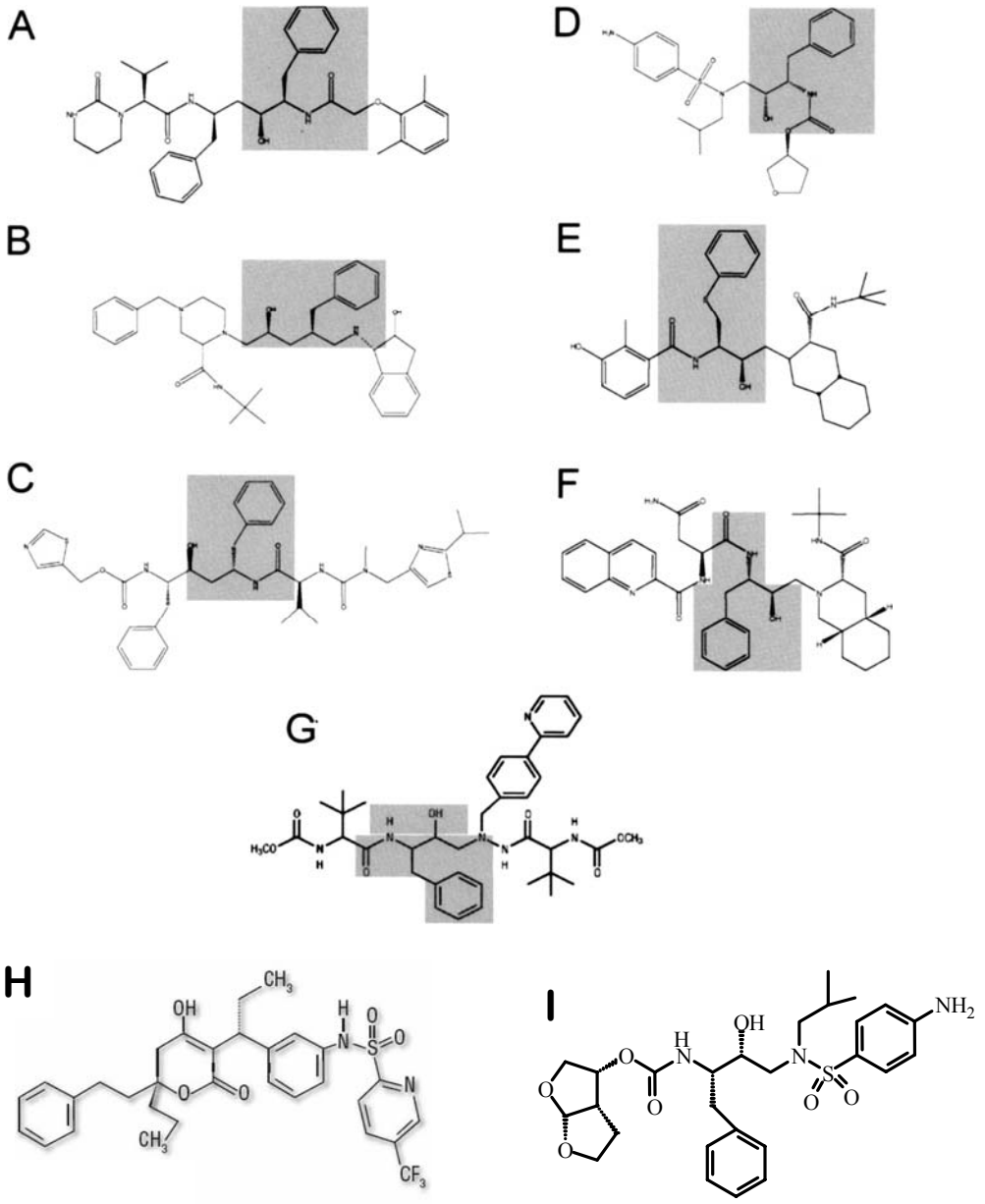

Figure 9: Structural features of HIV protease inhibitors. The core peptidomimetic structure found within all HIV protease inhibitors is shown in the shaded regions. A. lopinavir; B. indinavir; C. ritonavir; D. amprenavir; E. nelfinavir; F. saquinavir; G. atazanavir; H. Tipranavir; I. darunavir (Hertel, 2004).

tipronavir and darunavir (Figure 9). Except for tipronavir, all other PIs contain a core motif mimicking the P1' proline-containing substrate (Roberts 1990). Compared with the substrate analog, those clinical drugs are smaller and make few interactions with PR (Figure 10A and B). All of these drugs bind to the active site of PR by hydrogen bonds and van der Waals interactions, depending on the nature of the groups at each position. Some conserved hydrogen bond interactions are observed between the NH and CO groups of inhibitor and PR, involving the amide and carboxylate oxygen of Asp29, the carbonyl oxygen of Gly27 and the amide and carbonyl of Gly48 from both subunits (Figure 10). Moreover, the interactions between the amide of Ile50 from both subunits and the carbonyl oxygen of P2 and P1' mediated by a conserved water molecule are also conserved in the PR/inhibitor structures. The interactions between PR and inhibitor are the major focus for structure-based drug design.

Based on the key role of a conserved water molecule, which bridges the inhibitor and PR, cyclic urea inhibitors have been designed to bind to the PR active site and replace this water molecule (Lam 1994; Ala 1998). Also inhibitors preventing the dimerization of the PR have been proposed (Zhang 1991; Schramm 1993). Those endeavors have not provided any successful clinic inhibitors so far.

5.3 HAART

Both RT and PR inhibitors cannot fight HIV effectively in monotherapy because their effectiveness is undermined quickly by the emergence of drug resistant strains. Instead, the cocktails known as the highly active antiretroviral therapy (HAART), typically including two reverse transcriptase inhibitors with one or two PR inhibitors, are administered to infected patients. Since initiated 10 years ago, HAART

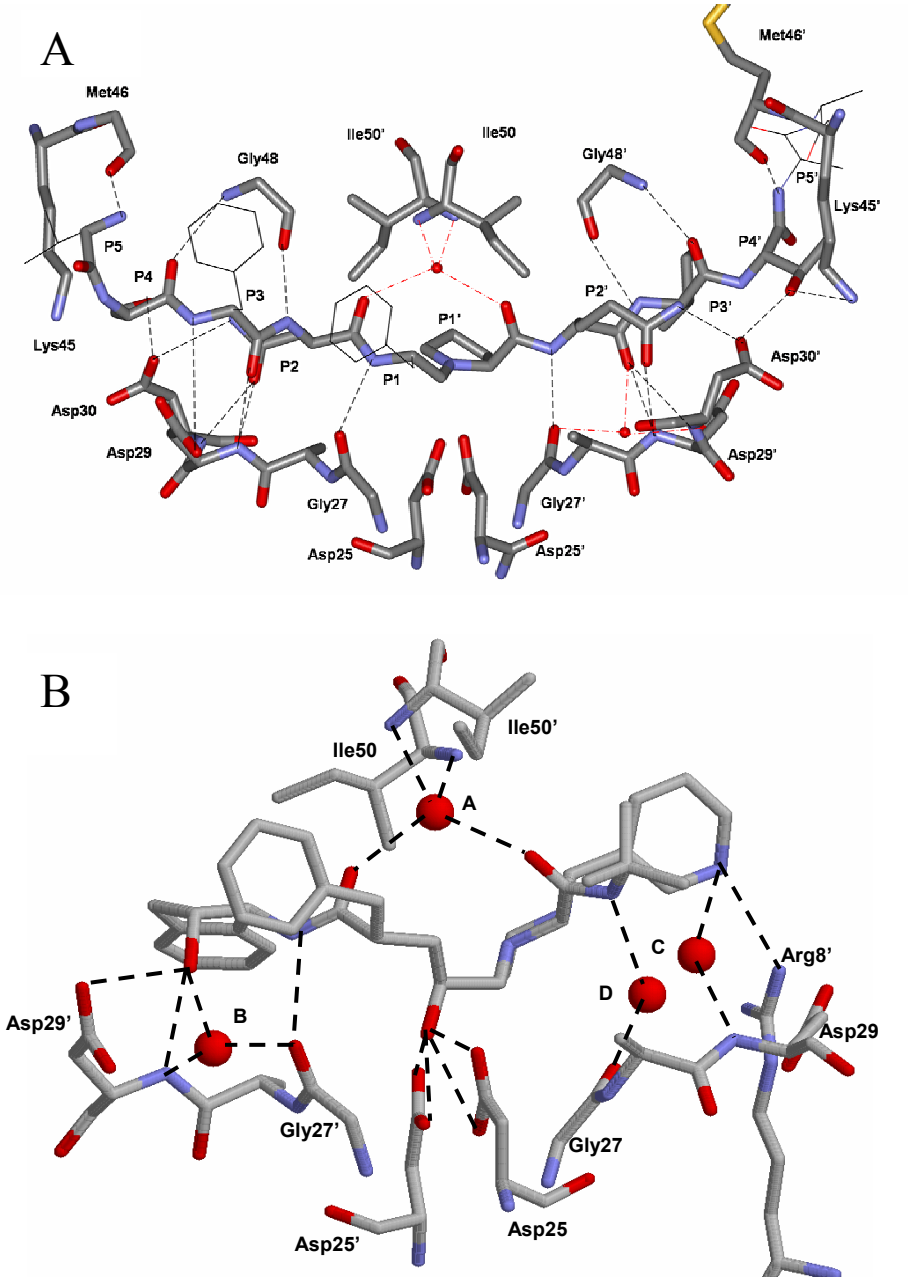

Figure 10A: The H-bonds between the PR and a substrate analog of the cleavage site p6/PR (Tie, 2006); B: The H-bonds between the PR and the clinical drug indinavir (Liu, 2005).

has successfully diminished both mortality and morbidity in HIV-infected patients (Palella 1998). When administered over prolonged periods, However, HAART cannot completely prevent the emergence of drug resistant strains and those drugs also bring substantial toxicity to patients.

5.4 Other Inhibitors

Prodigious efforts have been made to discover and design new anti-HIV compounds with unique structures and mechanisms of action. Besides RT and PR inhibitors, a new class of anti-HIV drug, the fusion (entry) inhibitor, has been approved by the FDA. Enfuvirtide is the first and the only one in this category now and is much more expensive than other antiretroviral drugs. Combined with optimized therapy, it significantly improves virological response for highly treatment-experienced patients who harbor drug resistant strains (Hornberger 2006). Drugs targeting other steps in HIV infection have also been considered, including attachment inhibitors, coreceptor inhibitors, integrase inhibitors and maturation inhibitors (Greene 2004).

Other strategies have been proposed to target cellular enzymes such as the helicase. The helicase is required for the replication of HIV, both the wild type and mutants. It has been supported by the preliminary evidence that helicase inhibitors (nucleoside analogues) have significantly blocked the HIV activity in cell culture at non-cytotoxic doses (Kwong 2005). However, this type drugs block the function of cellular proteins and thus bring potential cytotoxicity to the host cells. This is the major concern for this type drugs although they have a better chance of avoiding drug

resistant problem. Endeavors to develop this type drugs have made various levels of advancement but have not resulted in the manufacture of successful medicines.

5.5 The Development of Vaccines

The ideal and traditional way to prevent infectious disease is to develop vaccines. However, the development of vaccines for HIV is still in the early phase, confronted with various challenges (Girard 1999). The viral envelope glycoprotein gp120 has been a promising target to generate neutralizing antibodies. Nevertheless, it has been proved that HIV can escape the binding of antibodies at the distinct areas of the viral envelope proteins (Smith 2003). So generation of neutralizing antibodies is very difficult to achieve by HIV vaccines. Some vaccine trials have been performed in animal models and human (most in developing countries), but no vaccine candidates have constantly induced good immune response. And moreover, the genetic diversity of HIV is another big obstacle for the development of abroad spectrum vaccine for HIV variants (Emini 2002).

6. Methods of Testing for Drug Resistance

Since the drug resistance has become a substantial problem in antiviral therapy, testing for drug resistance is recommended in HIV treatment guidelines. The information of the drug-resistance profile of patients helps physicians gain insight into the patient's viral makeup and provides the information for optimizing treatment regimens.

Currently, the two basic methods to detect drug resistance are phenotypic resistance testing (PRT) and genotypic resistance testing (GRT) (Romanelli 2000).

PRT is a method to quantify the HIV susceptibility to various antiviral drugs in the human lymphocyte culture. The viruses are considered to be less susceptible or drug resistant to a particular drug if a larger quantity of the drug is required to block the replication of mutants than for the wild type viruses. However, the difficulty for this method is to determine how much variation of the drug dose for mutants from the dose of wild type virus is still considered as sensitive.

In contrast, GRT does not directly test the drug susceptibility but rather investigates the mutations in genomic sequences of target genes, currently RT and PR. So it indirectly assesses the viral resistance which is associated with genetic changes. The advantages of this method are that it is more rapid, less technically demanding and cheaper than PRT. Moreover, it can detect the mutations before they are expressed into functional proteins; thus GRT is more commonly used in the clinic. However, the mutants have to occupy at least 20-30% of the total viral population to be detected by GRT. In order to detect resistance for both methods, the minimum viral load for the test has to be over 500-1000 copies/ml. Although the interpretation of drug resistance profiles is not straightforward, both genotypic and phenotypic tests have shown good reliability and are cost-effective. It is reported that the concordance between PRT and GRT is about 80-90% for the susceptibility to NRTIs, NNRTIs, and PIs (Dunne 2001).

Combining the two basic methods, the virtual phenotype test is actually a genotype test by using a database, comprising resistance results of both genotyping and phenotyping tests from the same patients, to improve the genotype results. In fact, the virtual phenotype is a prediction of drug susceptibility based on genotypic

analysis and database matches. It is generally considered to be an advancement over standard genotypic testing. The database commonly used is the Stanford University HIV Drug Resistance Database (http://hivdb.stanford.edu/index.html). It is a collection of almost all published RT and PR sequences associated with drug exposure as well as unpublished data in other databases such as GenBank. Source sequences in the database are related to the antiretroviral drug treatment history of the person from whom the isolates are taken. In the protease inhibitor (PI) resistance notes, a series of possible drug resistant mutations are correlated with the level of susceptibility to all available FDA approved PR drugs (Figure 11). With the assistance of drug resistance tests, not only the antiretroviral treatment strategies can be enhanced but also drug resistance mechanisms of a variety of mutants in response to different drugs can be better understood.

7. Drug Resistance Mechanisms of RT and PR Inhibitors

Viruses with mutations are rapidly selected under the drug pressure, so those mutations should provide viruses with some selective growth advantage over the wild type viruses in the presence of drugs. In contrast, most of drug resistant mutations are deleterious for viral replication in absence of drugs. However, the drug resistance, in some cases, is difficult to explain completely by genetic changes, involving a single or multiple mutations.

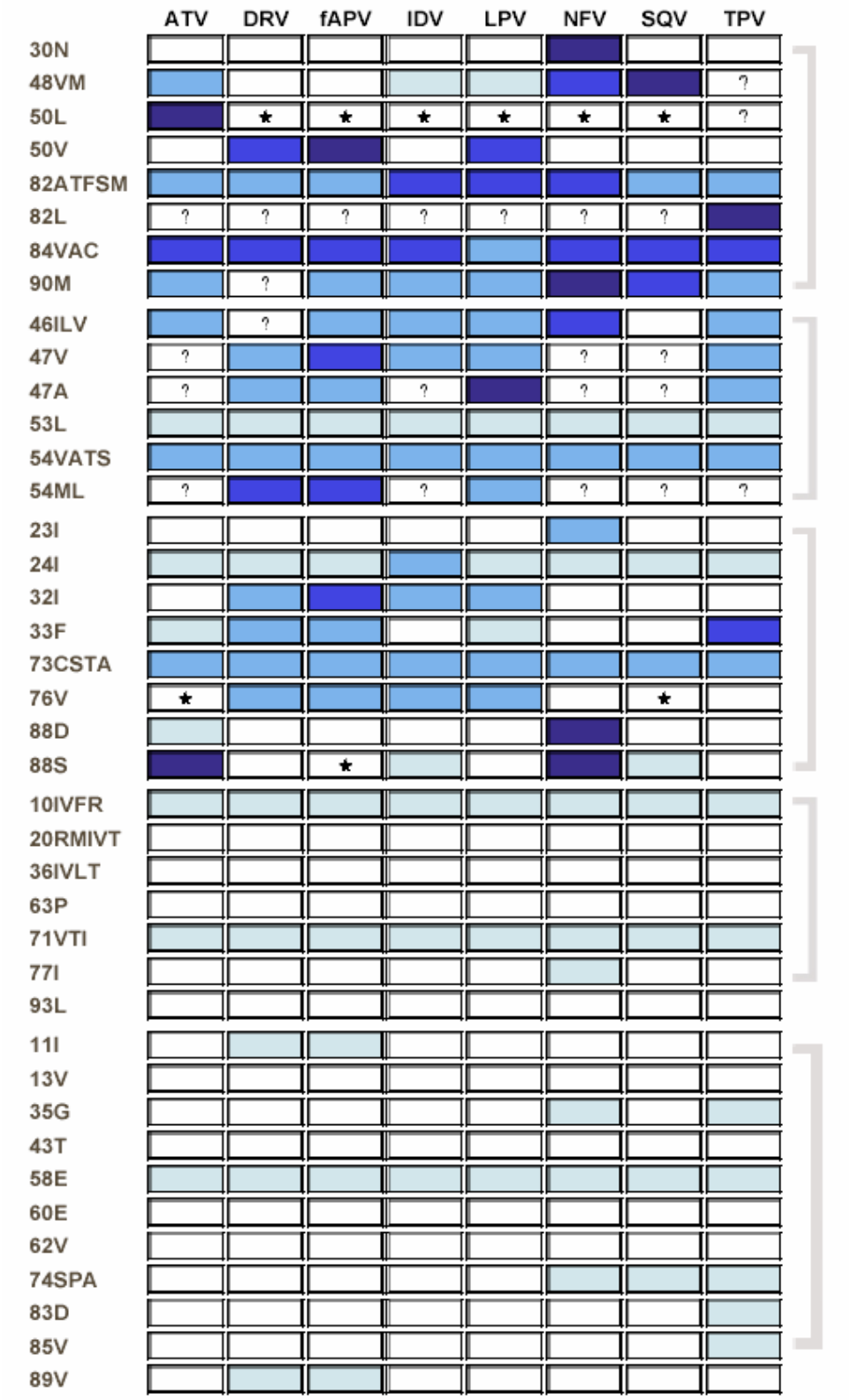

Figure 11: The PI drug resistance notes from the Stanford HIV drug resistance database (Shafter, 1999). The darker the color means the higher level of resistance.

7.1 Drug Resistance Mechanisms of RT Inhibitors

The treatment with the reverse transcriptase inhibitors (NRTIs and NNRTIs) results in severe drug resistance. Two major drug resistance mechanisms for NRTIs have been proposed (De Mendoza 2002). In some mutants, the RT gains the ability to recognize the structural difference between the phosphorylated NRTIs and dNTPs, so NRTIs lose their competitive advantage over dNTPs (Naeger 2001; Clavel 2004). The other mechanism is that the NRTIs incorporated in the DNA chains are removed by the attack of ATP or pyrophosphate and the DNA chains continue to grow (Meyer 1998; Meyer 2000). For NNRTIs, resistant mutants reduce the affinity of drugs for the binding site (Hsiou 2001; De Mendoza 2002).

7.2 Drug Resistance Mechanisms of PR Inhibitors

Similar to RT, the drug resistance is also a major issue in PI treatment. The drug resistance mechanisms of PIs have been studied extensively and appear to be very complicated. On long exposure to the drugs, not only the mutations in PR change the enzyme properties but also the mutations in the cleavage sites of substrates can arise to compensate for the changes caused by PR mutations.

7.3 Mutations in PR

The mutations in PR alter single or multiple residues which can cause multidrug resistance and cross-resistance (Figure 12). Mutations in 45 out of 99 residues of the PR have been associated with the treatment with PIs (Schinazi 1997; Hertogs 2000; Wu 2003; Johnson 2005). A clinical isolate of the HIV has accumulated as many as 10 mutations in PR at diverse positions and is resistant to all

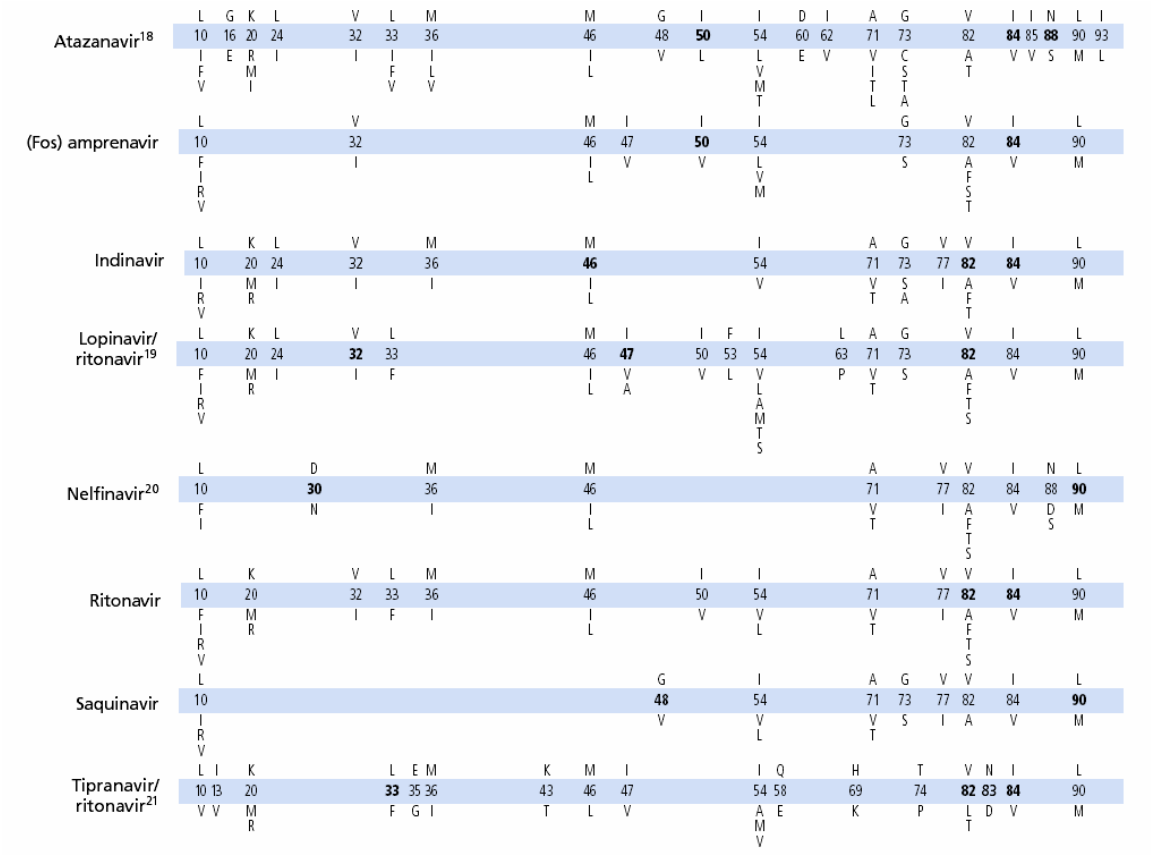

Figure 12: Mutations in the protease gene associated with resistance to PIs (Johnson, 2005).

available PIs (Condra 1995; Vickrey 2003). However, drug resistant mutations in PR cannot be at any position and altered to any amino acid. The potential mutations have been constrained to permit proper protein folding, structural stability, and catalytic activity on diverse substrates (Erickson 1996). Many PR mutants coupled with diverse inhibitors have been studied by crystallography and kinetics (Chen 1995; Mahalingam 1999; Hong 2000; Mahalingam 2001; Mahalingam 2002; Clemente 2004; King 2004; Mahalingam 2004; Tie 2004; Tie 2005; Kovalevsky 2006; Liu 2006). Those drug resistant mutants have shown diverse changes in catalytic activity, inhibition constants, and stability by the combinations of different mutations with substrate or inhibitor (Gulnik 1995; Ermolieff 1997; Ridky 1998; Mahalingam 1999; Xie 1999; Mahalingam 2001; Prabu-Jeyabalan 2002; Prabu-Jeyabalan 2003). Combinations of different mutations may lead to additive, synergistic or compensatory effects (Erickson 1996; Mahalingam 2002). In some cases, the observed structural changes in mutations are in agreement with kinetic and stability changes. However, other mutants do not demonstrate understandable relationships of catalytic activity, inhibition, and structural changes. Drug resistant mutation cause independent changes in any one of the above factors or combinations of those factors.

Drug resistant mutations can be simply classified as active site (inhibitor binding site) mutations and non-active site mutations. They also can be categorized as the major or primary mutations, the secondary mutations, the flap mutations, the dimer interface mutations and other distal mutations. The major mutations are normally by themselves able to cause drug resistance to one or multiple PIs. On the other hand, the secondary mutations frequently appear with those drugs resistant

mutations (Shafer 2002). These categorizations are mainly for the purpose of convenience and a mutation may belong to multiple categories at the same time.

The active site mutations or major mutations

The binding of inhibitor is stabilized by hydrogen bonds and van der Waals interactions between PR and inhibitor. So mutations of the residues forming at the inhibitor-binding site can potentially disturb the interactions between PR and inhibitor, thus leading to the diminished affinity of the inhibitor to the mutated PR (Hong 2000; Prabu-Jeyabalan 2003; Wartha 2005). This mechanism has been confirmed by the crystal structures of HIV-1 PR with single or double mutations at active sites complexed with inhibitors (Mahalingam 2001; Mahalingam 2002; Mahalingam 2004; Tie 2004). In addition, mutations of one residue not only directly alter the inhibitor interaction of that residue but may also indirectly modify the interaction of other residues with the inhibitor. Since the clinical drugs are always smaller than the natural substrates, the altered active site would have much larger effects on the binding of inhibitors than on the binding of substrates. So the inhibitors lose competitive advantage over the natural substrate in mutants. In many cases, such as mutations of V82A and I84V, the active site mutations are also the major resistant mutants. It seems that reducing drug affinity is a primary drug resistance mechanism which has been adopted by many targets of fungicides, antibiotics and so forth (Yotsuji 1988; Hayes 1997).

Non-active site or secondary mutations

The mutations of non-active site residues have been frequently observed and also significantly contribute to drug resistance (Muzammil 2003; Clemente 2004; Liu

2005). Although they do not directly interact with inhibitors, the mutated side chains may perturb the subunit-subunit interactions in the PR dimer. The perturbation may be transferred to the active site through an extended structural network, which can indirectly interfere with the binding of the inhibitor, and (or) diminish the dimer stability of the PR, and consequently impair the enzyme activity and lower the inhibitor binding affinity (Xie 1999; Mahalingam 2001; Mahalingam 2004; Liu 2005; Kovalevsky 2006).

Flap mutations

Due to the important role of the flap in substrate or inhibitor binding at the active site, mutations in the flap can potentially disturb the PR activity, dimer stability and conformation. Some HIV PR mutants are predicted to alter the equilibrium of conformations of fully open, semi-open and closed (Rose 1998). In the case of M46I, the mutated flap is predicted to be more stable in a closed conformation (Collins 1995). Some flap mutants have been suggested to have wider open flap than that of the wild type (Logsdon 2004). So the effect of the mutations on the equilibrium of different conformations could be one of the mechanisms of drug resistance (Perryman 2004).

7.4 Compensatory Mutations in the Cleavage Sites of Substrates

After the mutations in PR, mutations in substrate cleavage sites have been observed at NC/p1 and p1/p6 of the Gag gene in drug resistant strains (Doyon 1996; Zhang 1997; Robinson 2000; Feher 2002; Shafer 2002). The cleavage sites at NC/p1 and p1/p6 are the slowest to be cleaved in the polyprotein processing and those sites in the short peptides representing natural substrates have the lowest binding

specificity (kcat/Km) (Tozser 1991; Doyon 1996). In the presence of PR inhibitors, mutations of cleavage sites are able to partially compensate for the reduced activity, restore the efficiency of substrate processing and enhance the viral replication capacity (Doyon 1996; Croteau 1997; Zhang 1997; Feher 2002). Nevertheless, mutations of cleavage sites alone have not been found to cause PI resistance.

8. A Paradigm for Structure-Assisted Drug Design

Anti-viral drugs are likely to remain the mainstay for treating diseases caused by viral infection. The development of anti-retroviral drugs has made substantial progress in the past two decades. Within the past 20 years, the number of licensed clinical anti-viral drugs has grown from 5 to over 50 (De Clercq 2004) and 2/5 of them are anti-HIV drugs. Nevertheless, new drugs with better efficiency and specificity against viral resistance are still remarkably in demand. Besides the well studied classic models of HIV, hepatitis B and C, the emergence of new viruses such as the SARS (Severe Acute Respiratory Syndrome) coronavirus and the haemorrhagic fever viruses as potential bioweapons has also increased the need for anti-viral drug discovery (De Clercq 2004).

Structure-assisted (also called rational) drug design is one of the most powerful approaches among the technologies in drug research if the molecular structures are available or can be predict accurately. This drug design method involves multiple-disciplines of crystallography, NMR (Nuclear Magnetic Resonance), computational modeling and chemical synthesis. X-ray crystallography has proven to be the central technology to understand the structural binding modes of

proteins and small molecules. In an addition, crystallography provides the starting point for molecular dynamics modeling, docking of ligands, virtual screening for potential leads and optimizing of lead compounds in the design of drugs and vaccines.

The development of PIs is a typical representative of the success of structure-assisted drug design through the collaboration of pharmacology, medicinal chemistry and structural biology (Wlodawer 1993; Kempf 1995; Wlodawer 1998; Prabu-Jeyabalan 2003). Some initial PIs were substrate analogs (peptide derivatives) that replace the scissile-bond with a non-cleavable bond. They are normally large in size, cannot easily penetrate into cells and are easily digested by cellular enzymes. Consequently, smaller inhibitors with fewer peptide bonds have been developed. Except for tipranavir, all other PIs hold a peptidomimetic core and large hydrophobic moieties binding in the substrate-binding cleft of the PR (Figure 11).

The general steps for screening and structure-assisted drug design are summarized as below, concentrating on HIV PIs (Tomasselli 1994; Coffin 1997; Tomasselli 2000). First, inhibitory activities are measured to screen some compounds with low inhibition constants. The cocrystal structures of PR/inhibitors demonstrate the comprehensive pattern of hydrogen bond, hydrophobic and van der Waals interactions formed by the compound and protein. The guidance from crystal structures can speed up the screening. Further structural optimization can be made to introduce or modify the functional groups to improve the binding affinity and minimize the binding energy. It typically takes several rounds of inhibition studies, structural analyses and chemical synthesis until the discovery of some compounds with the desired potency and affinity for the protein. For instance, in the process of

designing indinavir (Merck), more than 150 intermediate compounds were produced before the final product was obtained (Lyle 1991; Vacca 1994). Then subsets of inhibitors are evaluated for their ability to penetrate cells and inhibit various strains of viral particles. Further inhibitors with high potency, satisfactory pharmacokinetic properties, toxicity and bioavailability tests in animal models are developed (Coffin 1997). Finally the compounds go to the lengthy clinical trials to test the dose and side effects before they become commercial drugs.

An ideal HIV PI should be effective against both wild type PR and structurally similar mutants. However, most PIs are designed to have a constrained shape in order to have high specificity and binding affinity for PR. Thus, they preferentially target wild type PR and cannot easily adapt to mutants. In order to minimize the drug resistance problem, the new inhibitors should be designed to have critical interactions with conserved regions of PR while they retain the adaptive ability through flexible functional groups (Ohtaka 2005). Thus the knowledge of design of effective anti-HIV drugs provides significant insight for designing drugs against other retroviral infections.

9. Limitations of PI in Anti-HIV Therapy

Besides drug resistance, the adverse metabolic side effects are another major issue involving the PI treatment. The adverse effects have been reported include peripheral lipodystrophy, visceral adiposity, hyperlipidemia, diabetes mellitus, cardiovascular disease, hypertension and insulin resistance (Hruz 2001; Grinspoon 2005; Barbaro 2006). As more and more evidence accumulates, it has been confirmed

that PIs do not specifically target HIV PR as designed and they disturb the function of a number of unrelated molecules. The glucose tolerance, for instance, has been disturbed in 10–16% of the patients on PI regimens (Hruz 2001). It is found that the activity of the glucose transporter (GLUT-4) is noncompetitively inhibited by indinavir and lopinavir (Hertel 2004; Grinspoon 2005). And indinavir must be administered with a large amount of water in order to prevent kidney stones. So one of the major considerations for the development of safer and potent PIs is to minimize toxic metabolic consequences (Hruz 2001). Despite the severe side effects of PI, the therapy cannot be terminated since no better alternatives are available for the patients at present.

Successful long-term chemotherapy treatment of HIV-1 infection remains an unrealized goal confronted by various challenges. First, antiviral drugs can not eliminate virus from an infected individual because the viral DNA is integrated into the host cell genome. Another difficulty is that the virus retains in reservoirs that the current drugs are hard to reach (Chun 1997; Finzi 1997). So drugs may only diminish the infection to a lower level. Second, the development of inhibitors with the double features of potency and no adverse effects for HIV positive individuals who harbor wild type and drug resistant viruses is an extremely difficult task. However, most of the mutations have deleterious effects on key viral proteins. Therefore, the hope for effective therapeutic for HIV is still there since the replication of resistant variants seems to be less efficient, or the virus loses its virulence (Clavel 2004). After blocking the replication of the wild type and some mutants, the viral load in the body can be reduced to a lower level at which the host immune system can control of it.

Once the therapy initiates, however, the drugs have to be maintained at a certain dose for the whole life because the incomplete suppression of viral replication facilitates the appearance of drug resistant virus and leads to a resurgence of high-level viral replication and treatment failure.

MATERIALS AND METHODS

Preparation of HIV-1 PR mutants

An HIV-1 PR (Genbank HIVHXB2CG) clone with five optimizing mutations (Q7K, L33I, L63I, C67A and C95A) was used as the template (called as wild type PR) to introduce the mutations. Those mutations have been proved to stabilize the protein and the optimizing mutants have similar kinetic properties to the protease without those mutations (Louis 1999). Plasmid DNA (pET11a, Novagen, Madison, WI) encoding PR was used with oligonucleotide primers with the base corresponding to the mutation to generate the mutant constructs by the Quick-Change mutagenesis kit (Stratagene, La Jolla, CA). The sequences of primers used for introducing the mutations are listed in the Table 1. The PCR mixture (total 50 µl) contained: 5 µl (10X) of reaction buffer, 1µl (25 mM) of dNTP, 1µl (125 ng/µl) of forward primer, 1µl (125ng/µl) of reverse primer, 1µl (2.5 U/µl) of Pfu turbo DNA polymerase, 1µl (10-20 ng) of DNA template. PCR setting was 1 cycle at 95 °C for 30 sec, followed by 12 cycles at 95 °C for 30 sec, 55 °C for 1 min, 68 °C for 12 min and held at 4 °C. A small fraction of each reaction mixture (5-10 µl) was applied to 1.0% agarose gel electrophoresis to estimate the quantity of DNA. The PCR products (5-25µl) were digested with 1 µl DpnI at 37 °C for an hour to dispose of wild type template then were transformed into XL-blue competent cells from Stratagene according to the protocols.

Table 1: The DNA sequences of primers for introducing mutations

Mutant	5'-3' primer sequences (number of nucleotide)
L24I	Forward: GGTCAG CTG AAA GAA GCT CTG ATC GAT ATC GGC GCT GAC GAT ACC (45nt) Reverse: GGT ATC GTC AGC GCC AGT ATC GAT CAG AGG TTC TTT CAG CTG ACC (45nt)
I50V	Forward: CCA AAA ATG ATA GGG GGA GTT GGA GGT TTT ATC AAA GTA AGA C (43 nt) Reverse: G TCT TAC TTT GAT AAA ACC TCC AAC TCC CCC TAT CAT TTT TGG (43 nt)
F53L	Forward: G ATA GGG GGA ATT GGA GGT TTG ATC AAA GTA AGA CAG TAT G (41 nt) Reverse: C ATA CTG TCT TAC TTT GAT CAA ACC TCC AAT TCC CCC TAT C (41 nt)
I54V	Forward: G ATA GGG GGA ATT GGA GGT TTT GTC AAA GTA AGA CAG TAT G (41 nt) Reverse: C ATA CTG TCT TAC TTT GAC AAA ACC TCC AAT TCC CCC TAT C (41 nt)
I54M	Forward: G ATA GGG ATT GGA GGT TTT ATG AAA GTA AGA CAG TAT G (41 nt) Reverse: C ATA CTG TCT TAC TTT CAT AAA ACC TCC AAT TCC CCC TAT C (41 nt)

Protein Purification

The PR mutants were expressed using pET11a vector and *Escherichia coli* BL21 (DE3) protein expression competent cells. PR was purified from inclusion bodies, as described previously (Mahalingam 1999). Cells were grown at 37°C in Luria-Bertani medium with 100ug/ml carbenicillin and shaken at 225 rpm until the OD600 reached 0.4 - 0.5. Protein expression was induced by IPTG (2 mM) (Louis 1989). After inducing for 3-4 hours, cells were harvested and suspended in 20 volume of buffer A (50 mM Tris-HCl, pH 8.2, 10 mM EDTA) and lysed by sonicating (5 of 1 minute intervals, 40-50% duty, 4-5 output) on ice. After centrifugation (12,000 rpm, 20 min in SS34 rotor at 4°C), the pellets (inclusion bodies) were then washed by resuspending in buffer B (buffer A plus 2 M urea and 1% Triton X-100) and then in buffer A again. The pellet was solubilized in 50 mM Tris-HCl, pH 8.0, 7.5-8 M guanidine-HCl, 10 mM EDTA.

After filtering through an 0.2-0.8 um syringe filter, the solution was applied to a Superdex-75 column (HiLoad 2.6 cm × 60 cm, Amersham Pharmacia Biotech, NJ) equilibrated in 50 mM Tris-HCl, pH 8, 4 M guanidine-HCl, 5 mM EDTA at a flow rate of 1 ml/min. Peak fractions were pooled and subjected to reverse-phase high-performance liquid chromatography (HPLC) on a RPC15 ST 4.6/100 column (Amersham Pharmacia Biotech, NJ). The peak appearing at gradient 40% of buffer B (0.05% TFA in Acetonitrile for buffer B and 0.05% TFA in water for buffer A) was collected and confirmed by molecular weight shown on SDS-PAGE. In both cases, the chromatography was run at room temperature. The protein was appropriately

folded by dialysis in 0.05 M formic acid at pH 2.8 for at least 3 hours, followed by 0.05 M sodium acetate buffer, pH 5.0 for at least 3 hours at 4°C. The protein was concentrated to the desired concentration (usually 2-6 mg/ml) for the kinetic study and crystallization. Concentrated protein remained stable at least one year at -80°C. The mutation was confirmed by both nucleic acid sequencing and protein mass spectrometry.

Enzyme Kinetics

The chromogenic substrate Lys-Ala-Arg-Val-Nle-p-nitroPhe-Glu-Ala-Nle-amide (Sigma, St. Louis, MO) is a CA/p2 analog and was used to determine the kinetic parameters. PR at a final concentration of 70-120 nM was added to varying concentrations of substrate (25-400 μM) maintained in 50 mM sodium acetate pH 5.0, 0.1 M NaCl, 1 mM EDTA, and assayed by monitoring the decrease in absorbance at 310 nm within the first 1-2 min using a PerkinElmer Lambda 35 UV-Vis spectrometer.

The absorbance was converted to substrate concentration via a calibration curve. The enzyme concentrations were based on active site titration data. The Michaelis-Menten curves were fitted using SigmaPlot 8.0.2 (SPSS Inc.). PR hydrolysis of the peptides K-A-R-V-L-A-E-A-M-S (CA/p2) and V-S-F-N-F-P-Q-I-T-K-K ($p6^{Pol}$/PR) was assayed using HPLC as described (Mahalingam 2001). The reduced peptide analogs R-V-L-r-F-E-A-Nle (CA/p2) and Ace-T-I-Nle-r-Nle-Q-R (p2/NC) (r is the reduced peptide bond and Nle replaces M) were purchased from BACHEM. Indinavir was a gift from Merck & Co and TMC114 and saquinavir from

Dr. Arun Ghosh (Purdue University). The K_i values were obtained from the IC_{50} values estimated from an inhibitor dose-response curve with the spectroscopic assay and the chromogenic substrate using the equation $K_i = (IC_{50} - [E]/2) / (1 + [S]/K_m)$, where [E] and [S] are the PR and substrate concentrations, respectively (Maibaum 1988).

Urea Denaturation Assays

The denaturing effect of urea was measured using the spectroscopic assay. PR activity was measured with increasing concentration of urea (0 – 4.0 M) at the final concentrations of 300–500 nM enzyme and 400 μM substrate (Feher 2002). The UC_{50} values at half-maximal velocity were obtained by plotting the initial velocities against urea concentration and fitting to a curve for solvent denaturation of protein using SigmaPlot 8.0.2 software.

K_d Determination

The K_d was determined by measuring specific activity as a function of dimeric enzyme concentration at a final substrate concentration of 375 μM in 50 mM acetate pH 5.0, 0.1 M NaCl at 25 °C (Wondrak 1996).

Crystallographic Analysis.

Crystals were grown at room temperature by vapor diffusion using the hanging drop method. The protein concentration was 1.8 - 5 mg/ml. The reservoir contained precipitant, buffer at various concentrations and pH as described in Table 2.

Table 2: The crystallization conditions

PR/PI	PR/PI Ratio	Precipitate/salt	Buffer	Additives
L24I/ p2-NC	1:20	6-20% saturated $(NH_4)_2SO4$	0.1 M citrate/0.2 M phosphate buffer, pH 5.4-5.8	5-10% DMSO
L24I/ IDV	1:5	20-40% saturated $(NH_4)_2SO4$	0.1 Mcitrate/0.2 M phosphate buffer, pH 5.0-6.0	10% DMSO
I50V/ p2-NC	1:20	6-20% saturated $(NH_4)_2SO4$	0.1 M citrate/0.2 M phosphate buffer, pH 5.4-5.8	10-15% DMSO
I50V/ IDV	1:5	20-40% saturated $(NH_4)_2SO4$	0.1 M citrate/0.2 M phosphate buffer, pH 4.6-5.8	6-10% MPD, 10% DMSO
G73S/ IDV	1:5	20-40% saturated $(NH_4)_2SO4$	0.1 M citrate/0.2 M phosphate buffer, pH 4.6-5.8	6-10% MPD, 10% DMSO
F53L	1:5*	20-30% saturated $(NH_4)_2SO4$, 0.1 M sodium citrate	0.2M sodium citrate, phosphate buffer, pH = 6.0-6.4	10% DMSO
M46L/ DRV	1:2	25% NaCl	0.2 M sodium acetate buffer, pH = 3.8	
D25N/ p2-NC	1:20	10% NaCl	0.1 M citrate/0.2 M phosphate buffer, pH 5.4	5-10% DMSO
D25N/ DRV	1:2	30% NaCl	0.2 M sodium acetate buffer, pH 5.0	
WT/ p2-NC	1:20	10-15% saturated $(NH_4)_2SO4$, 0.1 M sodium citrate	0.2M sodium citrate, phosphate buffer, pH 6.0-6.2	10-15% DMSO 5-10% dioxide
I54M/ DRV	1:2	25-30% NaCl	0.2 M sodium acetate buffer, pH 4.4-4.6	
I54M/ SQV	1:5	10-15% NaCl	0.2 M sodium acetate buffer, pH 4.8-5.2	
I50V/ SQV	1:5	30-35% saturated $(NH_4)_2SO4$	0.2M sodium citrate, phosphate buffer, pH 6.0-6.2	
F53L/ SQV	1:5	1.75M KCl	0.2 M sodium acetate buffer, pH 5.4	5-10% dioxide
G48V/ DRV	1:2	1.3 M KCl	0.1 M citrate/0.2 M phosphate buffer, pH 5.6-5.8	7-10% MPD
L90M/ DRV	1:2	20% NaCl	0.2 M sodium acetate buffer, pH 4.2	

*The molecular ratio of F53L and indinavir was 1:5 in the crystallization mixture; however, indinavir was not bind to the PR revealed in the crystal structures. Similar crystals were also obtained in the absence of indinavir in the PR solution.

Some additives such as DMSO (dimethylsulfoxide), MPD (2-Methyl-2,4-Pentanediol), and dioxide were added in order to improve the quality of crystals. The crystallization drops had a 1:1 v/v ratio of the reservoir solution and the protein. The crystals grew from overnight to 10 days into tetrahedral bipyramids, bricks, plates, and rod shapes. Some of them formed crystal clusters and were cut into small crystals before mounting. Crystals were frozen in liquid nitrogen after soaking in the 20-35% glycerol as a cryoprotectant. All protein was mixed with inhibitors in a certain ratio that depended on whether the inhibitor had higher affinity (1:2) or low affinity (1:20) for the protein. One exception was that PR_{F53L} crystallized in the unliganded form although the molar ratio of PR_{F53L}: inhibitor was 1:5 in the solution. Some mixtures of PR and inhibitor were more difficult to crystallize than others.

X-ray diffraction data for the crystals were collected on the SER-CAT beamline of the Advanced Photon Source, Argonne National Laboratory in Chicago. Data were processed with HKL2000 (Otwinowski 1997). The structures were solved by molecular replacement using the AmoRe (Navaza 1994) and CPP4i suite (Collaborative Computational Project 1994; Potterton 2003) programs. The structures were refined by SHELX97 (Sheldrick 1997) and refitted using O 8.0 (Jones 1991). Alternate conformations were modeled for residues when obvious in the electron density maps. The solvent was modeled with 180-300 water molecules per dimer including partial occupancy sites and ions present in the crystallization solutions, as described previously (Tie 2004). Anisotropic B factors were refined for the structure. Hydrogen atom positions were included in the last stage of refinement using all data after all other parameters including the disorder had been modeled. The

published structures have been deposited in the Protein Data Bank (Berman 2000), with the accession codes listed in the Table 3. The mutant structures were compared with the wild type structures or other by superimposing their main chain atoms or Cα using the program ALIGN (Cohen 1997) or FUD. Figures were made using RasMol (Sayle 1995), Molscript (Kraulis 1991) and Bobscript (Esnouf 1997; Esnouf 1999).

Chapter One: Kinetic, Stability, and Structural Changes in High Resolution Crystal Structures of HIV-1 Protease with Drug Resistant Mutations L24I, I50V, and G73S

(Published: Liu F., Boross P.I., Wang Y.-F., Tozser J., Louis J.M., Harrison R.W., Weber I.T. (2005) *J Mol Biol.* 354(4):789-800.)

INTRODUCTION

Indinavir was one of the first PR inhibitors in clinical use. High levels of resistance to indinavir were associated with substitutions of up to 11 PR residues in different combinations (Brown 1999). The crystal structures of drug-resistant HIV PRs with multiple mutations have been reported in complexes with indinavir (Chen 1995; Munshi 2000; King 2002). Our analysis of the high resolution crystal structures of HIV PR, and the common indinavir-resistant mutants PR_{V82A} and PR_{L90M} in complexes with indinavir, showed structural changes consistent with differences in their enzymatic activity (Mahalingam 2004). However, biochemical and biophysical analyses have not been performed for other mutations that are consistently observed at lower frequency. Mutations L24I and G73S are observed in about 10% and 5%, respectively, of patients exposed to indinavir. These rare mutations are generally observed in combination with other resistant mutations. Mutations of Gly 73 appear in patients failing multiple PR inhibitors, and are often found in combination with L90M (Shafer 2002). The effects of these mutations have been compared to that of

I50V, which is rarely observed on exposure to indinavir (0.2%), however, it is found in 30% of patients exposed to amprenavir as their first PR inhibitor. PR_{I50V} showed higher Ki values for saquinavir, indinavir, and nelfinavir in biochemical studies (Partaleis 1995). Mutations L24I, I50V, and G73S alter residues in different regions of the PR dimer structure as shown in Figure 1.1. I50V alters a residue at the tip of the flexible flap that forms part of the inhibitor-binding site. L24I is next to the catalytic Asp 25 but has no direct contact with inhibitor, while G73S is located far from the inhibitor binding site. These mutants provide good models to help dissect the varied molecular mechanisms of drug resistance.

Here, we report the kinetics, dimer stability, and crystal structures of the HIV drug-resistant mutants PR_{L24I}, PR_{I50V}, and PR_{G73S}. Crystal structures were determined for PR_{L24I}, PR_{I50V}, and PR_{G73S} in complexes with indinavir, while PR_{L24I} and PR_{I50V} structures were also determined with a peptide analog of the p2/NC cleavage site in order to analyze the interactions with both substrate and inhibitor. Atomic details from these new crystal structures will be important for the design of second-generation inhibitors to circumvent the development of drug-resistance.

RESULTS AND DISCUSSION

Kinetics and Stability

Kinetic parameters were determined for the resistant mutants using the spectrophotometric substrate (K-A-R-V-Nle-p-nitroPhe-E-A-Nle-amide), which is an analog of the HIV-1 CA/p2 cleavage site (Table 1.1). The two mutants PR_{L24I} and PR_{I50V} showed lower k_{cat}/K_m values of 3.7% and 18%, respectively, relative to PR.

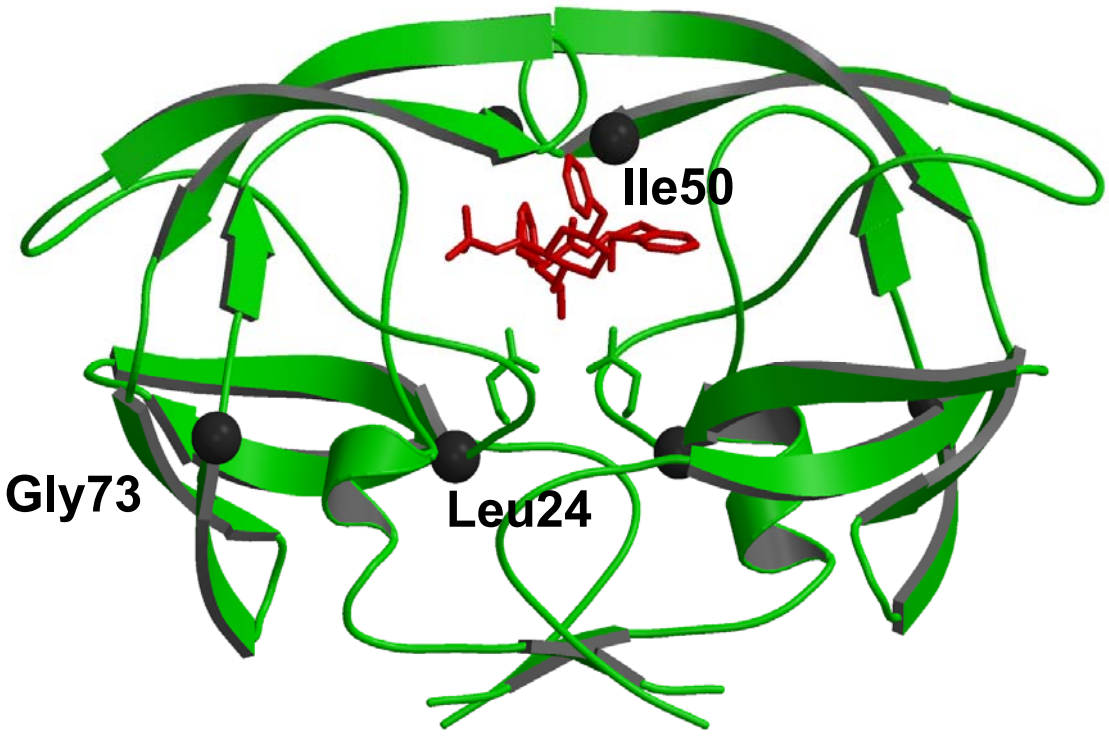

Figure 1.1. PR dimer structure (green ribbons) with indinavir (red bonds). The sites of mutation are indicated by black spheres for Leu 24, Ile 50 and Gly 73. Only one subunit is labeled.

Table 1.1: Kinetic parameters for hydrolysis of spectroscopic substrate (KARV-Nle-p-nitroPhe-EA-Nle-amide) (CA/p2#). [a]PR values were taken from (Mahalingam, 2004).

Protease	**Substrate**	**K_m (μM)**	**k_{cat} (min^{-1})**	**k_{cat}/K_m ($min^{-1}\mu M^{-1}$)**	**Relative k_{cat}/K_m**
[a] PR	CA/p2#	55 ± 7	290± 10	5.2± 0.2	100
PR_{L24I}	CA/p2#	310 ±45	61 ± 4	0.19 ± 0.03	3.7
PR_{I50V}	CA/p2#	500±36	480±19	0.93±0.08	18
PR_{G73S}	CA/p2#	46±4	280±65	6.1±0.6	117

The decrease in k_{cat}/K_m for PR_{I50V} was primarily due to an increase in K_m, whereas for PR_{L24I}, it was due to both an increase in K_m and a decrease in k_{cat}. PR_{G73S} and PR showed similar k_{cat}/K_m values for this substrate. Therefore, PR_{G73S} was tested for the hydrolysis of three other peptide substrates, representing different cleavage sites in Gag and Gag-Pol polyproteins: K-A-R-V-L*A-E-A-M-S (CA/p2) and V-S-F-N-F*P-Q-I-T-K-K ($p6^{Pol}$/PR) and E-R-Q-A-N*F-L-G-K-I (NC/p1) (where * indicates the hydrolyzed peptide bond) (Table 1.2). PR_{G73S} showed more variation in the K_m values than in the k_{cat} values. The relative k_{cat}/K_m values were 14%, 27.5% and 390% for the CA/p2, NC/p1 and $p6^{Pol}$/PR peptides, respectively, suggesting significant differences in substrate specificity compared to PR.

The stability of these three mutants, as assessed by urea denaturation, was reduced to 50-60% for PR_{L24I} and PR_{I50V}, and about 80% for PR_{G73S} relative to the PR value (Figure 1.2A). Consistent with the lower catalytic activity and susceptibility to urea denaturation, the dissociation constant (K_d) was approximately 20 nM for both PR_{L24I} and PR_{I50V} (Figure 1.2B). In contrast, PR_{G73S} exhibited no significant decrease in specific proteolytic activity at the lowest measured protein concentration similar to PR, which showed no dissociation at 5 nM concentration.

Inhibition

The three mutants were assayed for inhibition by the clinical inhibitor, indinavir, and two substrate analog inhibitors, R-V-L-r-F-E-A-Nle (CA/p2) and Ace-T-I-Nle-r-Nle-Q-R (p2/NC) (r is the reduced peptide bond), that represent two cleavage sites in Gag (Table 1.3). PR_{I50V} was poorly inhibited by indinavir with about

50-fold higher inhibition constant (K_i), and about19-fold higher K_i with the p2/NC analog, and about 3-fold with the CA/p2 analog as compared to PR. In contrast, PR_{L24I} showed relatively strong inhibition by the CA/p2 analog with K_i of 0.05-fold of the PR value, while the inhibition by indinavir was 2.6-fold and by p2/NC was similar to PR value. Inhibition of the hydrolytic reaction catalyzed by PR_{G73S} was similar to PR for indinavir and p2/NC, and was 4.4-fold of the PR value for CA/p2 (Table 1.2). Therefore, the mutant PR_{I50V} had the largest effect on inhibition, while PR_{G73S} was most similar to wild type PR.

Crystal Structures

The crystal structures were determined of mutants PR_{L24I}, PR_{I50V}, and PR_{G73S} in complex with indinavir, and mutants PR_{L24I} and PR_{I50V} with the substrate analog p2/NC in order to determine any structural changes compared to the wild type PR. Good diffraction data were not obtained for crystals of PR_{G73S} with p2/NC. The crystallographic data collection and refinement statistics are shown in Table 1.4. The crystal structures of PR_{L24I}-p2/NC, PR_{L24I}-IDV and PR_{I50V}-IDV were refined to R-factors of 10.6 to 10.8% at the highest resolution of 1.10 Å. The structures of PR_{I50V}-p2/NC, and PR_{G73S}-IDV were refined to an R-factor of 11.1 to 14.4% at resolutions of 1.30 to 1.50 Å. The crystal structures had one dimer in the asymmetric unit of space groups $P2_12_12_1$ or $P2_12_12$, except for PR_{G73S}-IDV. In PR_{G73S}-IDV, the two alternate conformations of inhibitor in $P2_12_12_1$ were resolved by refining in $P2_1$ with two dimers in the asymmetric unit, as observed previously (Gulnik 1995). Overall, the main chain structure of the dimers was very similar and superimposed with RMS

Table 1.2: Kinetic parameters from the HPLC assay for hydrolysis of peptides KARVL*AEAMS (CA/p2) and VSFNF*PQITKK ($p6^{Pol}$/PR) and ERQAN*FLGKI (NC/p1). [b]PR values were taken from (Mahalingam, 2001).

Protease	**Substrate**	**K_m (μM)**	**k_{cat} (min^{-1})**	**k_{cat}/K_m ($min^{-1}\mu M^{-1}$)**	**Relative k_{cat}/K_m**
[b]PR	CA/p2	164±9	26±2	0.16	100
PR_{G73S}	CA/p2	680±170	15±1	0.022	14
[b]PR	$p6^{Pol}$/PR	253±15	105±2	0.42	100
PR_{G73S}	$p6^{Pol}$/PR	61±11	100±4	1.64	390
PR	NC/p1	234±68	187±35	0.80	100
PR_{G73S}	NC/p1	347±25	76.2±3.6	0.22	27.5

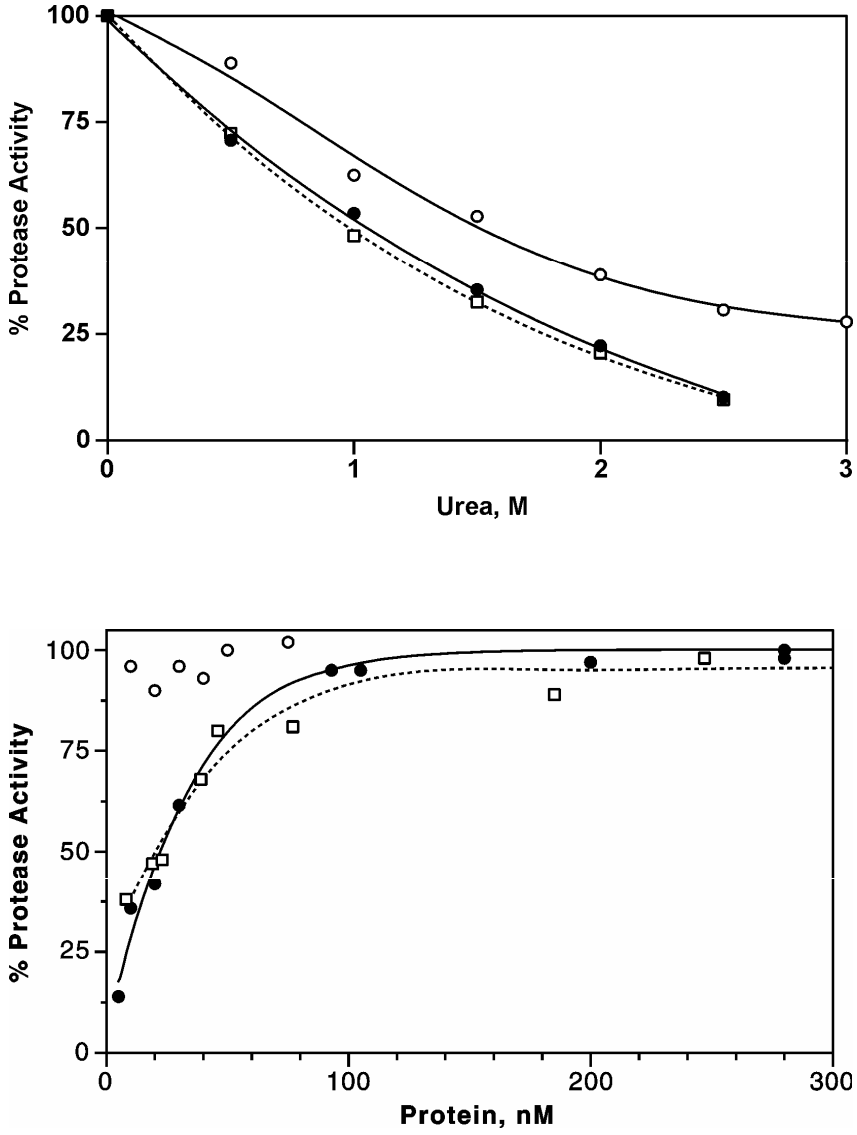

Figure 1.2 Protease stability. 1.2A. Sensitivity to Urea. L24I: closed circles and continuous line (UC_{50}=1.05M); I50V: open squares and dotted line (UC_{50}=0.97 M); G73S: open circles and continuous line (UC_{50}=1.54M). 1.2B. Dimer dissociation. L24I: closed circles and continuous line (Kd=22 nM); I50V: open squares and dotted line (Kd=19 nM); G73S: open circles (No dissociation observed).

Table 1.3: Inhibition constants for indinavir (IDV), the reduced peptide analogs CA/p2 (RVL-r-FEA-Nle) and p2/NC (Ace-TI-Nle-r-Nle-QR), where r is the reduced peptide bond. Values relative to PR are given in parentheses.

Protease	**Inhibition Constant (K_i)**		
	IDV (nM)	**CA/p2 (nM)**	**p2/NC (μM)**
PR	0.54	75	2.17
PR_{L24I}	1.40 (2.6)	3.5 (0.05)	2.0 (0.9)
PR_{I50V}	27.0 (50)	230 (3.0)	41 (19)
PR_{G73S}	0.55 (1.0)	330 (4.4)	3.3 (1.6)

Table 1.4: Crystallographic Data Statistics

Protease Mutant		**L24I**	**I50V**	**L24I**	**I50V**	**G73S**
Inhibitors		**p2/NC**	**p2/NC**	**IDV**	**IDV**	**IDV**
Space group		$P2_12_12$	$P2_12_12$	$P2_12_12_1$	$P2_12_12_1$	$P2_1$
Unit cell dimensions (Å)	a	58.2	57.9	51.5	51.3	51.3
	b	85.9	86.0	58.6	58.4	62.7
	c	46.5	46.5	61.6	61.0	59.2
Unique reflections		91188	57183	75564	72654	56309
R_{merge} (%)		6.8	5.8	5.7	5.6	6.5
Overall (final shell)		(13.2)	(28.1)	(12.2)	(17.7)	(23.9)
I/sigma(I)		25.24	26.79	28.23	33.81	17.42
Overall (final shell)		(9.9)	(4.14)	(7.38)	(5.07)	(4.51)
Resolution range for refinement (Å)		10-1.10	10-1.30	10-1.10	10-1.10	10-1.50
R_{work} (%)		10.62	11.14	10.84	10.72	14.43
R_{free} (%)		13.22	14.41	13.81	14.12	21.62
No. of waters		252.0	313.0	202	240.5	257.5
Completeness (%)		95.9	92.2	98.9	98.0	94.1
Overall (final shell)		(84.0)	(93.9)	(90.0)	(85.9)	(70.5)
RMS deviation from ideality						
Bonds (Å)		0.016	0.013	0.015	0.015	0.008
Angle distance (Å)		0.035	0.029	0.034	0.036	0.027
Average B-factors ($Å^2$)						
Main chain		7.8	10.1	11.0	9.3	18.3
Side chain		10.9	12.7	13.2	11.3	23.4
Inhibitor		9.8	14.8	10.5	8.8	15.2/18.5[a]
Solvent		24.1	27.3	24.2	24.5	28.4

a: The two numbers represent the average B-factors for inhibitors in the two dimers in an asymmetric unit

differences of < 0.3 Å for pairs in the same space group, and 0.5-0.6 Å for comparison of dimers in two different space groups. The indinavir was bound in two alternate conformations in the dimers of PR_{I50V} and PR_{G73S} with relative occupancies of 0.81/0.19 and 0.58/0.42, respectively. The inhibitor showed one orientation in all the other structures. The electron density map of indinavir in PR_{L24I}-IDV is shown in Figure 1.3. The atomic B factors were especially low for the protein and inhibitor atoms in the structures at 1.10 Å resolution; the average B values were 8-11 $Å^2$ for main chain and inhibitor atoms and 11-13 $Å^2$ for side chain atoms. The average B factors increased as the resolution decreased. The 1.5 Å resolution structure of PR_{G73S}-IDV had average B factors of 18.3 and 23.4 $Å^2$ for main chain and side chain atoms, respectively, and 15.2 and 18.5 $Å^2$ for the atoms of the two inhibitors, consistent with the lower resolution and higher difference (7%) between Rwork and Rfree. From 202 to 313 solvent molecules were modeled for the different structures with average B factors of 24.1 to 28.4 $Å^2$.

Alternate conformations were observed for many amino acid side chains and some main chain atoms, especially for the highest resolution structures (Figure 1.4A). There were 42 side chains modeled with alternate conformations for PR_{L24I}-IDV, 39 for PR_{L24I}-p2/NC, 33 for PR_{I50V}-IDV, 28 for PR_{I50V}-p2/NC, and 44 for the two dimers in the PR_{G73S}-IDV structure. Main chain atoms with alternate conformations were modeled for residues in the surface turns of 39-41 in PR_{I50V}-IDV and 66-69 in PR_{L24I}-p2/NC. There were alternate conformations for the side chains of Nle P1' and Arg P3' of the peptide analog p2/NC in the two mutant structures. The crystal structures that were refined at 1.1 Å resolution had the most alternate conformations. However,

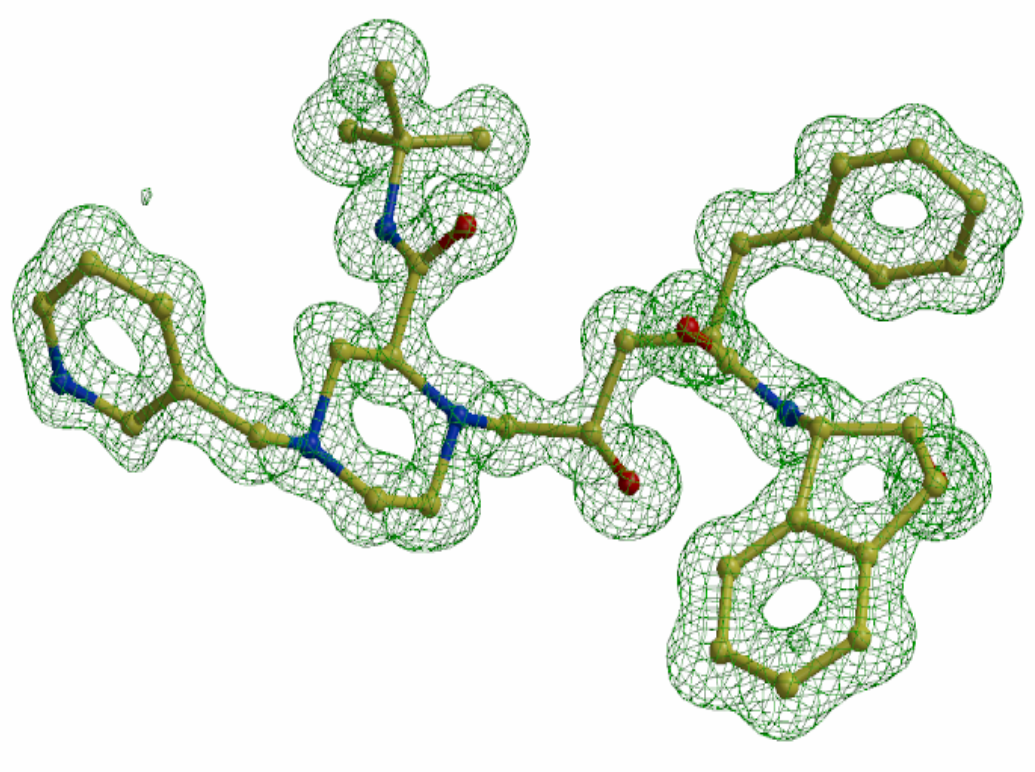

Figure 1.3. Omit map for indinavir in crystal structure of PR_{L24I}–IDV contoured at a level of 3.5 σ.

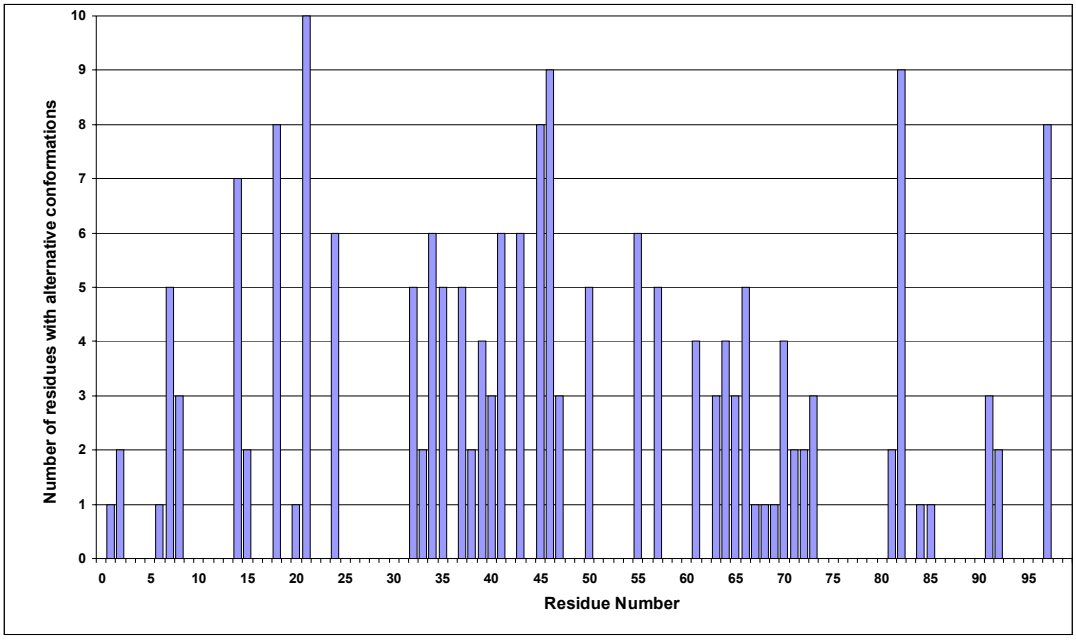

Figure 1.4A. Residues with alternate conformations. Alternate conformations of residues in 6 dimers of 5 new crystal structures. Alternate conformations for both side chain and main chain atoms were included.

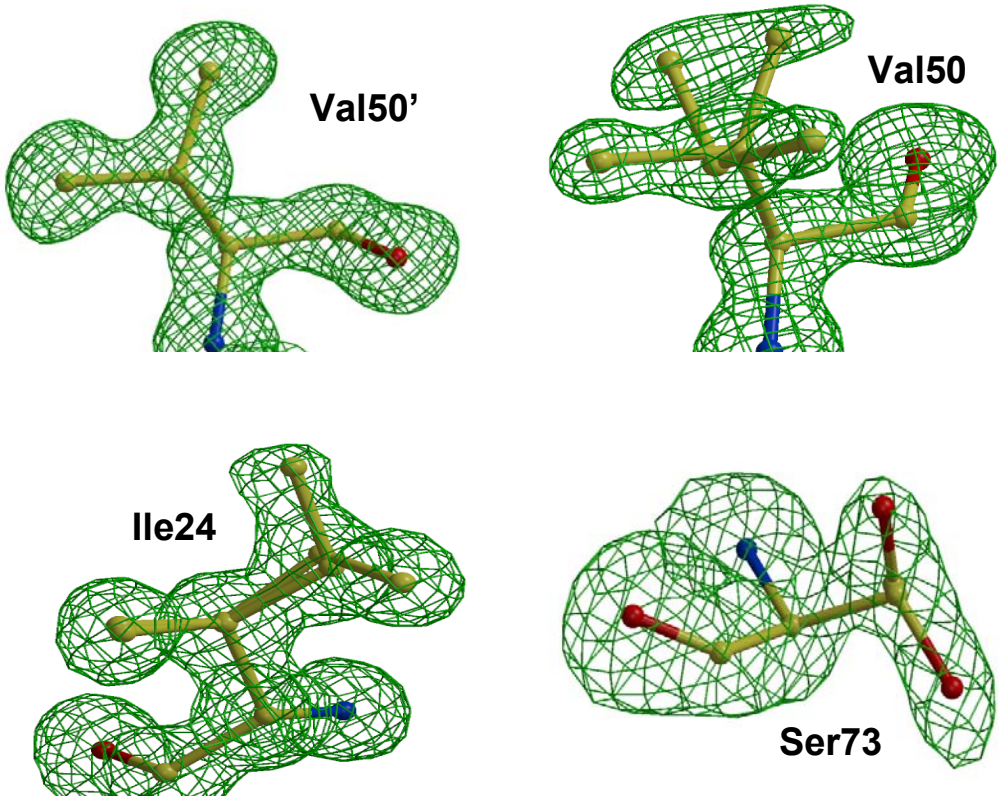

Figure 1.4B. Omit maps for mutated residues contoured at a level of 3.5 σ. Val 50' in PR_{I50V}–IDV had a single conformation for the side chain. Two alternate conformations are shown for the side chains of Val 50 (relative occupancy of 0.7/0.3) in PR_{I50V}–IDV, Ile 24 (relative occupancy of 0.6/0.4) in PR_{L24I}–p2/NC, and Ser 73 (relative occupancy of 0.5/0.5) in PR_{G73S}–IDV structures.

none of the residues consistently showed alternate conformations in both subunits of all structures. Moreover, the structures can show different relative occupancies for the alternate conformations of the same residue. The side chains of Glu 21, Met 46, Val 82 and Leu 97 had alternate conformations in both subunits of most structures. Met 46 and Val 82 are located near the inhibitor and frequently are mutated in drug resistant variants. All the mutated residues showed alternate conformations of the side chains (Figure 1.4B). The side chain of Ile 24 had alternate conformations in both subunits of both the PR_{L24I} structures, Val 50 had alternate conformations in one subunit of each of the PR_{I50V} structures, and Ser 73 showed alternate conformations in 3 subunits of the 2 dimers in the PR_{G73S}-IDV structure.

Structural Differences at Sites of Mutation

Each mutation introduced distinct structural changes compared to PR that can propagate to the inhibitor binding site and the dimer interface. The new mutant structures were compared to structures of PR-IDV and PR-p2/NC (Mahalingam 2004; Tie 2005). Leu/Ile24 lies in a hydrophobic internal pocket formed by residues from both subunits: Ile 3, Val 11, Ile 66, Ile 85, Leu 90, Leu 97', and Phe 99' in all the structures. The PR_{L24I} showed two alternate conformations for the Ile side chain in both subunits of the two crystal structures of PR_{L24I} – IDV and PR_{L24I} – p2/NC. The relative occupancies were about 0.8/0.2 for Ile 24 and about 0.6/0.4 for Ile 24'. Similar interactions were observed in both structures. The two alternate conformations of the side chains of Ile 24 and 24' in the mutant enabled the formation of similar van der Waals contacts to those of the side chains of Leu 24/24' in PR. One exception was the new interaction of the Cg side chain atom of Ile 24 with the side

chain of Leu 90, which was not observed for the wild type PR (Figure 1.5A). The mutant Ile 24/24' showed reduced interactions with Ile 85/85' and Phe 99'/99; for example, the shortest interatomic distance increased from 3.8 to 4.4 Å between the side chain atoms of residue 24 and Phe 99' (Figure 1.5A). Leu/Ile 24 interacted with Leu 97' and Phe 99' at the C-terminus of the other subunit. Therefore, structural changes can propagate from the mutated residue 24/24' to the dimer interface between the two C-terminal beta strands formed by residues 95-99. PR_{L24I} had one less intersubunit contact of residues 24/24' compared to PR in the complexes with p2/NC, and 2 less in the indinavir complexes. The altered contacts at the dimer interface appeared to be unfavorable consistent with the lowered stability in urea and increased dissociation of the dimer.

Residue 50 lies at the tip of the flap and interacted closely with the other flap of the dimer and the inhibitor (Figure 1.1). The interactions with inhibitor are described in the following section. The carbonyl oxygen of Ile/Val 50 from one subunit formed a conserved hydrogen bond interaction with the amide of Gly 51 from the other subunit. The mutated residue in one of the subunits, Val 50 in PR_{I50V}-IDV and Val 50' in PR_{I50V}-p2/NC, showed two alternate conformations for the side chain with relative occupancies of about 0.7/0.3 (Figure 1.4B). Ile/Val 50 and 50' showed slightly asymmetric van der Waals interactions (<4.2 Å) in all the structures (Table 1.5). In general, residue 50 interacted with residues from both flaps in the dimer (Gly 51, Gly 52, Ile 47', Gly 48', Gly 49', Ile/Val 50', Ile 54') and residues Thr 80', Pro 81' and Ile 84' in the 80's loop from the other subunit. Residue 50' in the other subunit interacted with similar residues except for Ile 47. PR-IDV differed slightly

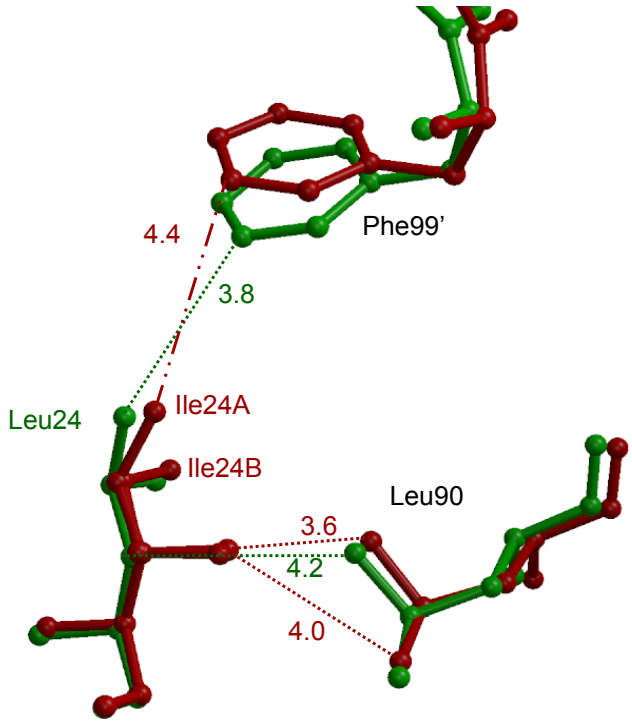
Phe99'
4.4
3.8
Leu24
Ile24A
Ile24B
Leu90
3.6
4.2
4.0

A

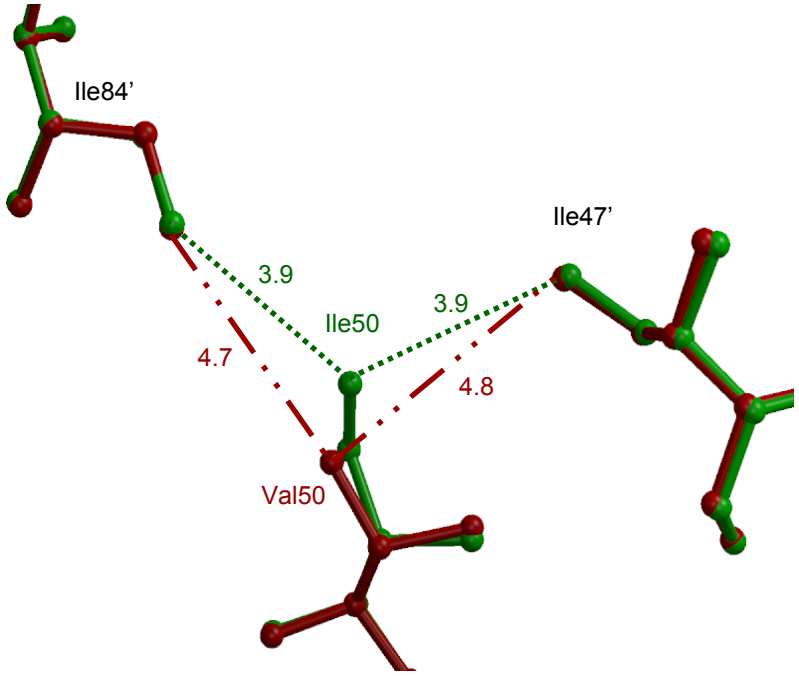
Ile84'
Ile47'
3.9
3.9
Ile50
4.7
4.8
Val50

B

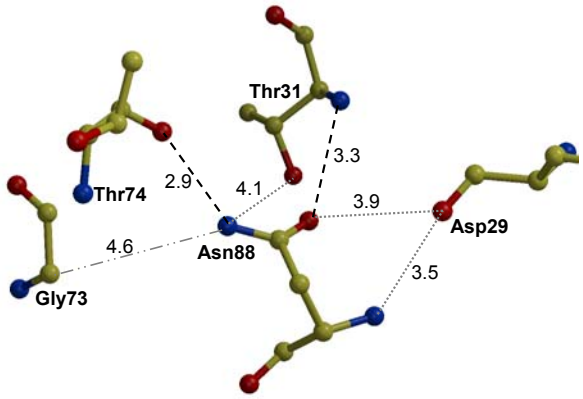

C

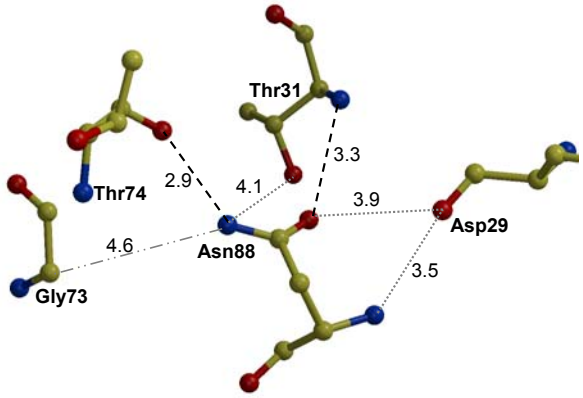

D

Figure 1.5. Structural differences at sites of mutation. Dashed lines indicate hydrogen bond interactions (2.6-3.3Å). Dotted lines indicate van der Waals interactions (3.5-4.2Å). Lines alternating dash and dots indicate distances over 4.2Å. Fig 1.5A. Interactions of Leu/Ile24 with Leu90 and Phe99' in the indinavir complexes. PR is green and PR_{L24I} is red. Figure 1.5B. Interactions of Ile/Leu 50 with Ile 47' and Ile 84' in the complexes with p2/NC. PR is green and PR_{I50V} is red. Figure 1.5C. Interactions of Gly73 with residues 74, 31, 29 and 88 in PR-IDV structure. Figure 1.5D. Interactions of Ser 73 with residues 74, 31, 29 and 88 in the second dimer of PR_{G73S}-IDV crystal structure. The side chain of Ser 73' has two conformations.

from the mutant PR_{I50V}-IDV in the loss of contact of Ile 50 with Thr 80', fewer interactions with Pro 81', more interactions of Ile 50 with 47' and 48', and additional interactions with Gly 49 and 49'. The interactions in the PR-p2/NC structure also showed small differences from the PR_{I50V}-p2/NC structure, such as the improved interactions of Ile 50 with Ile 84' and 47' (Figure 1.5B). Val 50/50' in both PR_{I50V}-IDV and PR_{I50V}-p2/NC had approximately 10 fewer intersubunit contacts than Ile 50/50' in the PR complexes (considering only major conformations). The loss of intersubunit interactions of Val 50/50' compared to those of Ile 50/50' was consistent with the lower stability and higher dimer dissociation constant of PR_{I50V}.

The mutant PR_{G73S} showed two alternate conformations for the side chain of Ser 73 in three of the four subunits in the crystal structure with indinavir (Figure 1.4B). In all four subunits at least one conformation of the Ser side chain hydroxyl formed a new hydrogen bond interaction with the side chain of Asn 88, a hydrogen bond interaction with the amide of Thr74, and new van der Waals contacts with Leu 89 (Figure 1.5C, 1.5D). The side chain of Asn 88 formed conserved hydrogen bond interactions with the carbonyl oxygen and the amide of Thr 74, and van der Waals contact with the carbonyl oxygen of Asp 29 in both mutant and wild type PR structures (Weber 1990). The new interactions of Ser 73 can propagate to the active site via the Asn 88 interaction with Asp 29 and Thr 31, since Asp 29, Asp 30 and Val 32 interacted directly with the substrate or inhibitor. This network of hydrogen bond and van der Waals interactions provides a mechanism for non-active site mutations to transmit energetic effects to the binding site for substrates and inhibitors. Little difference was observed in the inhibitory effect of indinavir on PR_{G73S} compared with

PR, probably because indinavir did not form hydrogen bond interactions with Asp 30, unlike the peptide analogs. Therefore, the new interactions of Ser 73 in PR_{G73S} are likely to be responsible for the observed differences in inhibition by the CA/p2 analog and the relative k_{cat}/K_m values for different substrates.

Protease-Inhibitor Interactions

Generally, the mutants and wild type PR showed similar interactions with inhibitors. Indinavir was bound by a set of 7 direct hydrogen bond interactions to protease residues (Figure 1.6A), as described previously for PR.(Mahalingam 2004) There were also conserved interactions mediated by four distinct water molecules. The mutants showed changes in the hydrogen bond interactions with the pyridyl group of indinavir. In PR_{L24I}-IDV, the major indinavir conformation in PR_{I50V}–IDV, and in the first dimer of PR_{G73S}–IDV, the pyridyl group of indinavir can form a hydrogen bond with the side chain of Arg 8' (Figure 1.6B). A similar interaction was previously observed in the indinavir complex with PR_{L90M} but not for PR and PR_{V82A}(Mahalingam 2004). The pyridyl group of indinavir appeared to have two possible positions, and the side chain of Arg 8' was frequently observed in alternate conformations. Consequently, Indinavir can form a hydrogen bond interaction with Arg 8' when the two groups are close enough. The minor conformations of indinavir in the complexes with PR_{I50V} and PR_{G73S} had lost interactions with Asp 29 and Gly 27. The first dimer of PR_{G73S} had lost interactions via water C, although it is possible that this water was not visible due to the lower resolution of the crystal structure.

The PR interacted with p2/NC substrate analog by 12 direct hydrogen bonds from PR residues Asp 25, Gly 27, Asp 29, Asp 30, and Gly 48 from both subunits that extended from the amide of P3 to the NH2 of P4' (Figure 1.6C). Seven of these interactions involved main chain amides and carbonyl oxygens in both PR and inhibitor, as described previously (Gustchina 1994). Additional PR-p2/NC interactions were mediated by eight water molecules. The highly conserved water 1 that interacted with the flaps and inhibitor was equivalent to water A in the indinavir complexes. Water 2 was structurally equivalent to B in the indinavir complexes, while the others were not in equivalent positions. Water 2 mediated interactions of P3 C=O with Gly 27 and Asp 29, while water 3 had pseudosymmetric interactions with P2' C=O, Gly 27' and Asp 29'. Waters 4-8 interacted with the P3 Thr side chain and with the termini of the inhibitor. The hydrogen bond interactions of PR with p2/NC substrate analog were highly similar in the mutant structures (differences of 0.1 Å or less in length) (Figure 1.6C), with only minor changes in the interactions with water. The hydroxyl of P3 Thr had one interaction with water in PR and two interactions in the mutants, while the P4' NH2 only had one hydrogen bond with water in PR_{I50V}.

Residue 50/50' was the only mutated residue that had direct contacts with inhibitor. Val 50 cannot form the van der Waals interactions of the Ile CD atom with indinavir. The loss of interactions was partially compensated by movement of the PR_{I50V} flaps toward indinavir by 0.4 Å at the Cα atoms of residues 50 and 50'. Both structures of PR_{I50V} showed two alternate conformations for inhibitor and for the side chain of Val 50 in one subunit of the dimer. The presence of alternate conformations clearly increased the number of protease-inhibitor contacts. However, the occupancy

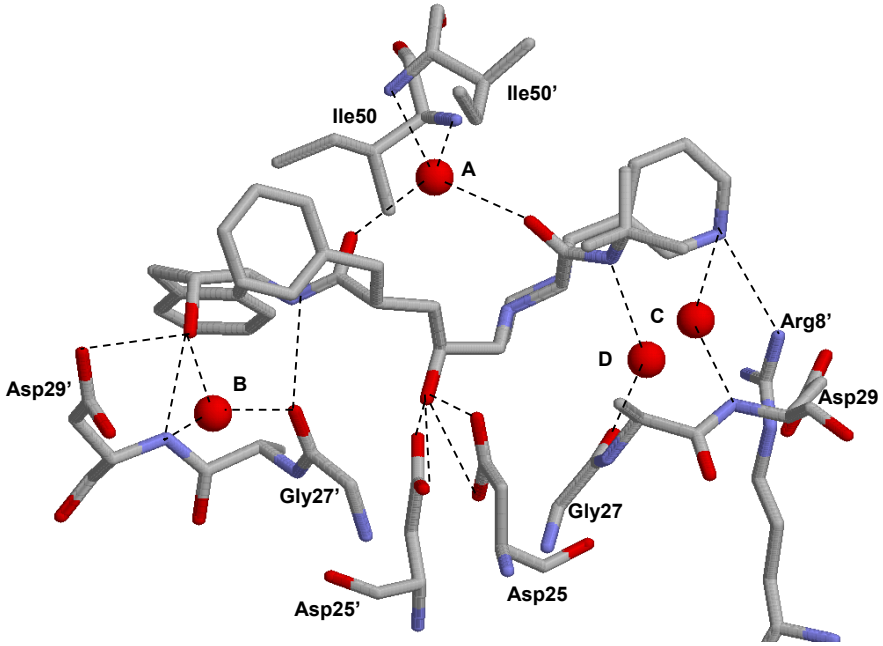
Ile50
Ile50'
A
C
Arg8'
D
Asp29'
B
Asp29
Gly27'
Gly27
Asp25'
Asp25

A

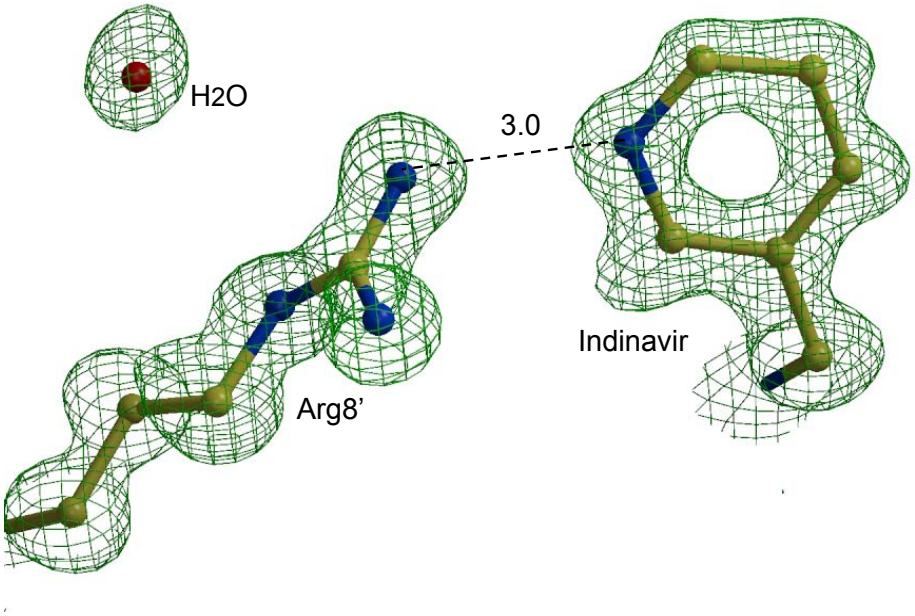
H2O
3.0
Indinavir
Arg8'

B

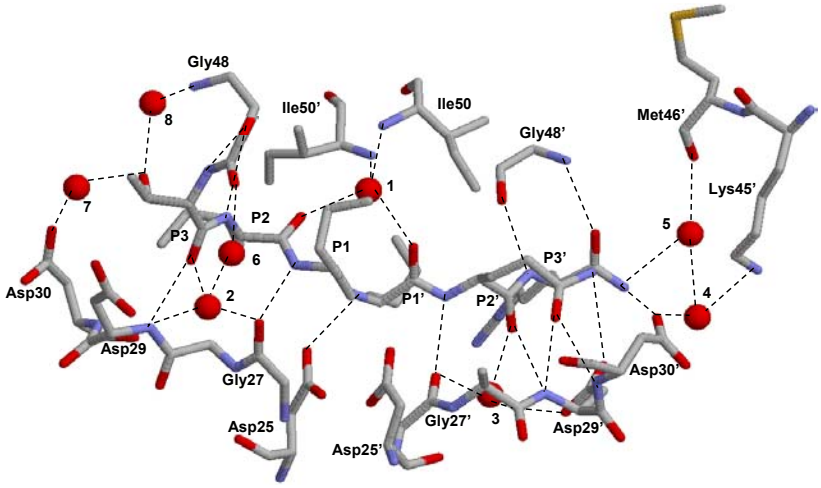

C

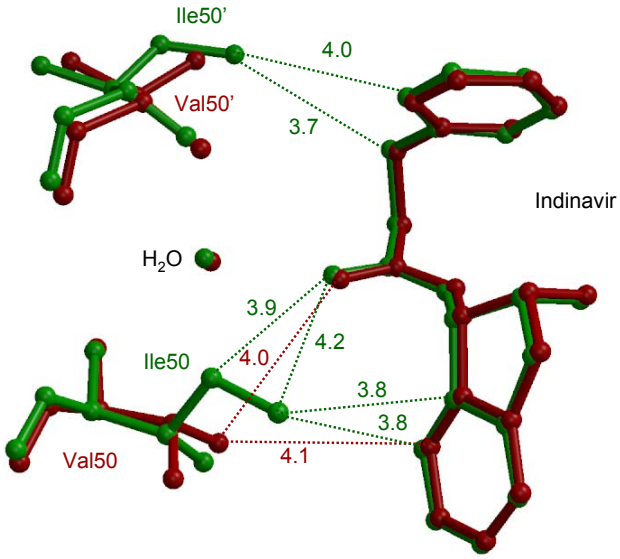

D

Figure 1.6. Protease-inhibitor interactions. Only the residues involved in hydrogen bond interactions are shown. Water molecules are represented as spheres. Hydrogen bonds are indicated by dashed lines. Fig1.6A. PR_{L24I} hydrogen bond interactions with indinavir. Water molecules are labeled A-D. Fig 1.6B. Interactions of Arg 8' in PR_{I50V} –IDV with the pyridyl group of indinavir. The omit map was contoured at 3.5 σ. Fig 1.6C. PR_{L24I} interactions with p2/NC. Water molecules are labeled 1-8. Arg 8 and Arg 8' are omitted for clarity. Fig 1.6D. Selected interactions of the side chains of Ile/Leu 50 and 50' with indinavir in the PR_{I50V} and PR indinavir complexes. PR-IDV is in green and PR_{I50V}–IDV is red. Only the central portion of indinavir is shown with van der Waals contacts indicated by dotted lines with distances in Å.

ratio was 0.8/0.2 for alternate conformations of indinavir, and about 0.7/0.3 for p2/NC and the Val 50/50' side chains. Therefore, the contacts involving major conformations were expected to be more significant. The side chain atoms of Ile 50 and 50' showed 9 van der Waals contacts with indinavir in PR-IDV, while Val 50 and 50' had 5 van der Waals contacts with indinavir for the major conformers. Some differences are illustrated in Figure 1.6D. Similarly, PR-p2/NC showed 6 van der Waals contacts between the side chains of Ile 50 and 50' and the p2/NC, while the mutant had 3 contacts of Val 50 and the major conformer of Val 50' side chains with p2/NC. In both cases the mutant had lost 3-4 contacts with inhibitor, consistent with the increased relative Ki values for PR_{I50V} of 50-fold for indinavir and 20-fold for p2/NC.

Catalytic Sites

The 1.1 Å resolution crystal structures of PR_{L24I}-IDV and PR_{I50V}-IDV showed more asymmetrical interactions between the carboxylate oxygens of the catalytic Asp 25 and 25' and the hydroxyl of indinavir than observed for PR. PR-IDV structure showed interatomic distances of 2.7-2.9 Å, while the mutant structures had two shorter interactions of 2.6-2.7 Å and two longer interactions of 3.0-3.2 Å. The peptide analog did not have a carbonyl group at the catalytic site and there was only one hydrogen bond formed between the amide of P1' and the OD2 of Asp 25, unlike the four possible with the hydroxyl group of indinavir.

Crystal structures of HIV PR-inhibitor complexes at resolution of at least 1.1 Å have shown potential difference density for the hydrogen associated with the

catalytic aspartates (Brynda 2004; Tie 2004). Positive difference density was observed near the catalytic aspartates in the 1.1 Å structure of PR_{L24I} – p2/NC. This difference density was between the two closest inner carboxylate oxygen atoms of Asp 25 and 25' (Figure 1.7). A smaller peak was observed between the Asp 25 and the CH2 of the reduced peptide group after adding hydrogen. The peak representing the proton between the Asp 25 and 25' oxygen atoms in the PR_{L24I} – p2/NC complex was not in exactly the same position as that in the PR_{V82A} - UIC94017 complex (Tie 2004). Therefore, the location of the proton may depend on the chemistry of the inhibitor.

CONCLUSION

Structural changes due to mutations may result in reduced affinity for inhibitor, altered protease activity or stability, and consequently provide resistance to drugs. All three protease variants showed distinct structural changes near the site of mutation and changes in catalytic activity or inhibition relative to wild type protease. The substantially reduced catalytic activity of PR_{L24I} agreed with the sensitive location of the mutation next to the catalytic Asp 25. Although this mutation has been observed in about 10% of patients exposed to indinavir there was only a small (2.6-fold) increase in Ki relative to PR. Hence, the drug resistance is expected to arise from the effect of L24I on reducing catalytic activity and dimer stability, which is consistent with the observed presence of this mutation only in combination with other indinavir-resistant mutations. In contrast, PR_{I50V} exhibited a dramatic 50-fold increase in Ki for indinavir, although this mutation is very rarely observed in isolates

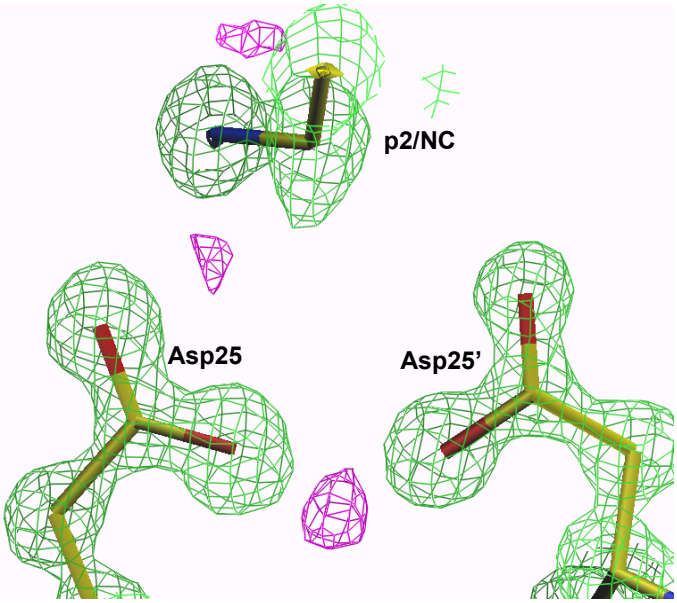

Figure 1.7. The catalytic site of PR_{L24I} – p2/NC at 1.1 Å resolution. The 2Fo-fc map is in green and contoured at 2.6σ and the positive Fo-Fc map is in purple at 3.5σ.

resistant to indinavir. The weaker inhibition appeared to arise from reduced van der Waals interactions of inhibitors with Val 50 in PR_{I50V} compared to Ile 50 in PR. PR_{G73S} was similar to PR in dimer dissociation and inhibition, consistent with the location of residue 73 at the protein surface and far from the active site. Interestingly, Ser 73 in PR_{G73S} formed new hydrogen bond networks that can transmit changes to the substrate binding site consistent with the variation in activity for different substrates. The rarity of this mutation, and its selection in combination with other resistant mutations, are consistent with the relatively minor effects on protease structure and catalysis.

Two of the three mutants PR_{L24I} and PR_{I50V} appeared to have the major effect of reducing intersubunit interactions and increasing dimer dissociation. The subunit-subunit interface in the PR dimer is formed mainly by residues from the N- and C-termini (below the active site), the catalytic residues, and the flaps (above the active site) (Figure 1.1). Increased dimer dissociation was observed for both the PR_{I50V} mutant that reduced the intersubunit interactions of the flaps, and PR_{L24I} that altered intersubunit interactions with the C-terminal residues located at the opposite side of the molecule from the flaps. This analysis has confirmed that drug resistance can arise when mutations alter the PR dimer interface at the flaps or the terminal beta sheet, as well as when mutations directly alter the inhibitor binding site. Furthermore, distal mutations with relatively minor effects can transmit changes to the substrate binding site and contribute to viral resistance.

Chapter Two: Mechanism of Drug Resistance Revealed by the Crystal Structure of the Unliganded HIV-1 Protease with F53L Mutation

(Published: Liu F., Kovalevsky A.Y., Boross P.I., Louis J.M., Harrison R.W., Weber I.T. (2006) *J Mol Biol*. 358(5):1191-9.)

INTRODUCTION

According to Shafer (Shafer 2002) the presence of the flap mutations results in intermediate-to-high-level resistance of the HIV-1 PR to the seven approved PR inhibiting drugs (nelfinavir, saquinavir, indinavir, ritonavir, amprenavir, lopinavir, atazanavir).The F53L mutation has been attributed to the use of the lopinavir/ritonavir treatment regimen. The mutations at positions 46-48, 50, 53 and 54 are the most commonly detected, and usually are accompanied by the mutations at positions 82 and 84 in the inhibitor binding site. Combinations of these mutations arise during the treatment of infected patients with over three PR inhibitors producing multidrug resistant variants of the HIV-1 PR.

In order to fully understand the molecular mechanisms of multidrug resistance it is necessary to analyze structures of both the inhibitor-complexed and uncomplexed HIV-1 PR. Although there are numerous reports on the PR structures complexed with a variety of inhibitors (Rodriguez-Barrios 2004), the structural information on the unliganded PR is extremely scarce. The crystal structures of only the wild-type PR (natural (Lapatto 1989; Navia 1989) and synthetic (Wlodawer 1989)) and a single

multidrug resistant PR variant (Logsdon 2004; Martin 2005) have been determined at the resolutions of 2.7-3Å and 1.30Å, respectively.

Therefore, in this study we have prepared the HIV-1 PR_{F53L} mutant, examined its kinetic properties and obtained a high-resolution X-ray crystal structure of the PR in its unliganded form. The structure is discussed in comparison with the previously reported unliganded PR structures. The crystal structure of the PR_{F53L} mutant is the first uncomplexed HIV-1 protease structure containing a single flap mutation important for drug resistance. It demonstrates that even a single mutation can produce substantial structural changes in the flap region.

RESULTS AND DISCUSSION

PR_{F53L} Showed Altered Kinetics and Stability

The enzyme kinetic parameters were measured and compared to those for wild type PR. PR_{F53L} showed lower catalytic efficiency (k_{cat}/K_M) at 15% of the PR value, due primarily to the ~6-fold increased K_M (K_M = 320±50 μM, k_{cat} = 245±18 min^{-1}, k_{cat}/K_M = 0.77±0.12 $\mu M^{-1} \cdot min^{-1}$ for PR_{F53L} and K_M = 55±7 μM, k_{cat} = 285±10 min^{-1}, k_{cat}/K_M = 5.2±0.2 $\mu M^{-1} \cdot min^{-1}$ for PR) (Mahalingam 2004). The mutant was assayed for inhibition by the clinical inhibitor, indinavir, and two substrate analog inhibitors, CA-p2 and p2-NC, that represent cleavage sites in HIV-1 Gag. PR_{F53L} was inhibited by indinavir with 20-fold higher inhibition constant compared to PR (K_i = 11.1±1.7 nM for PR_{F53L} and K_i = 0.54±0.07 nM for PR). However, the peptide analogs gave slightly better inhibition (0.7 and 0.8-fold) of this mutant relative to the K_i values of 0.075 and 2.2 μM for CA-p2 and p2-NC inhibition, respectively, of PR (Tie 2005).

The stability of PR_{F53L} was assessed using two approaches. Monitoring protease activity as a function of increasing urea concentration indicated that PR_{F53L} was more sensitive to urea denaturation with a transition mid-point value (UC_{50}) of ~ 1.2 M as compared to PR (UC_{50}=1.8 M) (Figure 2.1a). Consistent with this observation a gradual loss in catalytic activity of PR_{F53L}, when monitored as a function of enzyme dilution, was observed below 20 nM, with ~ 50 % decrease at ~5 nM (Figure 2.1b), which represents the apparent dimer dissociation constant (K_D) (Jordan 1992). Under the same conditions (50 mM sodium acetate pH 5, 0.1 M NaCl, 25 °C), wild type PR does not exhibit any loss in catalytic activity. The K_D of PR is expected to be lower than 5 nM, which is the lower limit of the assay.

In summary, PR_{F53L} exhibits significantly lower k_{cat}/K_m than the wild type PR. It is weakly inhibited by indinavir, but shows similar inhibition by substrate analogs as does the wild-type PR. In addition, PR_{F53L} has significantly decreased stability as assessed by urea denaturation and showed increased dimer dissociation relative to PR. Clearly, there is likely to be a correlation between the reduced activity and stability of this flap mutant.

Crystal Structure of Unliganded PR_{F53L}

The crystal structure of PR_{F53L} was determined in its unliganded form at 1.35 Å resolution, which is one of the highest resolution structures reported to date for unliganded PR. The crystallographic statistics are given in Table 2.1. The crystallographic asymmetric unit contains one monomer, and the dimer is constructed by the rotation around the crystallographic 2-fold axis of the $P4_12_12$ space group. The residues are numbered 1-99 and 1'-99' for the asymmetric and symmetry-related PR

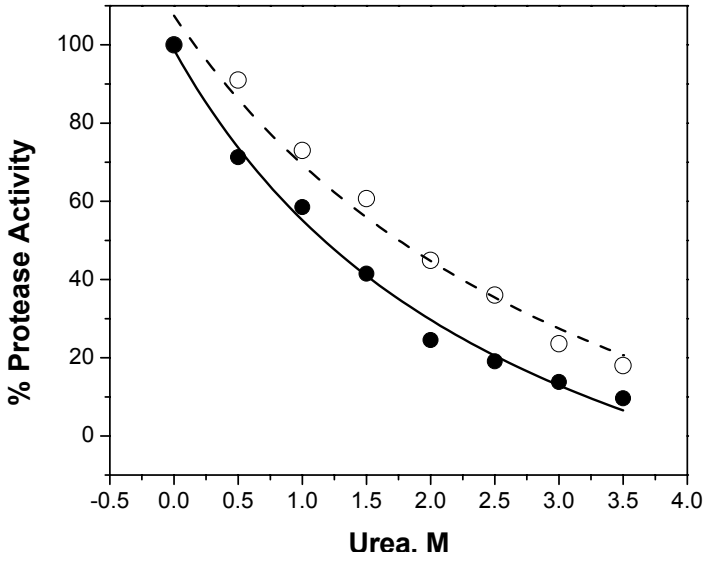

(a)

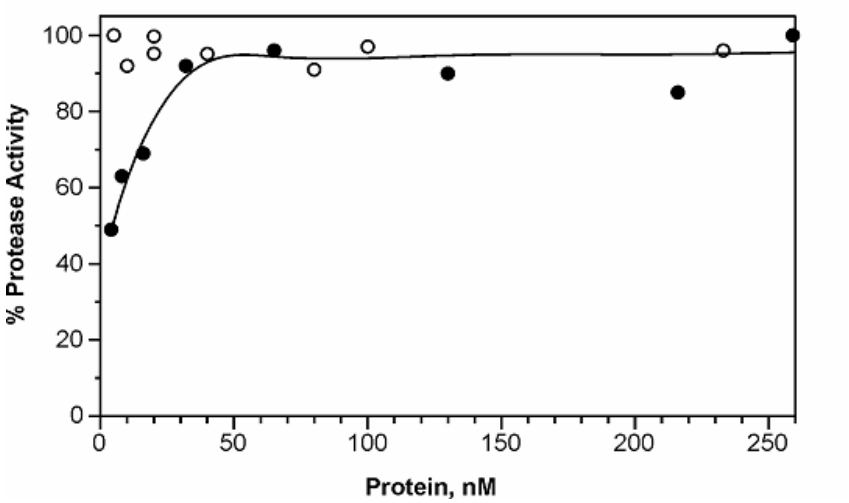

(b)

Figure 2.1. Specific activity as a function of urea concentration (**a**) and the dimeric enzyme concentration (**b**). Black circles and continuous line correpond to data for PR_{F53L}, while open circles and dashed line indicate PR.

Table 2.1. Crystallographic data collection and refinement statistics.

Space group	$P4_12_12$
Unit cell (Å)	60.95, 55.55
Resolution range (Å) (final shell)	50 – 1.35 (1.40 – 1.35)
Unique Reflections (final shell)	22,779 (2166)
Completeness (%) (final shell)	97.3 (95.1)
R_{merge} (%) overall (final shell)	6.8 (56.3)
Data range for refinement (Å)	10 – 1.35
$I/\sigma(I)$ (final shell)	22.2 (2.52)
R_1 ($I > 2\sigma(I)$)	15.5
R_{work}, R_{free} (%)	16.0, 23.4
No. of protein atoms refined	762
No. of solvent (total occupancies)	97 (83)
RMS deviation from ideality:	
Bonds (Å)	0.012
Angle distances (Å)	0.030
Average B-factors ($Å^2$):	
Main chain	26.7
Side chains	33.0
Solvent	44.6

subunits, respectively. The structure was refined using anisotropic atomic displacement parameters (B-factors) for all atoms, including 97 water molecules per asymmetric unit. Water O1050, which forms hydrogen bond interactions with the catalytic Asp25, has a unique position in the structure since it is located on the crystallographic 2-fold axis, and therefore equidistant from both Asp25 and Asp25' in the crystallographic dimer. Hydrogen atoms were added at the last stages of the refinement. The PR showed good electron density for almost all of the non-hydrogen atoms, except for several side chain atoms of Ile50 in the flexible tip of the flap (Figure 2.2a). The average B factors for all residues were calculated to be ~27Å^2 and ~33Å^2 for the main chain and side chain atoms, respectively. The average B factor for flap residues 45-56 was ~32 Å^2 and ~39Å^2 for main chain and side chain atoms, respectively, the values being very similar to the overall values. Alternate conformations were modeled for the side chains of Arg8 and Met46. The electron density for the mutation site at position 53 unequivocally showed the leucine side chain (Figure 2.2b). No electron density for inhibitor was observed in the binding site, although indinavir was present in the crystallization drops. Numerous attempts to crystallize PR_{F53L} in complex with various inhibitors (indinavir, TMC114, DMP323) were not successful in yielding crystals.

Structural Differences between Unliganded PR_{F53L} and the Unliganded PR_{WT}.

The unliganded structures of PR_{F53L} and PR (PDB code 1HHP) were compared to determine the differences due to the F53L mutation. PR_{F53L} differs in its sequence at 6 positions compared to PR. In addition to the drug resistant mutation

F53L, the mutations Q7K, L33I and L63I were introduced to significantly restrict auto-proteolysis and C67A and C95A to avoid aggregation due to cysteine-thiol oxidation of PR. These optimizing mutations did not alter the overall solution structure, stability or the catalytic activity of PR(Ishima 1999; Louis 1999). The overall RMS deviation of the main chain atoms was only 0.44 Å, a seemingly insignificant difference. However, the analysis of the conformational differences in the two structures demonstrated considerable disparity in the flap region, particularly, for the tips of the flaps (Figure 2.3a, 2.3b).

The deviation of the main chain atoms for the flap residues 48-54 was 0.8-2.5 Å from the corresponding atoms in PR, with the largest shift at Ile50. This shift resulted in a greater separation of the tips of the two flaps of PR_{F53L} dimer than in the wild type structure, although the overall conformation of the main chain remained very similar (Figure 2.3b). Such mutual reorientation of the symmetry-related flaps in the mutant opens up a channel with the closest inter-flap distance of 6.3 Å as measured between the carbonyl oxygen atoms of Gly51 and Gly51' (Figure 2.3c). Interestingly, however, no well-defined solvent molecules were visible in the 6Å-wide channel.

In contrast, in PR the tips of the flaps are much closer together (Figure 3b and 3d) and show both hydrophobic and hydrophilic interactions between each other. An unconventional C-H…O hydrogen bond Ile50 CD1…Gly49' O of 3.00 Å is present, which is supported by the hydrophobic interaction Ile50 CD1…Gly48' C_α of 3.7 Å (Figure 2.4).

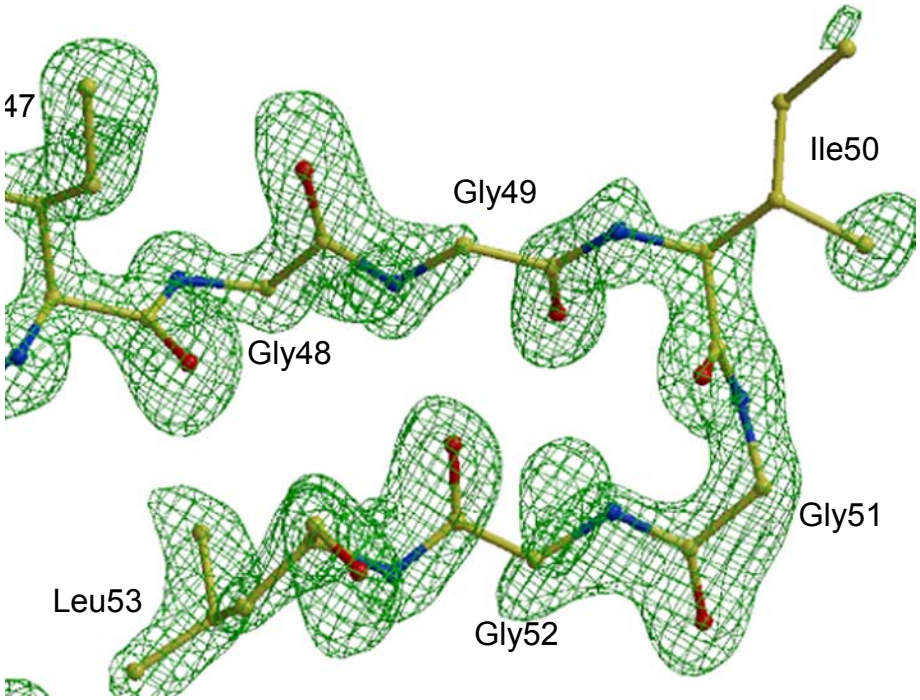

(a)

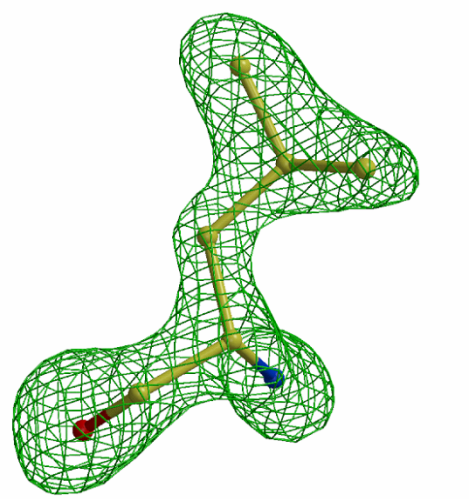

(b)

Figure 2.2 (a) The F_o-F_c omit map for residues 47 through 53 in the flap region of PR_{F53L} contoured at 2.6σ. **(b)** F_o-F_c omit map for residue 53 in PR_{F53L}, contoured at 2.7σ, unambiguously shows leucine. Figures were made with Bobscript (Esnouf 1997; Esnouf 1999).

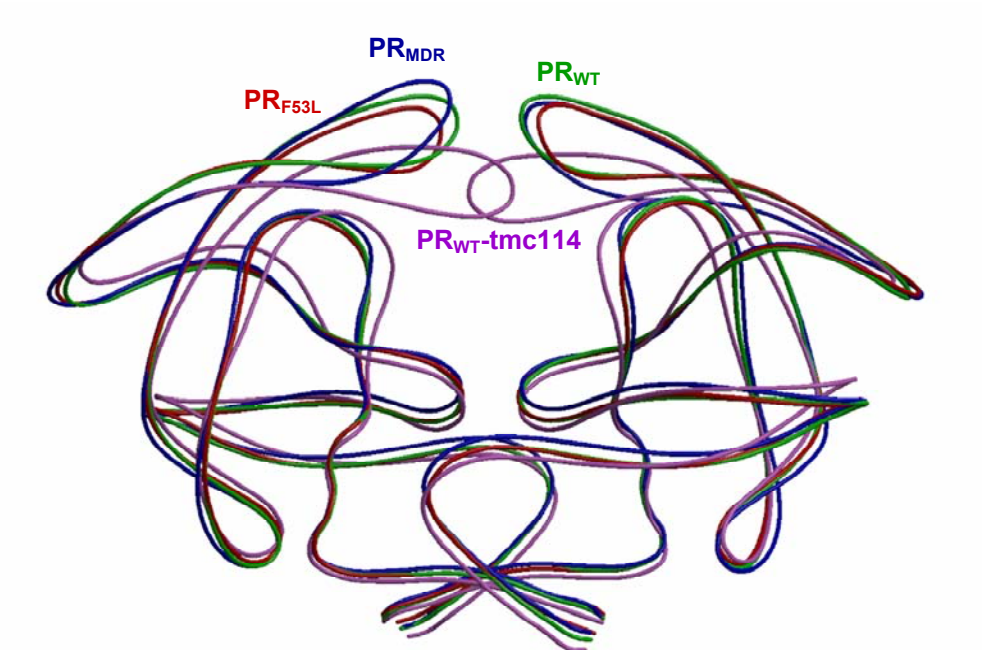
PRMDR
PRWT
PRF53L
PRWT-tmc114

(a)

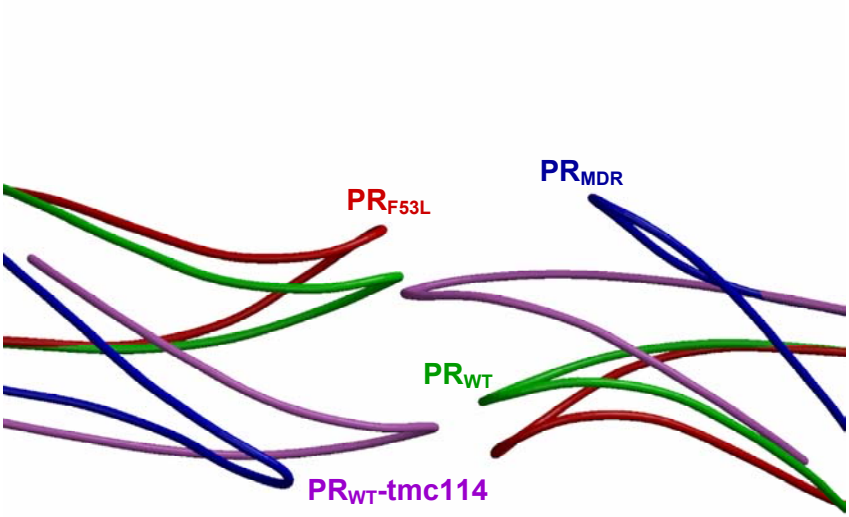
PRMDR
PRF53L
PRWT
PRWT-tmc114

(b)

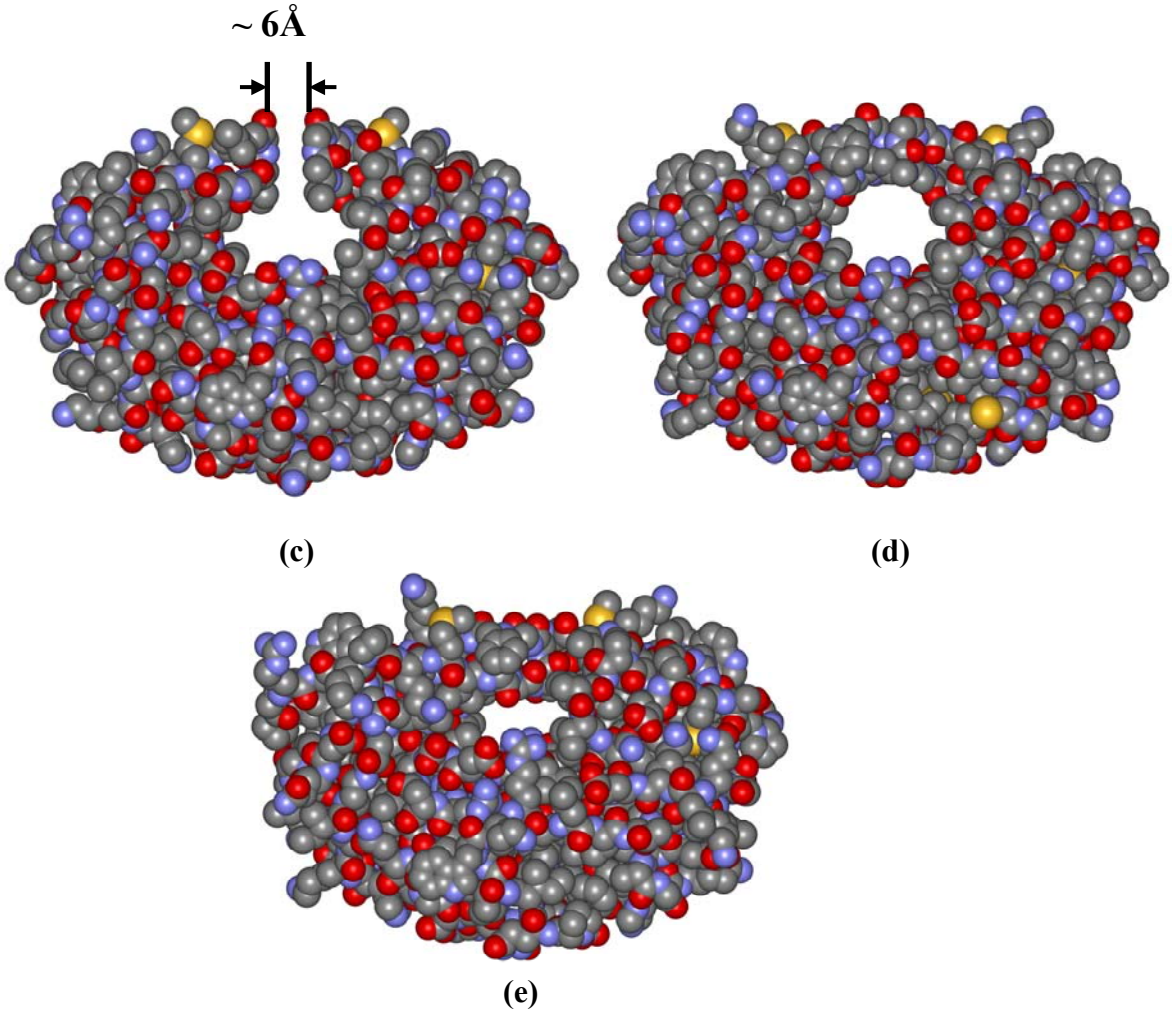

Figure 2.3. **(a)** Superposition of unliganded PR, PR_{F53L}, PR_{MDR}, and TMC114-complexed PR structures. **(b)** Superposition of residues 45-56 and 45'-56' in the flaps of unliganded PR, PR_{F53L}, PR_{MDR}, and PR_{WT}-tmc114 structures. PR_{F53L} is in red, PR in green, PR_{MDR} in blue and inhibitor-complexed PR_{WT} in pink. The F53L mutant structure was compared with the wild type structures and the MDR mutant protease by superimposing their main chain atoms using ALIGN (Cohen 1997). **(c)** Space-filling representations of the protease dimers showing a 6 Å separation between the tips of the flaps in PR_{F53L}, **(d)** the unliganded PR and **(e)** PR_{WT}-tmc114 with the inhibitor omitted for clarity. Figures were made using Bobscript (Esnouf 1997; Esnouf 1999) and WebLabViewer (Molecular Simulations Inc).

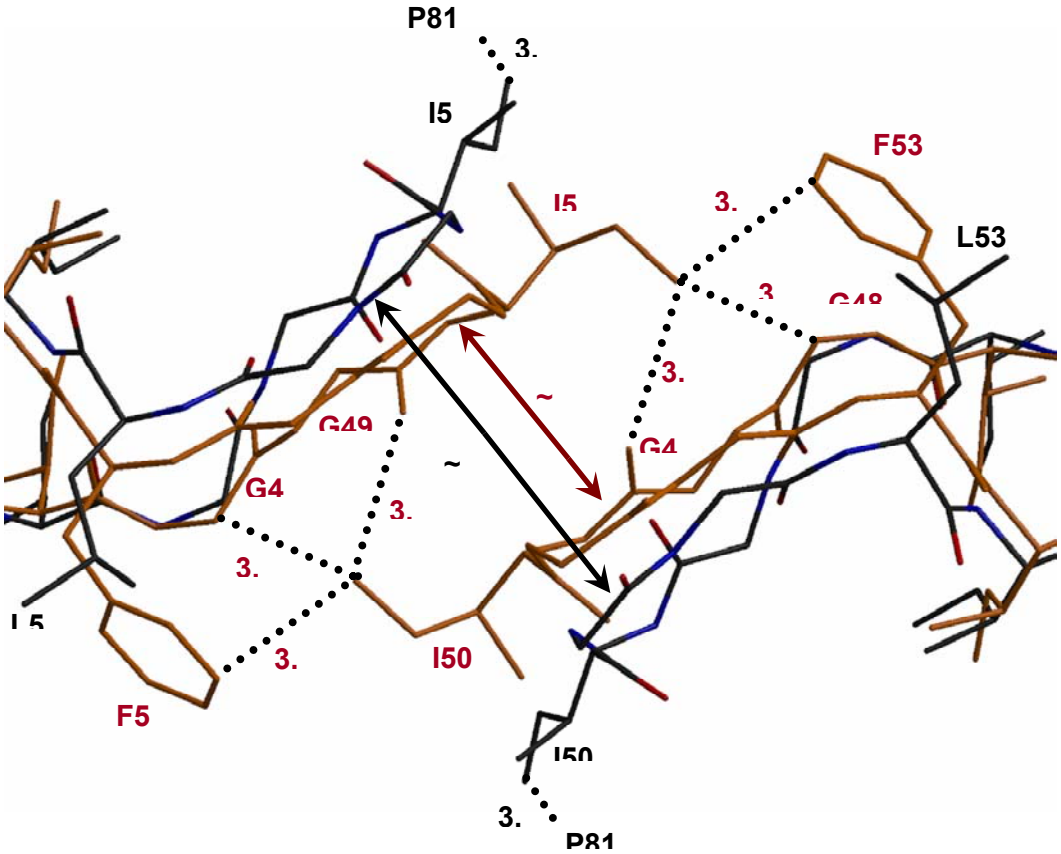

Figure 2.4. Comparison of inter-flap interactions in unliganded PR_{F53L} and unliganded PR structures. PR_{F53L} is colored by atom type; PR is in orange. Figure was made with Bobscript (Esnouf 1997; Esnouf 1999).

The other major difference between PR_{F53L} and PR is the absence of the large phenyl ring of phenylalanine in the former due to the mutation. The large aromatic ring is known to favor strong hydrophobic interactions, for instance, C-H…π interactions. In the wild-type structure the aromatic carbon atoms of Phe53 are in close contact with the Ile50' CD1 atom, and the closest intermolecular distance is just 3.4 Å (Figure 2.4). Moreover, the orientation of the terminal CH_3 group of Ile50 and the phenyl ring is such that they close the narrow flap-to-flap channel from both sides. By mutating residue 53 to the smaller non-aromatic leucine, which can only participate in much less energetically favorable C-H…H-C interactions, those C-H…π contacts are eliminated completely. Unlike in PR, where the terminal methyl group of Ile50 is directed into the space between the tips of the flaps, in PR_{F53L} it is pointed away from the wide channel towards the protein surface, making only weak hydrophobic interactions with Pro81 carbon atoms of ~ 3.9 Å. Furthermore, the side chain of Leu53 is directed into the channel between the flaps, and does not make any intermolecular interactions (Figure 2.4).

Therefore, we can speculate that the C-H…π interactions found between the aromatic carbon atoms of Phe53 and the terminal methyl group of Ile50' are essential to stabilize the conformation observed in PR. These contacts are absent in the mutant PR_{F53L}, which is likely to make the flap more conformationally flexible. The increased flexibility of the flaps could thus preclude the formation of PR_{F53L} complex with indinavir, despite its presence in solution during the crystal growth.

Structural Differences between Unliganded PR_{F53L} and Liganded PR_{WT}

The unliganded PR_{F53L} was compared with a wild-type PR complexed with an inhibitor to investigate the conformational change due to ligand binding. Our structure of PR_{WT}-tmc114 (PDB code 1S6G) was chosen for this comparison (Tie 2004). PR_{WT}-tmc114 contains the second generation antiviral inhibitor TMC114. The choice was also motivated by the fact that the two proteins have the same amino acid sequence, except for the primary mutation F53L.

The overall RMS deviation of the main chain atoms for PR_{F53L} and PR_{WT}-tmc114 was 2.27 Å. As expected the active site triad Asp25-Thr26-Gly27 had a very similar orientation in both structures. The Asp25 carboxyl groups in PR_{F53L} were shifted by just 0.6 Å into the active site cleft compared to their positions in PR_{WT}-tmc114. On the other hand, substantial differences were observed for the conformations of the flaps (residues 45-55) (Figure 2.3a and 2.3b) and of residues 79-82. The tips of the flaps in the wild type inhibitor-complexed structure were shifted by as much as 8.3 Å from their positions in the unliganded structure in order to close the active site cavity and embrace the inhibitor (Figure 2.3e). Moreover, in the PR_{F53L} structure the loop of residues 79-82 (the 80's loop) was about 2-2.5 Å away from the position in the wild type molecule, and the 80's loop changes in cooperation with the flap to open up the active site cavity even further. Molecular dynamics simulations (Ridky 1998) on the unliganded PR have suggested that the closed conformation of the flap observed in inhibitor-complexed structures is less favorable than the more open conformation found in PR_{F53L} and PR structures. Recent simulations by Meagher and Carlson (Meagher 2005) have strongly supported the

previous results. They concluded that the "semi-open" form of the unliganded PR is indeed a stable conformation and is not biased by the crystal packing effects.

Structural Variations between Unliganded PR_{F53L} and Unliganded PR_{MDR}.

Our unliganded structure of PR_{F53L} was compared with the unliganded structure of PR_{MDR} (PDB code 1TW7), which is a multi-drug resistant variant of HIV-1 PR (Martin 2005). These two proteins differ in amino acid sequence in several positions besides the F53L mutation. PR_{MDR} has ten mutations associated with drug resistance (L10I, M36V, S37N, M46L, I54V, I62V, A71V, V82A, I84V, L90M), and the inactivating D25N mutation. Furthermore, unlike PR_{F53L}, it does not bear the optimizing mutations of residues 7, 33, 63, 67, and 95. In contrast to PR_{F53L}, the PR_{MDR} mutant crystallized in $P4_1$ space group, with a dimer in the asymmetric unit. The comparison of the two structures showed an RMS deviation of the main chain atoms of 1.0 Å, which is in between the values for comparison of PR_{F53L} with PR and PR_{WT}-tmc114. Similar to the trend observed in case of comparing with PR_{WT}-tmc114, the largest variations are found for the flaps (residues 43-56) (Figure 2.3a and 2.3b), residues 35-38 and 79-82. The different conformations of residues 35-38 (RMS deviations are 1.0-2.0 Å, the largest values are at positions 35 and 37) can be explained by the S37N mutation present in PR_{MDR}. The longer side chains of the Asn37 and Asn37' form water-mediated interactions with the side chain nitrogens of Arg57 and Arg57', respectively. This interaction is unattainable for the shorter side chain of serine in PR_{F53L}. Ser37, therefore, has the opposite orientation, away from the protein surface.

The major difference in the geometries of the two molecules is in the mutual orientation of their flaps (Figure 2.3b). The flaps' orientation in PR_{MDR} is such that the active site cavity is even more open than in PR_{F53L}. The geometry can thus be regarded as "quasi-open" conformation, since the flaps are not yet opened enough for entry of a substrate or inhibitor. The mutual conformation of the flaps in the PR_{MDR} mutant can be viewed as if the flaps were simply moved away from each other from their position in the complexed structure to a separation of about 10 Å. Although there are several water molecules around the flaps' tips, such a large separation does not allow any water-mediated contacts between the flaps.

The orientation of the flaps' tips for both PR_{F53L} and PR_{MDR} leads to their proximity to residues in the 80's loop. In the PR_{MDR} structure, the terminal CH_3 groups of Ile50 and Ile50' have strong van der Waals contacts of 3.6 Å with one of the carbon atoms of Pro81' or Pro80, respectively. As mentioned above, similar C-H…H-C interaction in the PR_{F53L} structure has the distance of 3.9 Å and therefore might be slightly weaker. These interactions result in a slight movement of the 80's loop away from the active site cavity for PR_{F53L} compared to its position in the PR_{MDR}.

It has to be emphasized that different crystallization conditions were used for obtaining the crystals of unliganded PR_{F53L}, PR_{MDR} and PR. The three structures have different unit cells and therefore the protease molecules are packed in a different fashion, having disparate intermolecular interactions. Although the conformation of the flap region observed in PR_{F53L} is very plausibly due to the mutation, a partial effect of the crystal packing on the flap's geometry cannot be ruled out for these structures.

Implications for the Mechanism of Drug Resistance.

Drug resistant mutations in PR have been classified structurally as active site and non-active site, depending on whether they are located on the inside or the outside of the active site cavity (Erickson 1996). Additionally, these mutations are designated as "major" or "minor" mutations depending on whether they appear to have a major effect on phenotypic and clinical resistance or play an accessory role. Several molecular mechanisms have been described previously for drug resistant PR mutants. Major active site mutations have been shown to directly alter PR interactions with inhibitor and/or substrate analogs and consequently reduce the affinity for inhibitor (Erickson 1996; Hong 2000; Clemente 2004; Logsdon 2004). Non-active site mutations were observed to alter interactions with the catalytic Asp25, or the dimer interface (Xie 1999; Clemente 2004); these mutations can alter catalytic efficiency or PR stability.

The F53L mutation of the HIV-1 PR occurs in 5-10% isolates from patients treated with indinavir, saquinavir, lopinavir, atazanavir, or more than one PR inhibitor, and it is always accompanied by other resistant mutations (Shafer 2002; Wu 2003). Consequently, the F53L mutation is classified as a non-active site minor mutation. Interestingly, no crystal structures have been reported previously of the PR with the single F53L mutation, although Heaslet *et al.* reported two inhibitor-complexed HIV-1 PR structures that contain multiple mutations including F53L (Heaslet 2006). In inhibitor-complexed PR structures without the F53L mutation, both Phe53 and Phe53' side chains have conserved conformations directed away from the active site

and interacting closely only with the neighboring Gly48 or Gly48' of the same flap (Brynda 2004). However, in the unliganded wild type PR the two symmetric Phe53 residues play a major role in stabilizing the "semi-open" conformation of the flaps by means of the C-H…π interactions with the methyl groups of Ile50 and Ile50' (Figure 2.4). The substitution of the Phe53 by Leu eliminates these attractive interactions, although no new intramolecular contacts are formed. Thus, we theorize that the absence of such stabilizing short contacts produces more conformationally flexible flaps, especially at the tips. It was suggested previously that the hydrophobicity of Phe53 side chain was important for the capture of substrates and inhibitors (Shao 1997). According to the solution NMR experiments the very tips of the flaps are in a rapid conformational exchange on the order of nanoseconds, while the residues 48-55 move to open and close the active site on the order of ~ 100 μs (Ishima 1999). An approaching substrate or inhibitor can interact with the Phe53 aromatic ring and assist with the flap opening. In PR_{F53L} the flap might move significantly faster than in the wild type PR. Furthermore, a substrate or inhibitor would have much weaker interactions with Leu53 than with Phe. Thus, this mutant can hamper binding of a substrate or inhibitor. Accordingly, the drug resistance associated with F53L mutation can be attributed to the additional mobility of the PR flaps due to the loss of attractive interactions with residue 53. Therefore, we propose that the F53L mutation introduces a distinct mechanism for drug resistance.

Protein Data Bank Accession Code

The coordinates and structure factors have been deposited in the RCSB Protein Data Bank with accession code 2G6B

Chapter Three: Ultra-high Resolution Crystal Structure of HIV-1 Protease Mutant Reveals Two Binding Sites for Clinical Inhibitor TMC114

(Published: Kovalevsky A.Y., Liu F., Leshchenko, S., Ghosh A.K., Louis J.M., Harrison R.W., Weber I.T. (2006) *J Mol Biol*. 363:161-173)

INTRODUCTION

TMC114 (darunavir) is an exceedingly potent antiviral agent designed to inhibit HIV-1 PR by binding at its active site (Ghosh 1998). It is highly effective against various subtypes of HIV-1, including many drug resistant strains (Koh 2003; De Meyer 2005), Recently, it was approved by the FDA for treatment of drug resistant HIV. TMC114 is a non-peptidic transition-state analog, with the chemical structure as shown below. It differs from its closest chemical analog, amprenavir, by the presence of the bis-THF moiety (Wlodawer 1998).

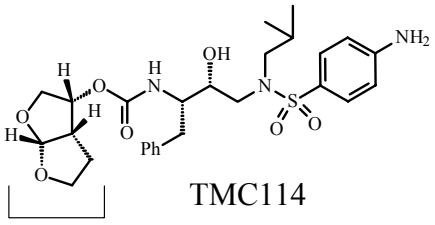

TMC114

The design rationale was to increase the number of favorable interactions with main chain atoms of PR. This objective has been achieved as evidenced by crystallographic studies on wild type PR and mutant complexes with TMC114 (King 2004; Tie 2004) and by quantum chemical calculations of interaction energies of TMC114, amprenavir, or nelfinavir with wild type PR (Nivesanond 2005).

No TMC114-specific resistant mutations in PR have been reported to date, so our approach has been to study PR mutants with a single substitution mutation that renders resistance to the other clinical inhibitors. Recently, we reported the analysis of TMC114 complexes with PR containing single multi-drug resistant mutations D30N, I50V, V82A, I84V and L90M (Tie 2004; Kovalevsky 2006). TMC114 adapted to the PR structural changes due to V82A and I84V mutations, with the K_i values increasing by no more than four times. In the case of PR_{L90M} TMC114 had even better inhibition than for the wild type enzyme. On the other hand, TMC114 exhibited less effective inhibition of PR_{D30N} and PR_{I50V}, where the K_i values were increased 12-17 times compared to the value for the wild type PR (Kovalevsky 2006).

Here, we focus on the multi-drug resistant mutations V32I and M46L (Wu 2003). The mutation V32I is observed in about 20% of isolates from patients treated with amprenavir, in 3-6% of patients treated with ritonavir, lopinavir, atazanavir and indinavir, and in about 4% of those on a multi-PI regimen (Wu 2003). It confers intermediate level resistance to amprenavir, ritonavir and indinavir. The mutation M46L is selected for resistance to seven of the eight FDA approved clinical PIs, and is a major mutation arising during treatment with indinavir (Johnson 2005). Structurally, V32I alters a residue in the substrate-binding site and can directly contribute to the drug resistance by unfavorable interactions with an inhibitor because isoleucine is larger than valine. Conversely, M46L alters a residue in the flexible PR flap (residues 43-58) and is not in direct contact with an inhibitor bound in the active-site cavity, although the main-chain atoms of Met46 form hydrogen bonds with substrate analogs (Tie 2005). The active dimer of HIV-1 PR employs the two flaps to

enclose the substrate or inhibitor within the active-site cleft. The PR flap is believed to be essential for substrate or inhibitor recognition and delivery to the active site (Shao 1997). Hence, the M46L mutation can influence the binding of inhibitor indirectly either by reducing the hydrophobic interactions during the binding process, or by strengthening interactions with a substrate.

We describe crystallographic analysis of the effects of TMC114 on mutants PR_{V32I} and PR_{M46L}. The crystal structures have been determined at 0.84Å and 1.22Å resolution for PR_{V32I}-TMC114 and PR_{M46L}-TMC114 complexes, respectively. The first ultra-high resolution structure of a PR-inhibitor complex showed two molecular species at 60% and 40% occupancy. The higher occupancy conformer has TMC114 bound at two distinct sites: the active site cavity and a second, new site on the surface of one of the flaps, while the lower occupancy conformer showed TMC114 only in the active site cavity. These results suggest an alternative mechanism for the effectiveness of TMC114 against many clinical drug resistant isolates of HIV-1 and may provide a distinct target for the design of novel inhibitors that bind to the second site on the flap.

RESULTS

Crystallographic analysis

The crystal structures of PR_{V32I} and PR_{M46L} drug resistant mutants complexed with the inhibitor TMC114 were solved in the space group $P2_12_12_1$ as summarized in Table 1. The asymmetric units contain the PR dimer and the residues in the two subunits are labeled 1-99 and 1'-99' (Figure 3.1a). The crystals diffracted to the ultra-high resolution of 0.84 Å for PR_{V32I}-TMC114 and near-atomic resolution (1.22

Å) for PR_{M46L}-TMC114. The final R-factors are 11.7% and 13.1% for PR_{V32I}-TMC114 and PR_{M46L}-TMC114, respectively. There was clear electron density for all atoms of the protease, the inhibitor and solvent molecules in the two structures. The $2F_O$-F_C electron density map had distinct peaks for each non-hydrogen atom in the ultra-high resolution structure of PR_{V32I}-TMC114, whereas the near-atomic resolution structure showed lower, less distinct peaks for atoms (Figure 3.1b and 3.1c). The average atomic B-factor values were approximately two-fold lower for the PR_{V32I}-TMC114 complex (Table 3.1) indicating the higher accuracy of atomic positions for this structure. The high resolution of the diffraction data allowed modeling of two shells of solvent, including more than 200 water molecules, chloride anions and dimethylsulfoxide (DMSO) molecules.

Of particular interest is the fact that TMC114 is found not only inside the active-site cleft, as observed in other structures (King 2004; Surleraux 2005; Kovalevsky 2006), but also on the protein surface in the flap region (Figure 3.1a and 3.1d). The inhibitor bound in the active site of PR_{V32I}-TMC114 and PR_{M46L}-TMC114 structures has two alternate conformations related by a 180° rotation and occupancies of 60/40%. TMC114 shares the second surface binding site with the solvent DMSO molecule, with the occupancies refined to 60 and 40%, respectively. Remarkably, TMC114 has different configurations when bound on the surface and in the active-site cavity. The amide nitrogen of the sulfonamide moiety has a pyramidal configuration and is chiral due to the presence of three chemically different

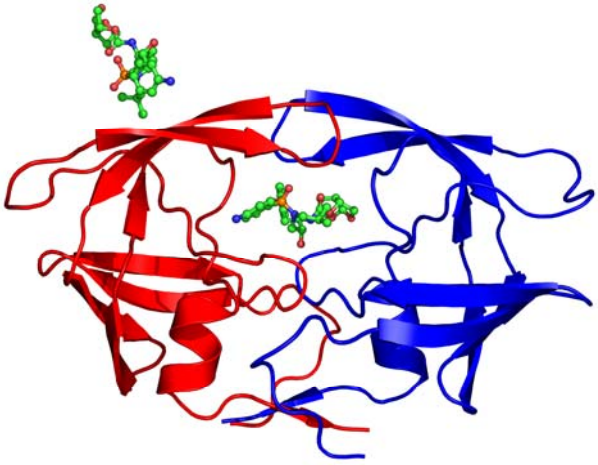

(a)

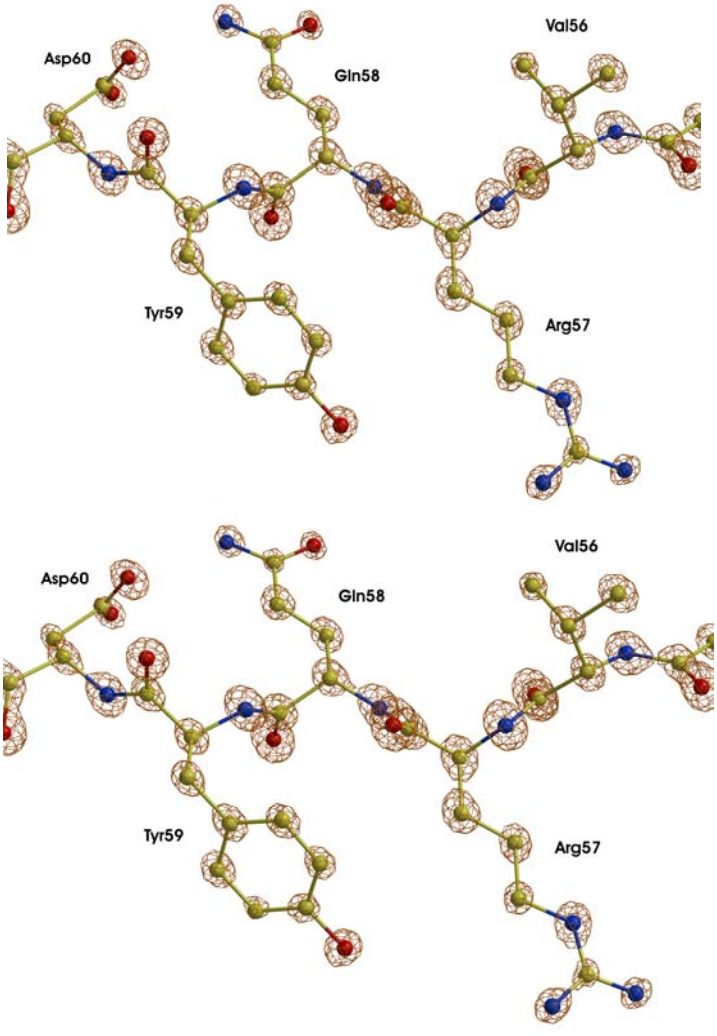
Asp60
Gln58
Val56
Tyr59
Arg57
Asp60
Gln58
Val56
Tyr59
Arg57

(b)

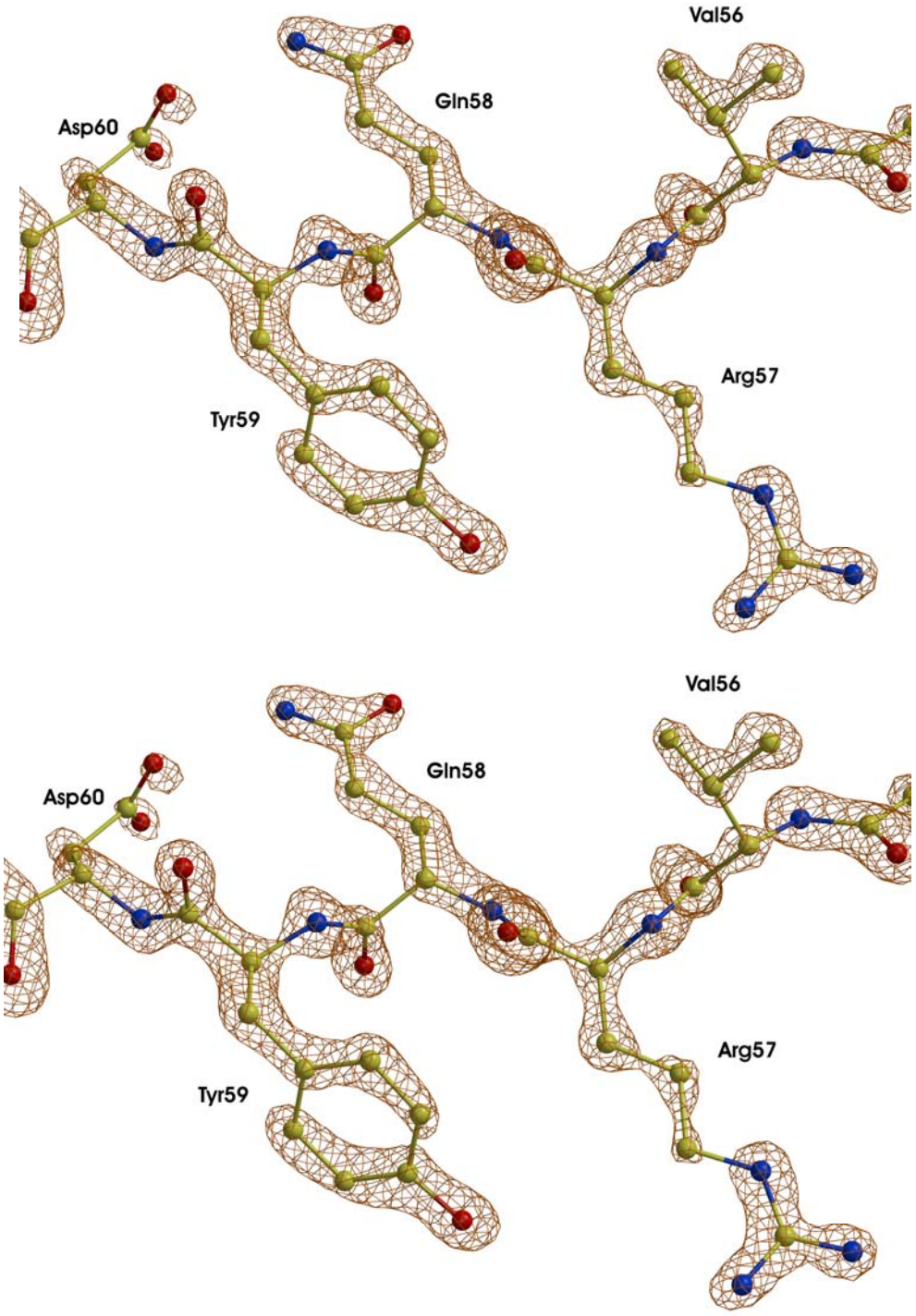
Val56
Gln58
Asp60
Arg57
Tyr59
Val56
Gln58
Asp60
Arg57
Tyr59

(c)

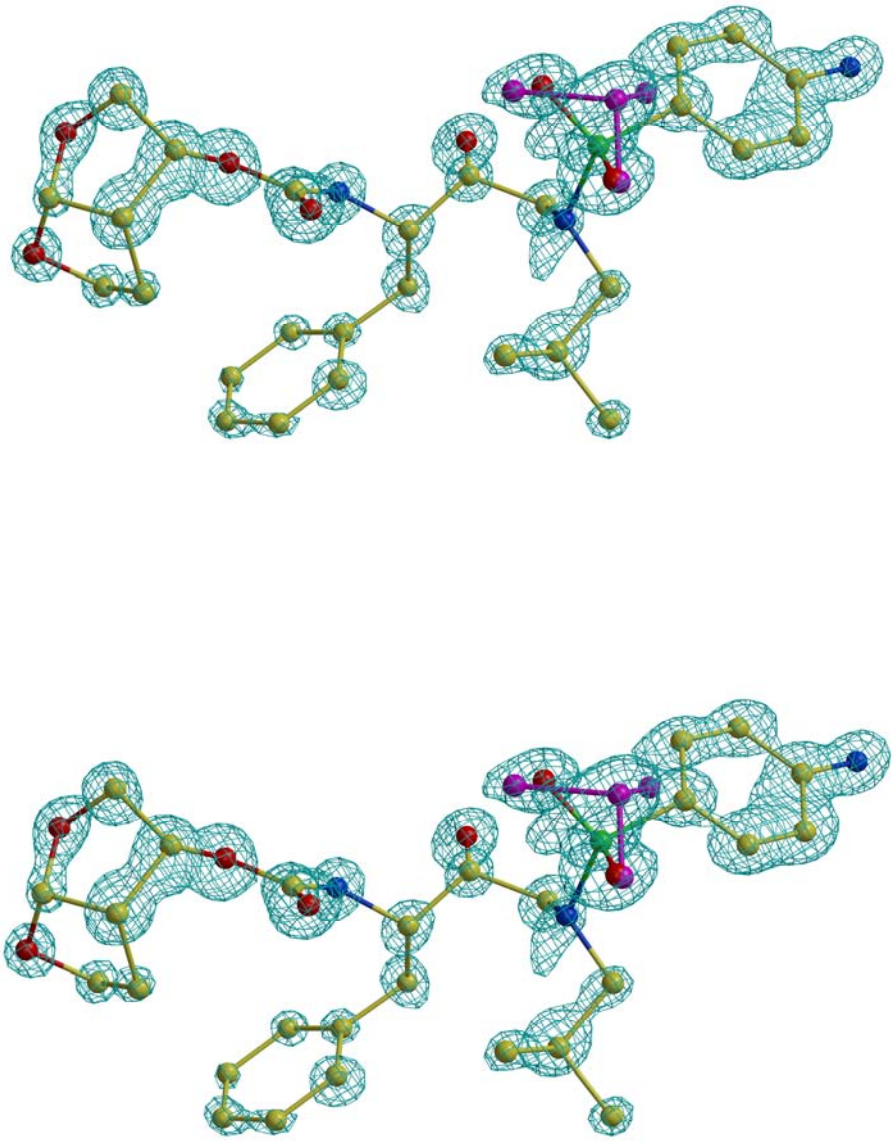

(d)

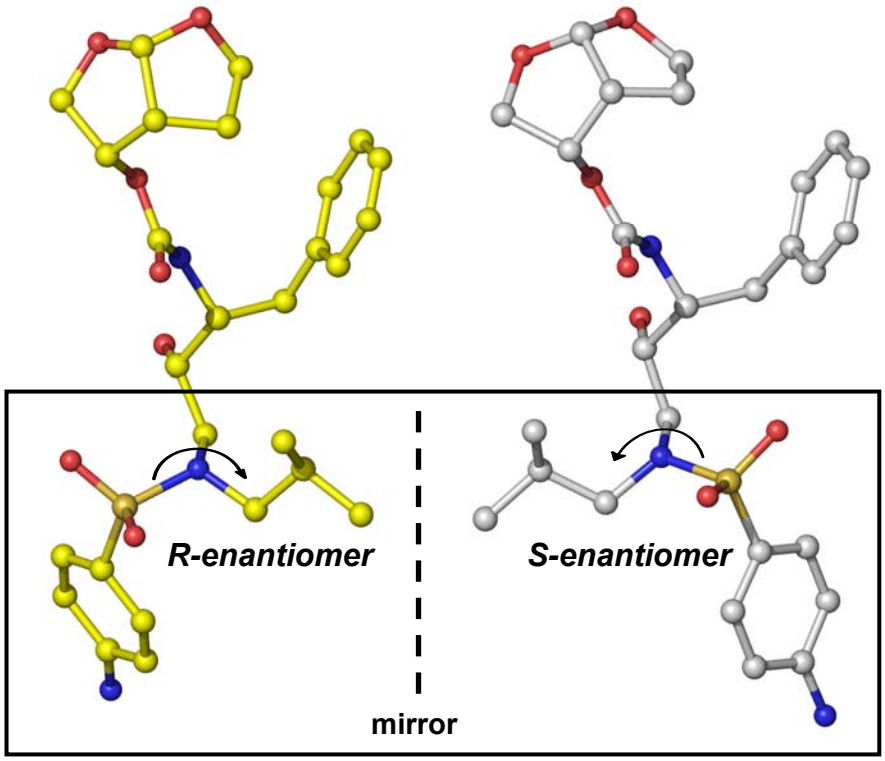

(e)

Figure 3.1 **(a)** – PR dimer structure. Two subunits (in red and blue) are drawn indicating the secondary structure. TMC114 is in ball-and-stick representation and is colored by atom type, and is bound in two sites as revealed in PR_{V32I} and PR_{M46L} structures. **(b)** and **(c)** – stereoview of the electron density ($2F_O$-F_C) for residues 55-60 in the PR_{V32I} and PR_{M46L} structures. Contour levels are 3.6σ for (**b**) and 2.4σ for (**c**). **(d)** – stereoview of the $2F_O$-F_C electron density for TMC114 bound to the flap in PR_{V32I}, drawn at 1.8σ. TMC114 has 60% occupancy, while the other 40% correspond to DMSO solvent molecule, depicted in magenta. **(e)** – the structures of TMC114 bound in the active site cavity (*R*-enantiomer) and in the flap region (*S*-enantiomer). The moieties in the box are related by reflection in a mirror and can be obtained by the sulfonamide nitrogen inversion.

Table 3.1. Data collection and refinement statistics for PR_{V32I} and PR_{M46L} in complex with TMC114.

	PR_{V32I}	PR_{M46L}
Data collection		
Space group	P 2_1 2_1 2_1	P 2_1 2_1 2_1
Unit cell dimensions		
a, b, c (Å)	28.70, 65.92, 92.53	28.9, 66.6, 93.1
Resolution Range (Å)	50–0.84 (0.87-0.84)[§]	50–1.22 (1.26–1.22)[§]
Unique reflections (obsvd. with I>2σ(I))	153847 (131172)	50541 (42888)
I / σ(I)	45.3 (2.0)	20.0 (3.1)
R_{merge} (%)	6.3 (35.8)	9.9 (31.9)
Completeness (%)	95.9 (63.3)	93.0 (73.2)
Refinement		
Data range for refinement (Å)	20–0.84	10–1.22
R_1 (I > 2σ(I))	11.7	13.1
R_{work} (%)	12.4	14.0
R_{free} (%)	14.8	19.6
No. of solvent molecules	258	212
No. of obsvd. reflections/No. of refined paramts.	6.6	2.5
RMS deviation from ideality:		
Bonds (Å)	0.018	0.013
Angle distance (Å)	0.039	0.033
Main-chain	8.4	15.1
Side-chain	13.3	21.2
Inhibitor at active site, at flap's site	10.2, 12.1	17.3, 24.5
Solvent	26.3	31.5
Occup. of alternate conf. of TMC114 (%) in active site cavity	60/40	60/40
Occup. of TMC114/DMSO at 2nd site in flap	60/40	60/40

[§] The numbers in parentheses are given for the highest resolution shell

substituents and a lone electron pair. The sulfonamide nitrogen has the *R*-enantiomeric configuration when TMC114 is bound in the active-site cavity, but an *S*-enantiomeric configuration in the flap binding site (Figure. 3.1e). The two diastereomers are related by the nitrogen inversion, a well-known geometrical change of a pyramidal nitrogen atom. The presence of two enantiomers of a ligand bound to different sites in a protein molecule is unusual.

Alternate conformations were modeled for 50 and 19 residues in the PR_{V32I}-TMC114 and PR_{M46L}-TMC114 crystal structures, respectively. Owing to the ultra-high resolution data for PR_{V32I}-TMC114, alternate conformations for main-chain as well as side-chain atoms were observed for many amino acid residues. On the contrary, the lower resolution data for PR_{M46L}-TMC114 resulted in less apparent disorder for the main-chain atoms; only the peptide bond connecting residues Ile50 and Gly51 has two alternate conformations. In the PR_{V32I}-TMC114 structure the main-chain and side-chain atoms of residues 23-25, 30-32, 47-52 and 22'-25', 30', 32'-33', 47'-55' have two alternate conformations, with the occupancies refined to 60 and 40%, the same as the relative populations of the two inhibitor conformations.

The high quality and 0.84 Å resolution of the X-ray data permit the decomposition of the PR_{V32I}-TMC114 structure into two distinct conformers with 60% and 40% occupancy. The remarkable conclusion is that two different molecular species have co-crystallized together; the 60% occupancy species has two inhibitor molecules bound to the protease at the active-site and the surface of the flap, while the other conformer has a single inhibitor bound in the active-site and DMSO occupies the surface site.

Effect of mutations on TMC114 binding in the active-site cavity of HIV-1 protease.

TMC114 forms a variety of interactions inside the active-site cavity. On average about a hundred different contacts are made, including:

a) strong O-H…O hydrogen bonds – normal distances are in the 2.6-3.0 Å range (Sarkhel 2004);
b) moderately strong N-H…O and N-H…N hydrogen bonds – normal distances are in the 2.8-3.2 Å range (Sarkhel 2004);
c) weaker C-H…O contacts – contacts are considered good when the distances are of 3.0-3.7 Å (Desiraju 2001);
d) C-H…π interactions - the distance to any atom of a π-system has to be < 4.0 Å, provided C-H is not in the aromatic ring plane (Nishio 1998);
e) the weakest van der Waals interactions such as C-H…H-C – when distances of 3.8-4.2 Å the interactions are attractive, while at distances of < 3.6 Å they are repulsive (Rowley 1999).

Although the V32I mutation introduces a bigger side chain next to the inhibitor, potentially reducing the size of the active-site cavity, in fact the inhibitor loses some favorable interactions with the protease, especially in its minor conformation, rather than gaining unfavorable contacts (Figure 3.3). A similar effect is observed in the PR_{M46L}–TMC114 structure, even though M46L has no direct contacts with the TMC114 molecule that occupies the active site cavity. The interactions are described below separately for the major and minor molecular species in the two mutant complexes.

The major conformation of TMC114 in the active site of PR_{V32I} and PR_{M46L} has interactions that are similar to those for the inhibitor in the wild type PR structure, except for the differences noted below. In PR_{V32I} C-H…π contacts between the aniline π-system of the inhibitor and the side chains of residues Ala28', Ile32' and Ile50 are preserved and the distances between non-hydrogen atoms of 3.4-3.8 Å are comparable to those calculated in the PR structure with residues Ala28, Val32 and Ile50'. However, a direct hydrogen bond of the N-H…O type with a distance of 2.7 Å from the aniline NH_2 group to a carboxylate oxygen of Asp30 is replaced by a weaker water-mediated interaction in PR_{V32I}, with the distances NH_2…H_2O…OOC (Asp30') of 3.0 Å and 2.7 Å, respectively. Additionally, an unconventional hydrogen bond C_α-H…O between Gly49' C_α and an oxygen of the sulfonamide moiety is weaker in the PR_{V32I} structure with a distance of 3.3 Å, which is significantly longer than the 2.9 Å observed in PR.

A quite symmetric pattern of hydrogen bonds is observed between the central OH group of TMC114 and the two Asp25 and 25' residues (Figure 3.2a) for the major and minor conformations of the inhibitor in PR–TMC114 co-crystal and for the major conformation of TMC114 in PR_{V32I} complex (Figure 3.2b). However in PR_{M46L}–TMC114, a strong asymmetry is apparent in the similar hydrogen-bond network (Figure 3.2c). The OH…OOC distances are 2.4, 2.8 Å and 2.9, 3.1 Å with Asp25' and Asp25, respectively. However, we cannot rule out the possibility that some of these differences may be an artifact of the lower resolution (1.3 Å) of the

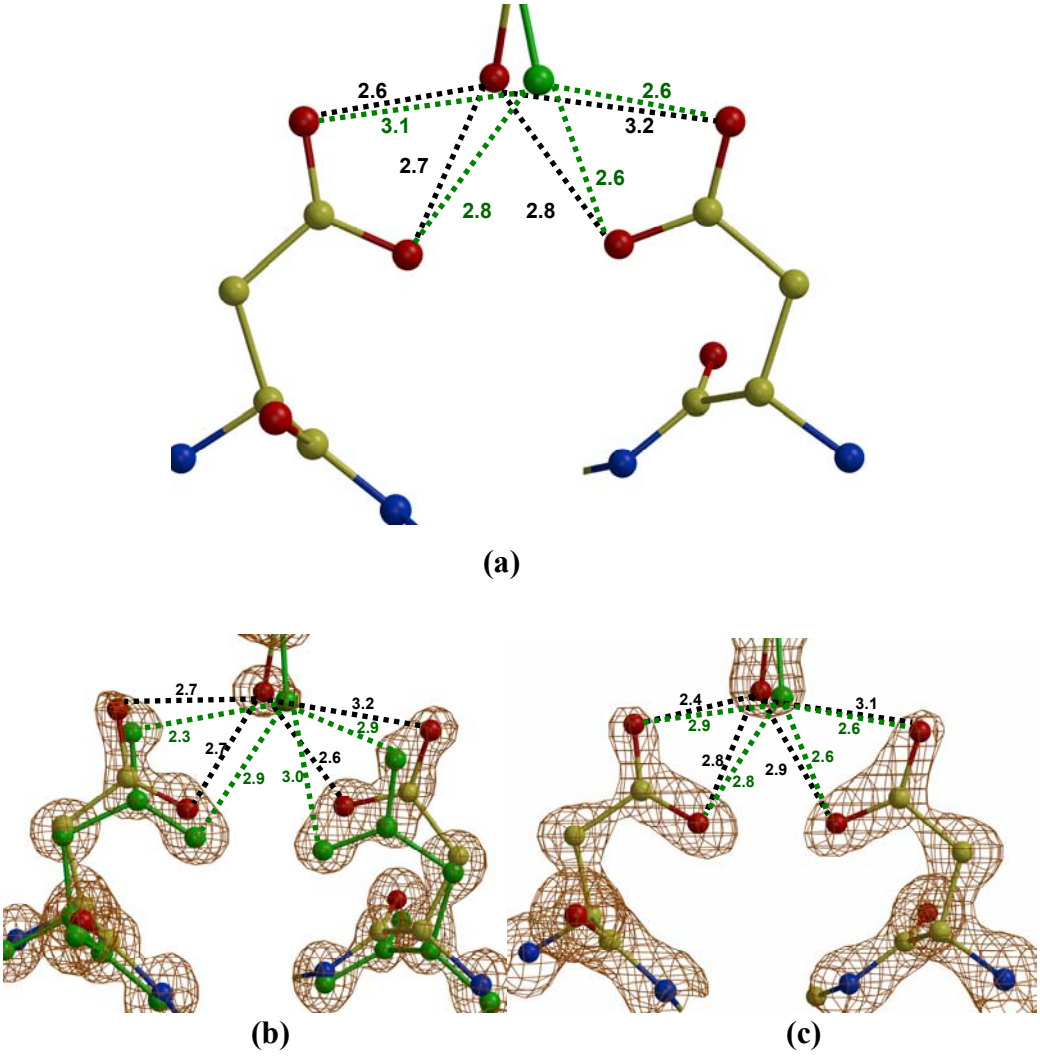

Figure 3.2 Comparison of hydrogen bonds between the central OH group of TMC114 and Asp25, Asp25' for major and minor inhibitor orientations. The $2F_O$-F_C electron density for the active site residues Asp25 and Asp25' is shown for PR_{V32I} (**b**) and PR_{M46L} (**c**). For PR-TMC114 the published structure is used with the PDB code 1S6G. Contour levels are 2.2σ in **b** and **c**. Distances between the central OH group of TMC114 in two orientations and carboxylate groups of 25 and 25' are indicated in Å. 60% populated orientation of TMC114 and protease atoms (60% populated conformation in PR_{V32I}) are colored by atom type. 40% populated orientation of TMC114 and 40% populated conformation of protease atoms in PR_{V32I} (**a**) are in green. The corresponding occupancies of TMC114's orientations are 55% and 45% in PR (**a**).

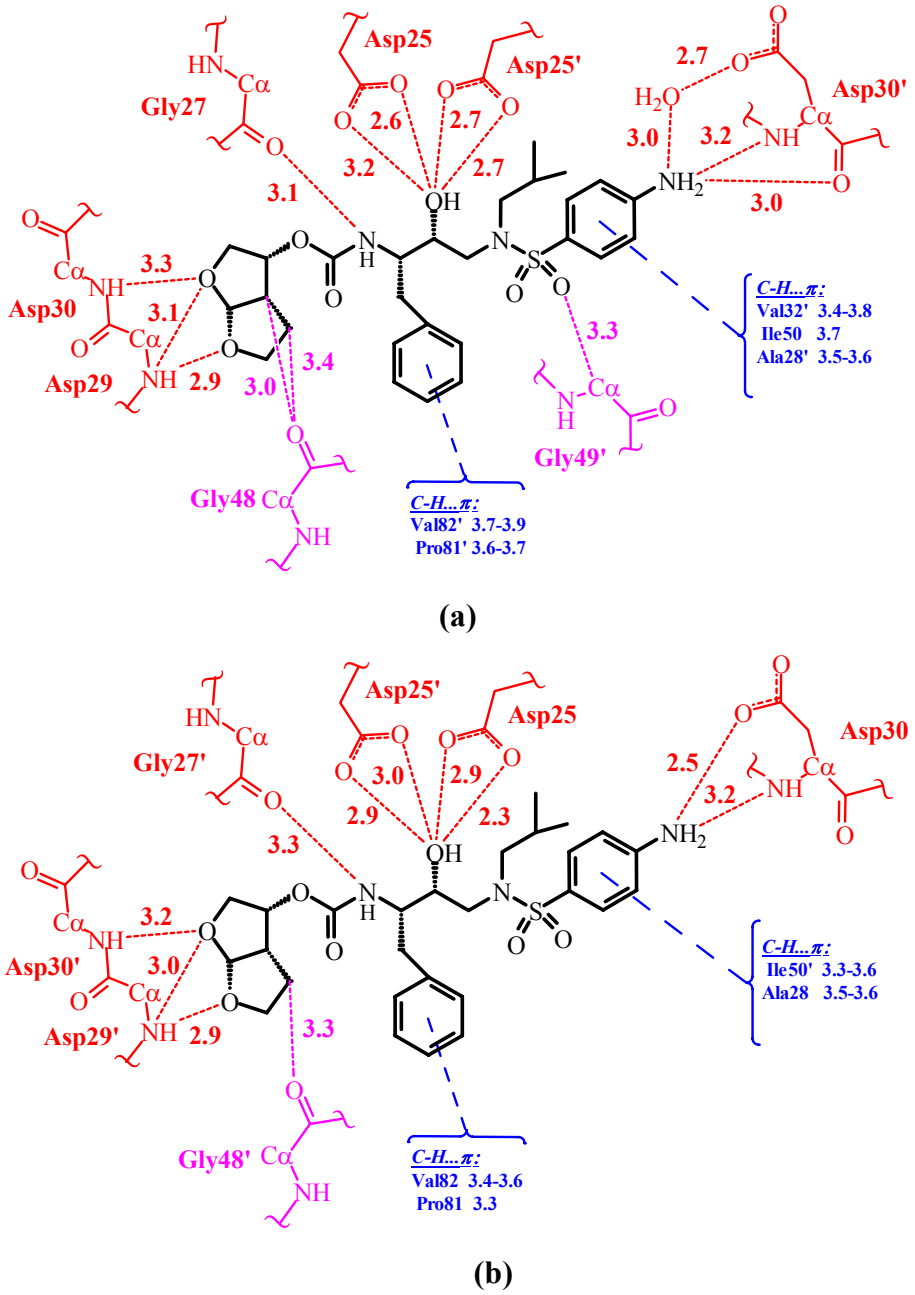

Figure 3.3 H-bond, C-H…O and C-H…π interactions of TMC114's major (**a**) and minor (**b**) orientations with PR_{V32I}.

wild type complex. The minor form in PR_{V32I}–TMC114 has an asymmetric hydrogen-bond network of the catalytic Asp 25 and 25' similar to that seen for the major conformation in PR_{M46L}-TMC114 (Figure 3.2b). However, the minor inhibitor conformation in PR_{M46L}–TMC114 has four very similar hydrogen bonds to the catalytic aspartates.

The minor (40%) species shows larger differences in the TMC114-protease interactions in the mutant complexes (Figure 3.3). Interestingly, the minor and major conformations of TMC114 show different binding in the active site cavity of PR_{V32I}, presumably related to the asymmetric hydrogen-bond network with Asp25 and 25'. On the other hand, the analogous asymmetry of the interactions of the major conformation of TMC114 with the catalytic aspartates in PR_{M46L}-TMC114 has little effect on its overall interactions with the protein. Therefore, it is surprising that the minor conformations in both mutant structures have similar absent or weaker interactions. A good hydrogen bond between NH_2 of the aniline and O=C of Asp30 of ~ 3.2 Å in PR-TMC114 is completely absent in the mutant structures where the corresponding distances are more than 4.3 Å. Similarly, only a single C-H…O contact (3.1-3.3 Å) of the bis-THF part with the main-chain carbonyl of Gly48' remains in the PR_{V32I} and PR_{M46L} complexes, whereas two such interactions with the distances of 2.9-3.4 Å are present in the wild-type structure. In addition, another C-H…O contact between C_α-H of Gly49 and an O of the sulfonamide, which can be considered a good non-conventional hydrogen bond with the distance of 2.8-2.9 Å in PR-TMC114, is considerably longer with the distances of 3.2 Å and 3.6 Å in PR_{M46L} and PR_{V32I}, respectively. Furthermore, the aniline moiety of TMC114 lacks the

aforementioned C-H…π interactions with residue 32 in both mutant complexes, since the corresponding C…C distances are > 4.4 Å. Finally, repulsive short van der Waals interactions are introduced in the mutant structures that include 3.4-3.5 Å contacts involving one methyl group of the *iso*-butyl moiety of TMC114 and the side-chain atoms of Val82 (Rowley 1999). Analogous contacts in PR-TMC114 are attractive van der Waals interactions with the distances of 3.9 Å.

Second binding site for TMC114 on the protease surface.

A second TMC114 molecule was found on the protein surface in the major conformer of the PR_{V32I} and PR_{M46L} complexes. The larger part of the inhibitor molecule is positioned in a groove located in the flap region of the protease (Figure 3.4a). The groove is formed by the residues Glu35', Trp42', Pro44'-Met46'(or Leu46'), Lys55'-Arg57' and Val77'-Pro79', and is less evident on the other protease subunit. The smaller part of the TMC114 molecule that is outside the groove consists of the phenyl and bis-THF groups that face two symmetry-related protein molecules. A similar, although shallower, groove is present in the PR-TMC114 structure where a 50% occupancy glycerol molecule is bound (Figure 3.4b). Thus, these structures suggest that the groove can open up to accommodate TMC114.

TMC114 has a larger number and significantly stronger interactions with the residues in the groove formed by the flap than with the residues of the symmetry-related protein molecules. A network of hydrogen bonds is formed between the aniline, sulfonamide and carbamate moieties of the TMC114 and the main- and side-chain atoms of PR_{V32I} or PR_{M46L} (Figure 3.5a). Two direct hydrogen-bonds of 2.9-3.3

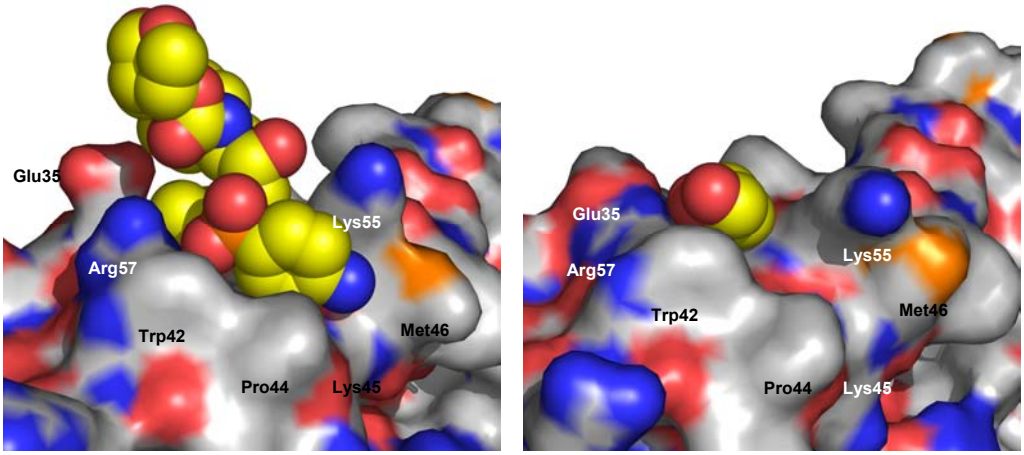

(a) **(b)**

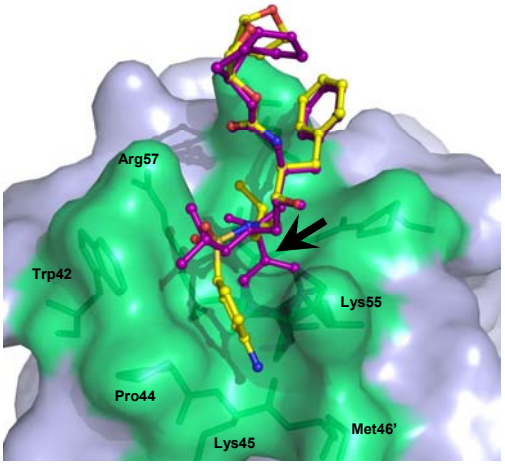

(c)

Figure 3.4 TMC114 bound to the flap binding site in PR_{V32I} (**a**), similar view in PR (**b**); superposition of *R*-enatiomer (magenta) from the active-site cavity with the *S*-enantiomer bound in the flap site. The inhibitor for PR_{V32I} and a glycerol molecule for PR are in a space-fill representation. Protease is represented as a surface. The aniline moiety of the R-enantiomer in **(c)** (indicated by arrow) collides with the PR residues; this would therefore prevent it from binding in the flap site. The figure is from PR_{V32I}; the geometry is similar in PR_{M46L}.The inhibitor's binding in PR_{M46L} is essentially unchanged. The residues forming the binding groove are labeled.

Å are made with the main-chain of Lys45' and side-chain of Arg57' in the two mutant structures (aniline NH_2 …O=C of Lys45' and S-O…H-N of Arg57'). Additionally, there are interactions mediated by two water molecules that involve the central OH group and the carbamate carbonyl oxygen atom of the inhibitor and the side chain amino groups of Lys55' and Arg57' of the mutants, with the distances in the 2.8-3.1 Å range (Figure 3.5a). The binding of TMC114 at the flap is also supported by other weaker interactions, such as non-conventional C-H…O hydrogen bonds. Two C-H…O interactions connect the main-chain carbonyl oxygens of Val56' and Val77' with the aniline and the iso-butyl group of TMC114, respectively. The distances are comparable in both mutant structures (3.2-3.3 Å). A slightly weaker C-H…O interaction exists between the sulfonamide oxygen and Cγ of Arg57', with 3.4 Å separation between heavy atoms in PR_{V32I} and PR_{M46L}. Moreover, the aniline group of TMC114 is bound more tightly in the groove by C-H…π interactions with side chains of Pro44' and Lys55' and interatomic distances as short as 3.4 Å. Similar van der Waals contacts of 3.9-4.0 Å are found with residue 46' in the V32I and M46L mutant structures. Hence, remarkably, the M46L mutation, though forming a part of the second binding site, does not alter the inhibitor binding in this site.

The phenyl and bis-THF groups are directed away from the groove in the flap and toward two symmetry-related protease molecules, while a third protease molecule is situated on top of the groove and above the inhibitor (Figure 3.5b). These groups make only a few hydrophobic contacts and no hydrogen bonds with residues of PR_{V32I} or PR_{M46L}. These symmetry-related interactions of the phenyl and bis-THF

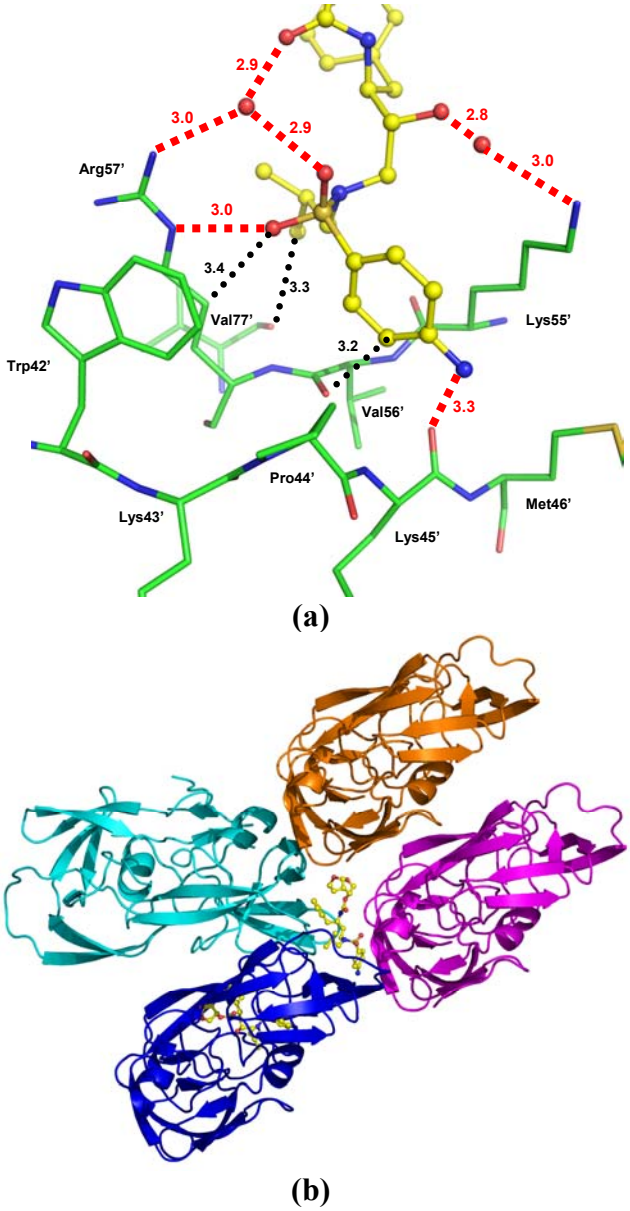

Figure 3.5 (a) Hydrogen bonds network and C-H…O interactions of TMC114 bound in the flap site for PR_{V32I}. All distances indicated are between the heavy atoms. Hydrogen bonds are colored in magenta, while C-H…O contacts are colored in black. Interactions in PR_{M46L} complex are very similar. **(b)** TMC114 bound to the surface site is surrounded by four protein molecules. The asymmetric unit consists of PR (blue) and two inhibitor molecules shown in ball-and-stick representations. The symmetry related protease molecules are in cyan, orange and magenta.

moieties are similar in both mutant structures. The π-system of the phenyl substituent is in the close vicinity of Arg41 from the first symmetry-related protease molecule and forms interactions of 3.4-3.7 Å with the main-chain amide and side-chain C_β atoms. The side-chain of Arg41 past the C_β atom is highly disordered, indicating the weakness of the protease/inhibitor intermolecular binding in this region. Similarly, bis-THF interacts with the indole group of Trp6 of the second symmetry-related molecule by C-H…π contacts with the distances of 3.4-3.8 Å. The side chain of Trp6 is also parallel to and about 3.5 Å away from the inhibitor's carbamate moiety and therefore can participate in π-π stacking interactions. Another set of C-H…π contacts involves residue Gly94' of the third symmetry-related protease and the aniline group. These interactions are very similar in PR_{V32I} and PR_{M46L} with distances of 3.4-3.6 Å.

Binding of the second inhibitor molecule induces conformational changes in the protease.

When the mutant structures are superimposed onto the PR-TMC114 structure (PDB code 1S6G) (Tie 2004) the overall main-chain root-mean-square deviation (rmsd) is 0.6 Å for both PR_{V32I} and PR_{M46L}. The rmsd value is analogous to that for comparison of HIV PR structures with different unit cells (Mahalingam 2004; Kovalevsky 2006), where the largest differences were observed for surface residues not involved in the inhibitor-protease interactions. However, the PR_{V32I} and PR_{M46L} complexes show dramatic conformational disparities relative to PR-TMC114 that go beyond the changes usually observed on comparison of closely related structures in

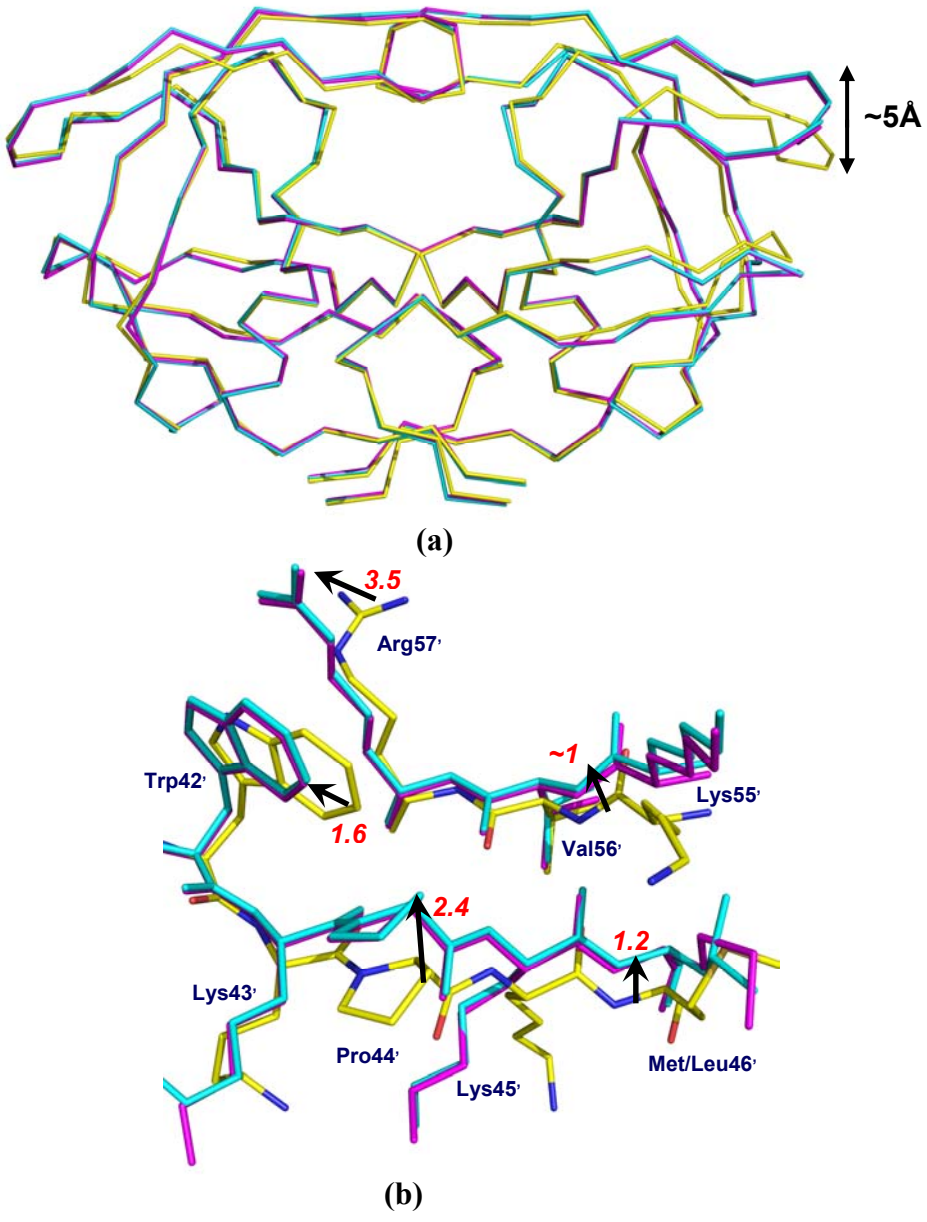

Figure 3.6 (**a**) The superposition of the mutant V32I and M46L structures on to the PR; (**b**) The residues (labeled) of the second binding site, which have the largest atomic shifts when PR, PR_{V32I} and PR_{M46L} are superposed, are illustrated. PR is colored by atom type, while PR_{V32I} and PR_{M46L} are colored in magenta and cyan, respectively. The atomic shifts (Å) are indicated as dashed arrows.

different unit cells (Figure 3.6a). The largest differences are in the conformations of the broad surface loop of residues 34-43, where the atomic shifts reach 5 Å compared with the position in the wild type structure. This large change of the flexible loop in the mutants is likely due to the close contacts with the symmetry-related surface-bound TMC114, in particular with Arg41. The second largest differences in the conformation of the proteases are evident for the flap residues that form the surface TMC114 binding site (Figure 3.6b). The main-chain atoms of residues 44'-46' shift by 1.2-2.4 Å towards the inhibitor in the mutant complexes and form hydrogen bonds (*i.e.*, aniline NH_2…O=C of Lys45') and hydrophobic interactions, while the side-chain of Arg57' moves by 3.5 Å, breaking its salt-bridge interactions in the PR and forming hydrogen bond interactions with TMC114. The residues that form hydrophobic interactions are shifted either toward the TMC114, like Pro44', or slightly away from it, like Lys55' and Trp42', and therefore either form good C-H…π contacts (Pro44' and Lys55') or avoid unnecessary close interactions with the sulfonamide group (Trp42'). The changes of the protease atoms in the other areas that are in contact with TMC114 do not exceed 0.4 Å, indicating much weaker inhibitor interactions. These structural changes confirm that TMC114 binding on the protease surface is mostly confined to the flap area. The protease adjusts in this area to accommodate the drug, while other symmetry-related interactions are mostly due to the crystal packing. Interestingly, the configuration of TMC114 also adjusts since the S-enantiomer is bound at this surface site.

Enzyme kinetics and inhibition.

The kinetic parameters of protease-catalyzed hydrolysis were measured for wild-type PR and the two mutants PR_{V32I} and PR_{M46L} using the chromogenic substrate that represents the CA-p2 cleavage site of the HIV-1 Gag precursor (Table 3.2). PR and PR_{V32I} showed essentially the same k_{cat}/K_m, while PR_{M46L} showed only 50% of the PR value. The lower activity of PR_{M46L} is primarily due to an approximately three-fold increase in the K_m value.

The wild-type PR and mutants were assayed for inhibition by the clinical inhibitor TMC114. TMC114 shows sub-nanomolar inhibition of PR, while the relative K_i values are about 7 and 10-fold higher for the inhibition of PR_{V32I} and PR_{M46L}, respectively (Table 3.2). This decreased inhibition for PR_{V32I} and PR_{M46L} is consistent with the loss of interactions with TMC114 observed in the crystal structures (Figure 3.3d-f). The PR_{V32I}
and PR_{M46L} mutants are significantly more resistant to the inhibition by TMC114 than the PR_{V82A} and PR_{I84V} mutants employed in our previous study (Tie 2004). Alternatively, TMC114 showed less effective inhibition of PR_{D30N} and PR_{I50V} (Kovalevsky 2006).

DISCUSSION

TMC114 is performing exceptionally well in clinical trials for treatment of HIV infection. It shows an outstanding resistance profile and high effectiveness against all the subtypes of HIV (Koh 2003; De Meyer 2005), and has been approved as a salvage therapy for those patients who fail other drug regimens. Remarkably,

Table 3.2. Kinetic parameters from the spectrophotometric assay for hydrolysis of peptide Ac-KARVNle(Phe-p-NO_2)EANle-CO-NH_2 and inhibition by TMC114 of PR, PR_{V32I} and PR_{M46L}.

Protease	**K_m, μM**	**k_{cat}, min^{-1}**	**k_{cat}/K_m, $min^{-1}•\mu M^{-1}$**	**K_i, nM (Relative)**
PR	106 ± 9	245 ± 10	2.3 ± 0.2	0.49 ± 0.13 (1)
PR_{V32I}	90 ± 8	198 ± 6	2.2 ± 0.2	3.3 ± 0.2 (6.7)
PR_{M46L}	286 ± 23	283 ± 11	1.00 ± 0.08	4.9 ± 0.4 (10)

there are no reports of resistant mutations in HIV-1 specifically selected by treatment with TMC114.

Similar to other drugs, TMC114 was designed to bind exclusively in the active-site cleft of the HIV-1 PR. Unexpectedly, the structures of PR_{V32I}–TMC114 and PR_{M46L}–TMC114 obtained with ultra-high 0.84 Å and near-atomic 1.22 Å resolution, respectively, have unequivocally shown that TMC114 binds at two sites: the active-site and a surface site on the flap. The subatomic resolution of the PR_{V32I}–TMC114 structure allowed us to definitively relate the major conformation of TMC114 in the active site and the surface flap site. Consequently, we concluded that two molecular species have co-crystallized: one has two TMC114 molecules bound to the protease, the PR_{V32I}-$(TMC114)_2$ species, and the other has just one TMC114 molecule in the active-site cavity and a DMSO solvent molecule in the second potential site on the protein surface. It is not unusual for an enzyme to have two binding sites for inhibitors, where one binds at the catalytic site and the other (allosteric) site is located in a different part of the protein molecule (Tian 2003). Detailed kinetic analysis may help to establish whether the second site for TMC114 has an inhibitory effect.

The crystal structures of PR_{V32I} and PR_{M46L} imply a biological role for the TMC114 binding site on the flap. Other types of compounds, like beta-lactams (Sperka 2005) or polyoxometalate anions (Judd 2001), have been demonstrated to inhibit the HIV-1 protease by exclusively binding to surface sites in the flap region. The part of TMC114 bound on the protease flap makes a number of strong stabilizing interactions to the main- and side-chain atoms of the protein. On the other hand, the

rest of the inhibitor that contacts three symmetry-related protease molecules has only a few hydrophobic contacts with each of them. Brynda *et al.* (Brynda 2004) reported another PR structure with a peptide inhibitor bound to a similar second site. In contrast to TMC114, this peptide inhibitor binds with a number of direct hydrogen bonds and water-mediated contacts with all four surrounding PR molecules in the crystal. Notably, the peptide inhibitor forms only water-mediated contacts with the flap residues, while direct hydrogen bonds are observed with other symmetry–related PR molecules. Thus, the authors concluded that the second site did not have any relevance for the inhibition of the PR. The analysis of the surface site in our PR_{V32I} and PR_{M46L} crystal structures suggests that TMC114 has significantly more interactions with the flap region than with the other parts of the protease. Another consideration is that the conformation of the protease in the flap site changes on binding of TMC114. In the complexes with PR_{V32I} and PR_{M46L} the residues in this flap site show substantial shifts from their positions in the wild-type PR that optimize the interactions with TMC114 (Figure 6b). Finally, TMC114 has two different configurations related by the sulfonamide nitrogen inversion: an *S*-enantiomeric configuration when bound on the surface and an *R*-enantiomeric configuration in the active-site cavity of the protease. If the active-site bound inhibitor configuration is superimposed onto the TMC114 bound in the flap site, the aniline moiety clashes with protease residues (Figure 4c). Thus, it is evident that the flap binding site is shaped to accommodate only the diastereomer with *S*-enantiomeric amide nitrogen. The other diastereomer with the *R*-enantiomeric amide nitrogen cannot bind at the

flap site due to the steric collisions with the protease atoms. Therefore, both the protease and TMC114 adapt to form a complex with two bound inhibitors.

We therefore propose that the second TMC114 binding site observed in the structures of HIV-1 PR_{V32I} and PR_{M46L} mutants can explain the remarkable effectiveness of TMC114 on the drug resistant strains of HIV-1.

Chapter Four: The Role of HIV-1 Protease with Flap Mutations in Drug Resistance of Saquinavir and Darunavir: Insights from High Resolution Crystal Structures

INTRODUCTION

HIV-1 (Human immunodeficiency virus type 1) protease (PR) is an effective drug target for protease inhibitors (PIs). The active HIV-1 PR homodimer possesses two glycine-rich regions, known as flaps. Each flap folds into extended anti-parallel β stands, comprising residues Lys^{45}-Met-Ile-Gly-Gly-Ile-Gly-Gly-Phe-Ile-Lys^{55}. The flap region is very flexible and binds substrate or inhibitor in the active site cavity of PR (Miller 1989; Gustchina 1990; York 1993; Collins 1995; Shao 1997). The importance of residues in the flap for PR activity has been characterized through large scale mutagenesis (Shao 1997). The residues Met46, Phe53 and Lys55 are the most tolerant to substitutions; residues Ile47, Ile50, Ile54 and Val56 only tolerate a few conservative substitutions; and the Gly-rich region at residues Gly48, Gly49, Gly51, Gly52 is the most sensitive to mutation (Shao 1997). Therefore, mutations in the flap residues potentially affect the enzyme activity and structural properties of the flap (Swairjo 1998). Mutations in flap residues 46, 47, 48, 50, 53, and 54 are frequently observed in drug resistant mutants of HIV and show various levels of reduced drug susceptibility to different protease inhibitors (PIs) (Shafer 2002).

Saquinavir (SQV) was the first PI to be approved (in 1995) and is still widely used in AIDS therapy. In the treatment with saquinavir, G48V, L90M and G48V/L90M are the primary drug resistant mutations selected (Noble 1996; Shapiro 1999). Darunavir (DRV, previously known as TMC114) was approved in 2006 and inhibits the wild type PR and most drug resistant mutants very well *in vitro* and *in vivo* (Koh 2003; De Meyer 2005; Kovalevsky 2006). Currently, darunavir (boosted with ritonavir) is recommended for treatment-experienced patients who respond poorly to other PIs. Mutations I54V and I54M are commonly reported during therapy with multiple PIs (Molla 1996; Condra 2000; Shafer 2002; Murphy 2004). The chemical structures of saquinavir and darunavir are shown in Figure 4.1. Saquinavir was designed to target the wild type PR, so it contains the peptidic main chain groups mimicking a natural substrate of PR. In contrast, darunavir was designed be less peptidic while introduce in more hydrogen bond interactions with the main chain atoms of PR in order to maintain the effectiveness on PR variants (Koh 2003).

In this study, mutations of four flap residues (G48V, I50V, I54V and I54M) of HIV-1 PR were analyzed to gain insights into their roles in the development of drug resistance. Residue 50 lies at the tip of the flap, while residues 48 and 54 are located at the opposite sides of the flap as shown in Figure 4.1. The crystal structures of flap mutants PR_{G48V}, PR_{I50V}, PR_{I54V}, and PR_{I54M} have been solved in their complexes with saquinavir (the first PI) and darunavir (the newest PI). Structural comparison revealed that the introduction of mutations in the flap caused changes in flap conformation, interactions between adjacent residues (45-55) in the flap region, inhibitor binding and conformation of residues 78-82 (called the 80's loop). The results from this study

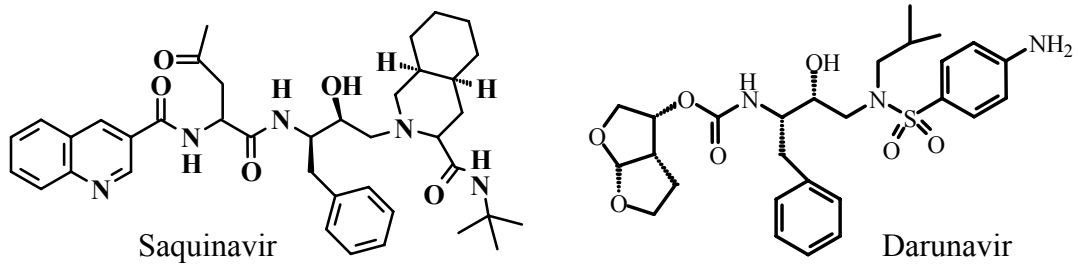

(a)

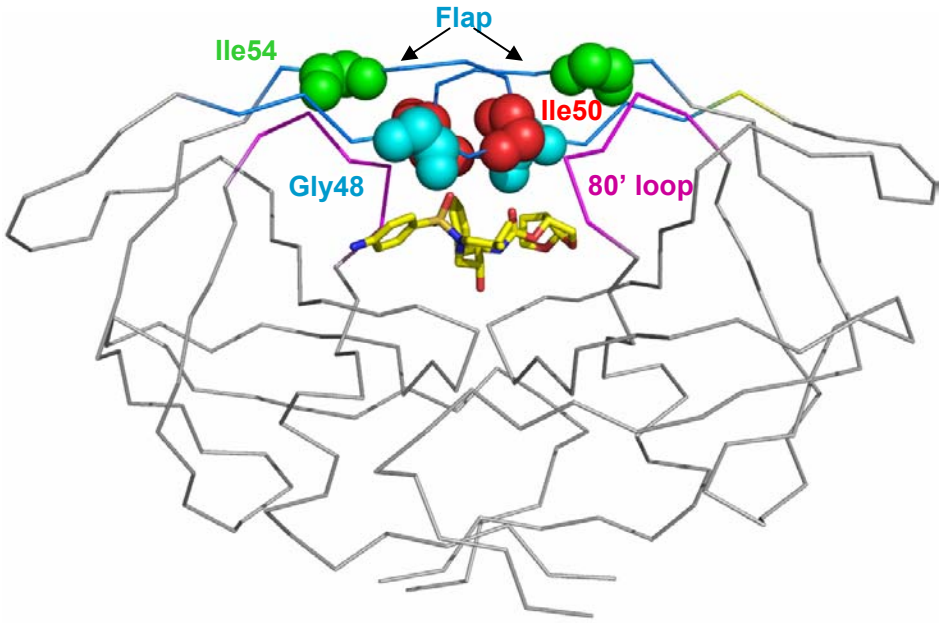

(b)

Figure 4.1: (a) The chemical structures of saquinavir and darunavir. (b) Structure of HIV-1 PR dimer with the locations of mutated residues 48, 50, 54 indicated in spheres (main chain atoms only for clarity) in both subunits. Gly48 is in cyan, Ile50 in red and Ile54 in green. Darunavir is shown in sticks colored by atom type. The flap residues (45-55) and the 80's loop (78-82) are colored in blue and purple, respectively.

confirmed the important roles of residues in protease flap region and enhanced our understanding of the drug resistant mechanisms used by the flap mutants. It also provides useful information for guiding the structure-based drug design to combat HIV.

RESULTS AND DISCUSSION

Dimer Stability

The dimer stability of four flap mutants (PR_{G48V}, PR_{I50V}, PR_{I54V}, and PR_{I54M}) and the wild type PR was evaluated by assessing the PR activity with increasing concentrations of urea. When the PR activity drops to 50% of the initial value, the concentration of urea is defined as UC_{50}. The UC_{50} value of PR_{I50V} was reduced to 60% of the value for the wild type PR, while the UC_{50} of the other three mutants (PR_{G48V}, PR_{I54V}, and PR_{I54M}) were very similar to that of the wild type PR (90-110%). In our previous study, the UC_{50} of PR_{F53L} was also reduced to 60% of the value for the wild type PR (Liu 2005). Therefore, the mutations of flap residues I50V and F53L adversely affected the PR dimer stability, while mutations G48V and I54V/M did not show significant effects on dimer stability.

Crystal Structures

The crystal structures of PR_{I50V}, PR_{I54V}, and PR_{I54M} complexed with saquinavir and PR_{G48V}, PR_{I54V}, and PR_{I54M} complexed with darunavir were determined at resolutions of 1.05-1.40 Å. Three crystallographic data sets (PR_{I54M}-SQV, PR_{I54V}-SQV, PR_{I54V}-DRV) reached atomic resolution (1.05 Å). The data

collection and refinement statistics are provided in Table 4.1. All six structures crystallized in isomorphous unit cells and the same space group $P2_12_12$. The R-factors were refined to the range of 0.12 to 0.16. One asymmetric unit accommodated one PR dimer, with residues labeled 1-99 and 1-99' for each subunit. The electron density maps clearly showed the correct mutations in all the complexes as illustrated in Figure 4.2. All atoms were clearly visible in the electron density maps. An example from the flap region of PR_{I54V}-SQV is shown in Figure 4.2. Darunavir was bound at the active site of PR with two pseudosymmetric conformations in the complexes with PR_{G48V}, PR_{I54V}, and PR_{I54M}, while saquinavir showed a single conformation in the complexes of PR_{I54V}-SQV and two conformations in the complexes of PR_{I54M}-SQV and PR_{I50V}-SQV. The electron density maps of saquinavir (in PR_{I54M}-SQV) and darunavir (in PR_{I54V}-DRV) are shown in Figure 4.3. Alternate conformations were modeled for side chain and main chain atoms when observed in the electron density map. The mutated residue Met54 showed alternate conformations of the side chain only in the PR_{I54M}-SQV complex (Figure 4.2) and Val54 showed alternate conformations of the side chain only in the PR_{I54V}-SQV complex. As observed previously in atomic resolution crystal structures, residue 50 showed alternate conformations for the main chain and side chain in the all the complexes, except the lower resolution structure PR_{G48V}-DRV, (Liu 2005; Kovalevsky 2006; Tie 2006). In addition, water molecules (161-223) and other solvent molecules including glycerol, phosphate, sodium ions and chloride ions with full or partial occupancy were modeled to fit the maps in the different structures.

Table 4.1: Crystallographic Data Statistics

Protease Mutant		**PR_{I50V}**	**PR_{I54V}**	**PR_{I54M}**	**PR_{G48V}**	**PR_{I54V}**	**PR_{I54M}**
Inhibitors		**SQV**	**SQV**	**SQV**	**DRV**	**DRV**	**DRV**
Space group		$P2_12_12$	$P2_12_12$	$P2_12_12$	$P2_12_12$	$P2_12_12$	$P2_12_12$
Unit cell dimensions (Å)	a	58.9	58.7	59.5	58.2	58.8	58.6
	b	86.0	85.9	85.7	86.2	86.1	85.7
	c	46.4	46.38	46.2	45.9	46.2	46.0
Unique reflections		69158	101144	103172	40435	100265	53524
R_{merge} (%) Overall (final shell)		8.9 (53.7)	10.0 (42.3)	8.8 (25.8)	9.4 (20.3)	10.8 (41.7)	8.9 (57.6)
I/sigma(I) Overall (final shell)		13.5 (1.8)	16.8 (2.5)	21.9 (7.0)	13.2 (3.0)	17.8 (1.8)	24.4 (2.2)
Resolution range for refinement (Å)		10-**1.20**	10-**1.05**	10-**1.05**	10-**1.40**	10-**1.05**	10-**1.30**
R_{work} (%)		15.0	15.0	11.9	16.0	15.9	15.1
R_{free} (%)		19.2	17.4	14.7	22.7	17.96	19.5
No. of waters		200	223	209	174	212	161
Completeness (%) Overall (final shell)		93.1 (79.4)	92.5 (58.1)	93.4 (79.3)	87.5 (55.8)	91.2 (58.7)	94.4 (80.8)
RMS deviation from ideality							
Bonds (Å)		0.014	0.017	0.017	0.011	0.017	0.013
Angle distance (Å)		0.032	0.033	0.036	0.029	0.037	0.034
Average B-factors (Å^2)							
Main chain		10.2	14.0	10.1	15.7	15.5	16.9
Side chain		18.7	19.9	19.1	25.8	21.4	26.4
Inhibitor		9.4	17.0	10.8	13.8	12.8	16.8
Solvent		26.1	33.5	26.0	29.8	32.0	19.0
Inhibitor occupancy (%)		80/20	100	75/25	60/40	60/40	70/30

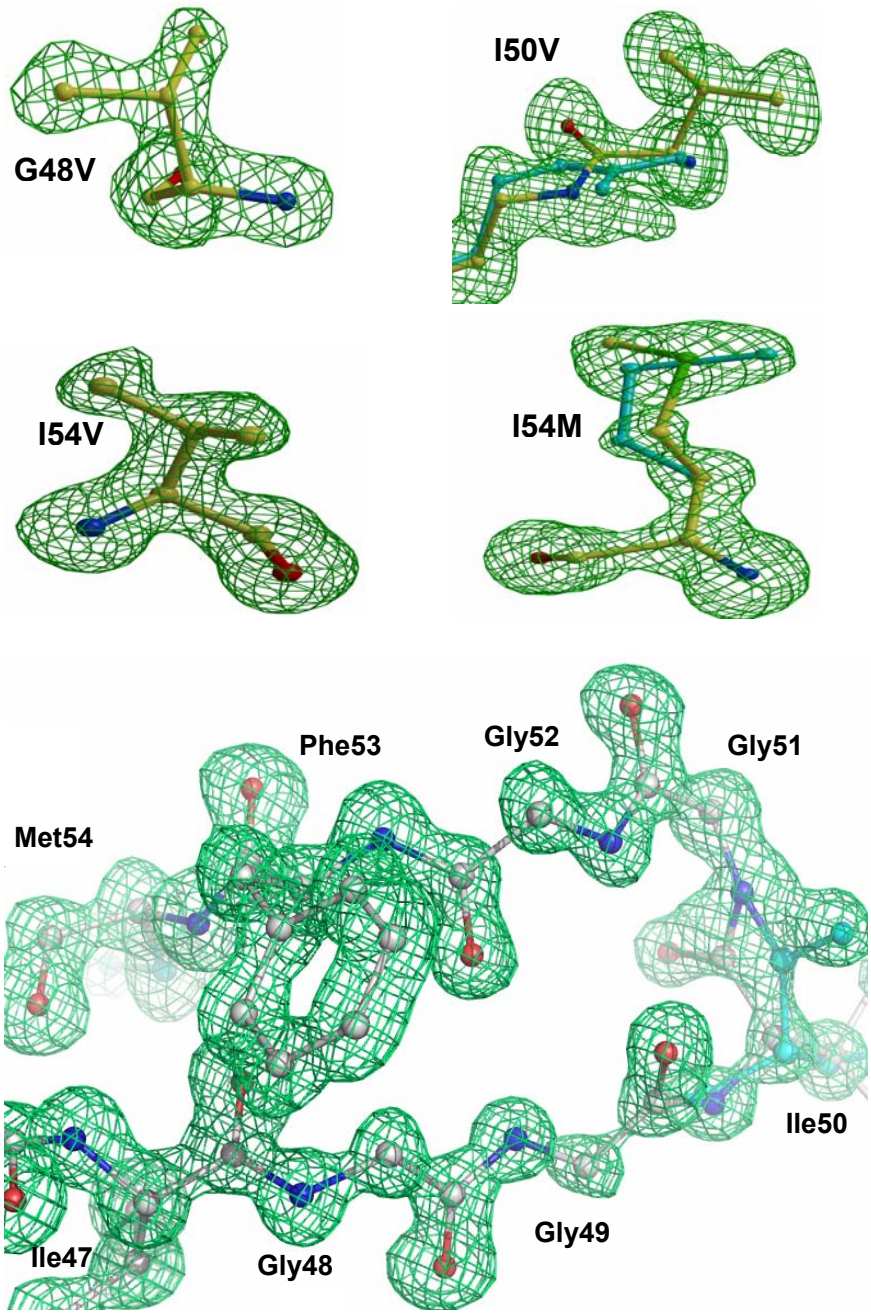

Figure 4.2: The Fo-Fc omit maps showing the mutated residues and the flap residues (47-54) contoured at 3.3 sigma. Val 48 is from PR_{G48V}-DRV, Val50 from PR_{I50V}-SQV, Val54 from PR_{I54V}-SQV, Met54 from PR_{I54M}-SQV and flap residues from PR_{I54M}-SQV. The cyan sticks indicate the alternate conformations of main-chain and side-chain atoms in Val50 and Met54.

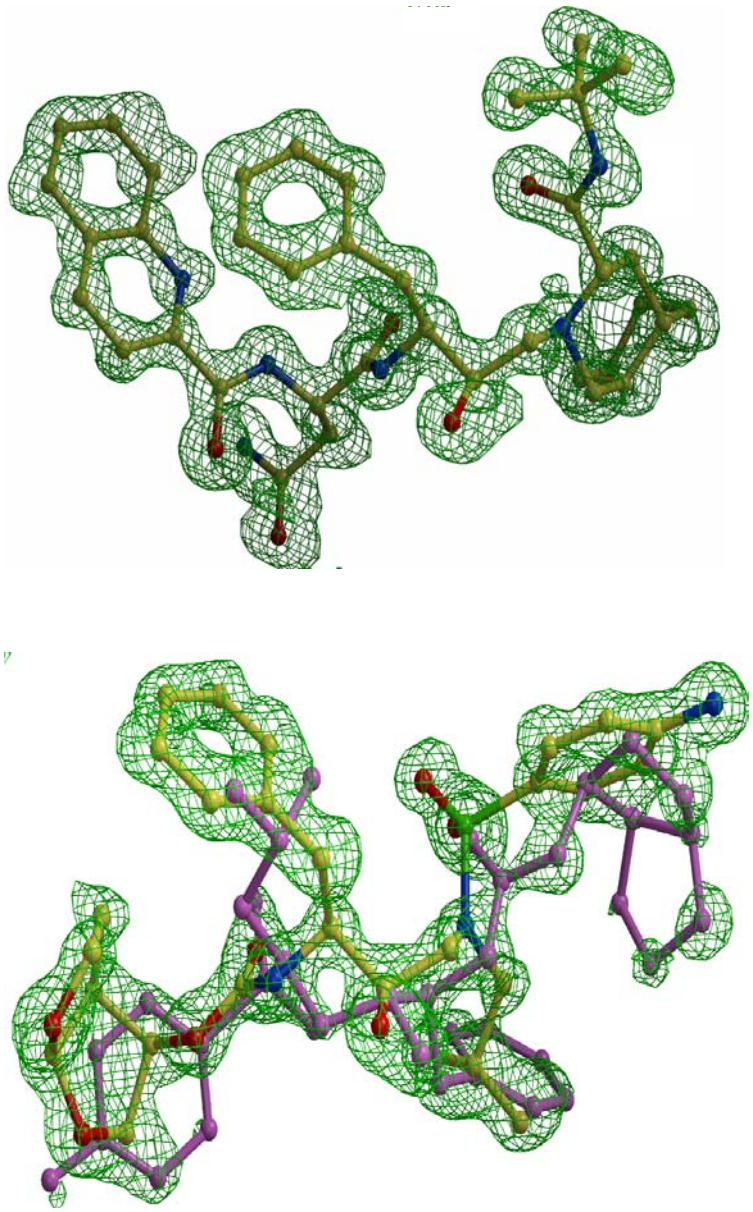

Figure 4.3: The Fo-Fc omit maps of saquinavir (upper panel) and darunavir (lower panel) contoured at 3.3 sigma. Saquinavir is colored by atom type from complex PR_{I54M}-SQV. Darunavir is from complex PR_{I54V}-DRV showing alternate conformations of 60/40% occupancy. The major conformation is colored by atom type and the minor is colored pink.

Comparison of Structures

The new mutant PR structures were compared with the structure of wild type PR complexed with the same inhibitor, which were determined in our previous studies. The wild type PR-DRV (1S6G) (Tie 2004) structure has been solved at 1.30 Å resolution in space group $P2_12_12$, while the PR-SQV has recently been determined to 1.16 Å resolution in $P2_12_12_1$ (Tie 2006). The mutations in the flap region possibly alter interactions with neighboring residues, the flap conformation and inhibitor binding. The structural differences between mutant PRs and the wild type PRs are indicated by the RMS deviations. The pairwise overall RMS deviations of Cα were 0.1-0.3 Å for complexes with darunavir in the same space group. The complex PR_{I54V}-DRV is the most similar to the wild type PR-DRV, while the other two complexes have similar deviations (0.3 Å) from the wild type PR. The pairwise overall RMS deviations of Cα for the three complexes with saquinavir were very close in the range of 0.6-0.7 Å. It is common for very similar HIV PR structures in two different space groups to have RMS deviations ~ 0.6 Å (Liu 2005). For all complexes, larger deviations were consistently located around residues 50 (the flap) and 80 (the loop) in both subunits. The alternate conformations of main chain residue 50/50' significantly contributed to the high RMS deviations in the flap regions. Structural deviations between residues 46-53 are shown in Figure 4.4. PR_{G48V} had the biggest difference from the wild type PR among all the complexes with darunavir, 0.8 Å at the Cα atom of Ile50 towards the active site cavity in one subunit and 0.5 Å at the equivalent position in the other subunit. In high resolution structures, a difference over 0.2 Å is significant.

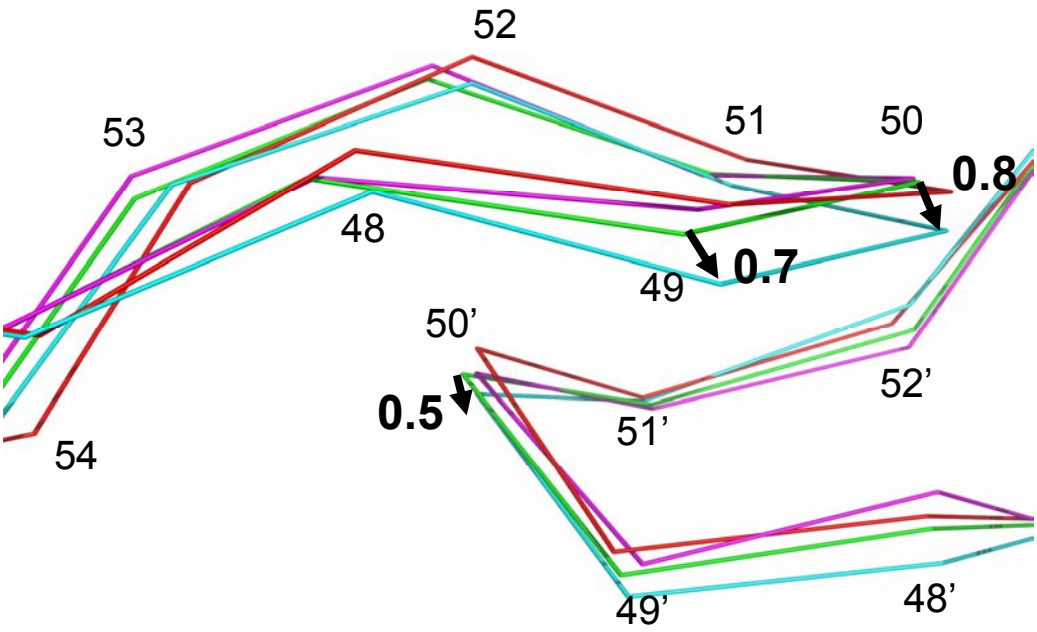

Figure 4.4: The flap regions for superimposed complexes with darunavir. The wild type PR is in green, PR_{G48V} in cyan, PR_{I54V} in magenta and PR_{I54M} in red. The distances between Cα atoms of PR_{G48V} and of the wild type PR are labeled in Å.

In all the mutant structures, the main chain atoms of residues 78-82 (the 80's loop) were notably shifted relative to their positions in wild type PR. The shifts appeared in both subunits of the dimer, and were slightly larger in one subunit than the other. The shifts of the 80's loop were directly related to the size of the side chain in the mutated residues, independent of the type of bound inhibitor. A certain separation seems to be required between residues 50, 54 and the 80's loop. However, the conformational changes in the 80's loop due to the mutations in the flap did not produce substantial changes in the inhibitor binding at the active site cavity in each of the complexes. Further, the flap mutants showed varied effects for the interactions of the mutated residues with the bound inhibitors, which is discussed for each mutant individually in the following sections.

PR_{G48V}-DRV

Residue Gly48 interacts with inhibitors in the wild type PR complexes. Replacing Gly48 by Val in PR_{G48V} is expected to disrupt the interactions with neighboring residues on the flap as well as with the inhibitor, thus destabilizing the flap and reducing the affinity for inhibitor. Despite extensive efforts, no crystals were obtained for the single mutant PR_{G48V} in complex with saquinavir. Fortunately, it was possible to cocrystallize PR_{G48V} with darunavir and the crystals diffracted to 1.40 Å. The comparison of PR_{G48V}-DRV with the wild type PR-DRV complex showed that Cα of Val48 in both subunits has lost interactions with the Phe53 aromatic ring, while new hydrophobic interactions were observed between the Val48 side chain and the Gly52 main chain atoms (Figure 4.5). In one subunit, the side chain of Phe53' has

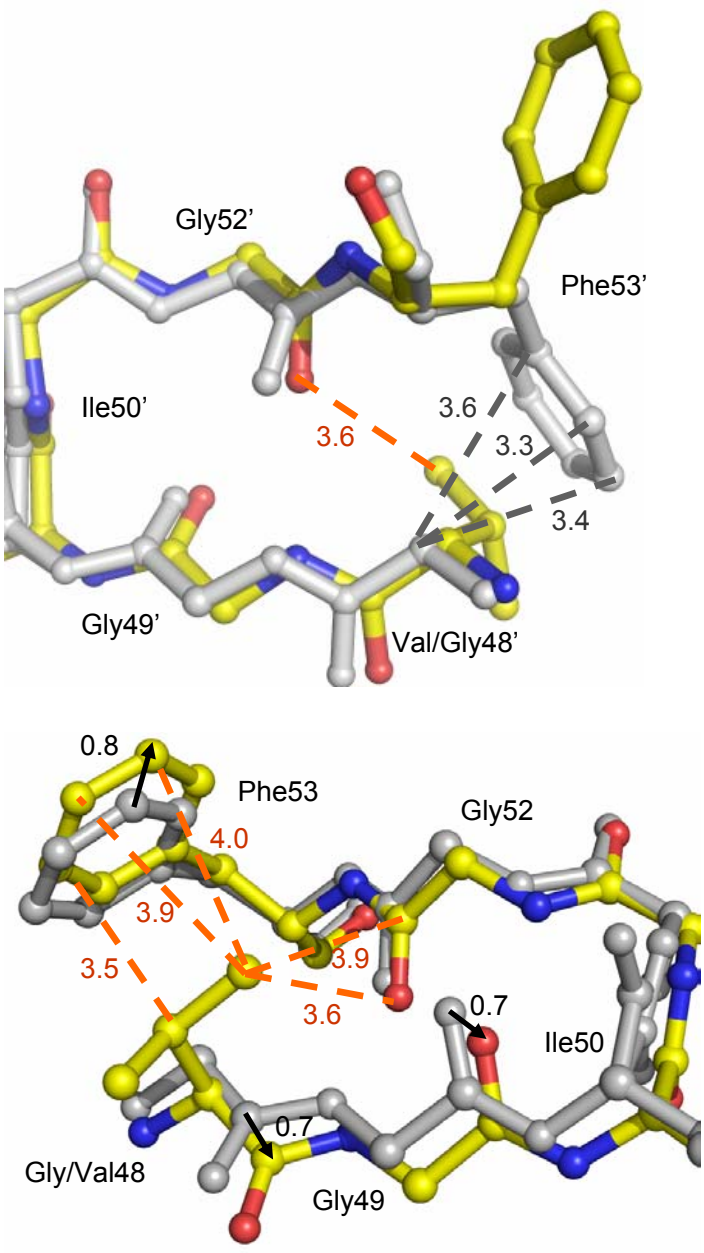

Figure 4.5: Comparison of the flaps of PR_{G48V}-DRV and of wild type PR-DRV in two subunits. The structure of PR_{G48V}-DRV is colored by atom type and wild type PR is colored grey. Dashed lines indicate van der Waals interactions with interatomic distances shown in Å. The arrows show the shifted distances in Å between the two structures.

rotated away from the position in wild type PR. Consequently, interactions between Cα of Gly48' and the ring of Phe53' were eliminated. However, a new interaction was formed between CG2 of Val48' and the carbonyl O of Gly52'. In the other subunit, the main chain residues around Val48 have shifted by 0.7 Å at the carbonyl C of Val48 while there is little change in the side chain of Phe53. As a result, the Cα of Val48 has lost most of the favorable van der Waals interactions with the ring of Phe53. However, the Cβ and CG2 atoms of Val48 have gained new interactions with the ring of Phe53. Similar to the other subunit, CG2 of Val48 has gained new interactions with carbonyl O and C of Gly52. Those new interactions may partially compensate for the missing interactions between Cα of Gly48 and the ring of Phe53 in the wild type PR. So Val48 did not simply disturb the interactions with the neighboring residues as expected, but structural adjustments partially compensated for lost interactions.

Other structural changes in PR_{G48V}-DRV were at the 80's loop. Residue 48 was near the 80's loop but there were no van der Waals contacts of less than 4.2 Å interatomic distance. The 80's loop in PR_{G48V}-DRV has shifted up to 0.7 Å at N of Pro81' towards Val48 from the position in the wild type PR-DRV, nevertheless the residues were still too far apart to make favorable interactions.

The carbonyl O of residue 48 makes direct interactions with at least four atoms of darunavir in both major (60%) and minor (40%) conformations. The carbonyl O of Val48 shifted 0.9 Å relative to the position in wild type PR-DRV. As a result, the carbonyl O of Val48 has gained more van der Waals interactions with both conformations of darunavir, mainly with the minor conformation. Also the

interactions (O….HC) with darunavir were 0.5 Å shorter and likely to be stronger as indicated in Figure 4.7. In addition, the side chain of Val48 has gained a new van der Waals interaction with the darunavir. Therefore, the PR_{G48V}-DRV structure showed compensating changes and new interactions with darunavir, suggesting that mutation G48V is unlikely to cause resistance in the treatment with darunavir.

A previously reported crystal structure of $PR_{G48V/L90M}$-SQV, however, shows that the position of bound saquinavir has adjusted to accommodate the side chain of Val48, so that larger gaps form between inhibitor and $PR_{G48V/L90M}$. Consequently, the carbonyl O of Val48 loses the hydrogen bond interactions with saquinavir (Hong 2000). In addition, there are fewer van der Waals interactions between saquinavir and the flap (residues 47–50) (Hong 2000). These structural changes may explain why G48V is a primary mutation observed in isolates that are resistant to saquinavir. Nevertheless, reduced interactions between PR and inhibitor were not observed in the structure of PR_{G48V}-DRV, which is consistent with the absence of mutation G48V in mutants resistant to darunavir.

PR_{I50V}-SQV

Residue 50 lies at the tip of the flap and the carbonyl O forms a hydrogen bond interaction with Gly51’ from the other subunit (Figure 4.1). The roles of Ile/Val50 in maintaining the flap conformation and binding of indinavir or darunavir have been described previously (Liu 2005; Kovalevsky 2006). In the wild type PR, the side chain of Ile50 forms van der Waals interactions with Thr80’ and Pro81’ from the other subunit of the PR dimer. Thr80 has been proposed to play an important role

in maintaining the mobility of the flap tips by pulling Ile50' in the other subunit out of a hydrophobic pocket (Foulkes 2006). In PR_{I50V}-SQV, the loss of a methyl group in Val50 induced the 80's loop to shift towards Val50 by 1.4 Å at the N atom of Pro81 in one subunit (Figure 4.6), so that contacts (within 4.2 Å) between Val50 and the 80's loop were maintained. Moreover, Val50 has gained new interactions with Ile54'. It appears that the mutation I50V in PR_{I50V}-SQV did not reduce the contacts between the two subunits at the flap tip as observed in the PR_{I50V}-indinavir complex (Liu, 2005).

Generally, the interactions of PR_{I50V} and saquinavir changed little relative to wild type PR-SQV, except at residue Val50. Compared with Ile50, Val50 is shorter by a methyl group. In one subunit, Val50 has lost two van der Waals interactions with saquinavir. However, in the other subunit Val50 has gained a new van der Waals interaction with saquinavir. In our previous studies, a number of attractive interactions between the side chain of Ile50 and inhibitor were lost in the complex of PR_{I50V} with darunavir and indinavir (Liu 2005; Kovalevsky 2006). This is in agreement with the fact that the mutation I50V is observed in isolates resistant to darunavir and shows relatively low inhibition by indinavir, but it is not commonly observed during the treatment with saquinavir.

PR_{I54M}-DRV, PR_{I54M}-SQV, PR_{I54V}-DRV, and PR_{I54V}-SQV

Residue 54 is located on the opposite side of the flap from residue 48 (Figure 4.1). Both mutations I54V and I54M are observed in isolates resistant to darunavir at intermediate and high levels, respectively. Mutation I54V appears in variants resistant

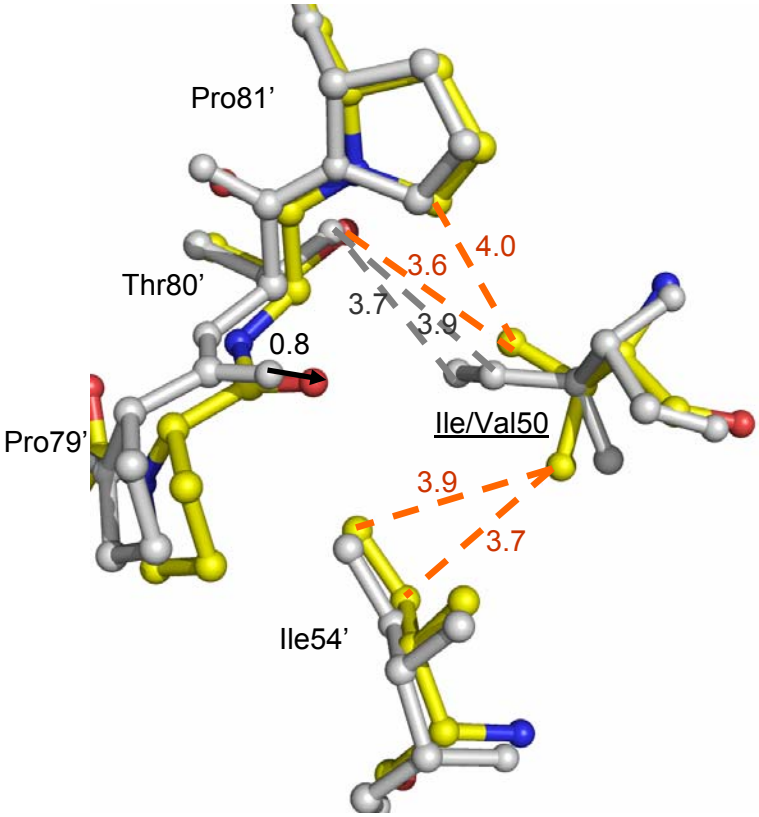
Pro81'
Thr80'
Pro79'
0.8
3.6
4.0
3.7
3.9
Ile/Val50
3.9
3.7
Ile54'

(a)

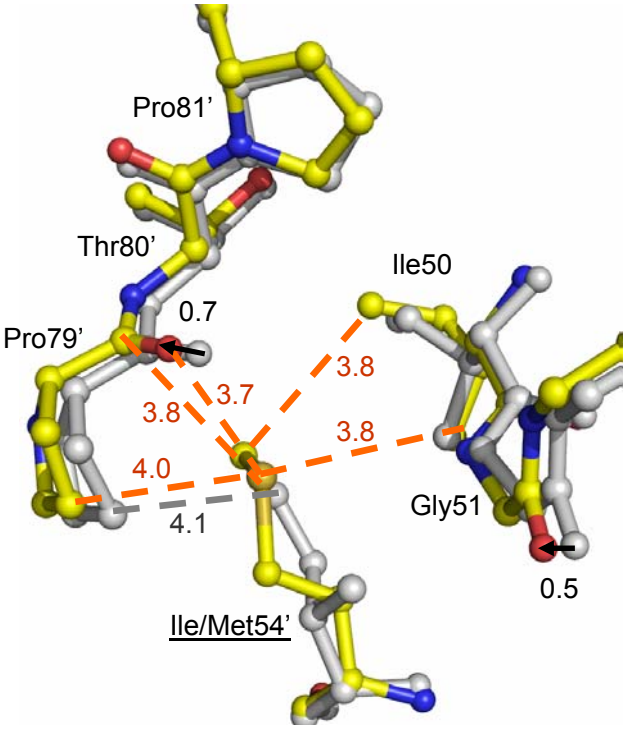
Pro81'
Thr80'
Pro79'
0.7
Ile50
3.8
3.7
3.8
3.8
4.0
4.1
Gly51
0.5
Ile/Met54'

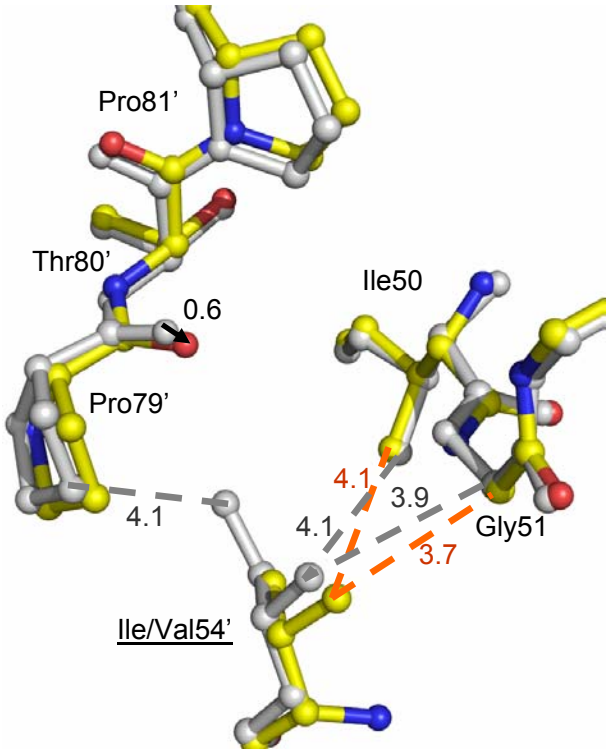

(c)

Figure 4.6: The interactions of residues 50, 51, 54 and 79-81 in (a) PR_{I50V}-SQV, (b) PR_{I54M}-DRV and (c) PR_{I54V}-DRV. The structures of mutants are colored by atom types and corresponding structures of wild type are grey. Dashed lines indicate van der Waals interactions with interatomic distances shown in Å. The arrows show the shifted distances in Å between the two structures.

to saquinavir, but mutation I54M has not been reported (Shafer 2002). Mutation I54M appears most frequently among mutations newly detected after amprenavir (chemically related to darunavir) treatment (Murphy 2004).

Significant structural changes were observed at the 80's loop in mutants complexed with saquinavir and darunavir in comparison with the corresponding wild type PR complexes. The 80's loop has shifted away from Met54 in PR_{I54M} and towards Val54 in PRI54V to adapt to the altered size of the side chains in residue 54 (Figure 4.6). In PRI54M-DRV, the carbonyl O of Pro79 has shifted away from Met54 by 0.7 Å and 1.4 Å in two subunits, respectively, in order to accommodate the longer Met side chain. Despite this movement, Met54 has gained new van der Waals interactions with Pro79 and side chain of Ile50 from the other subunit. In the other hand, the flap tip has shifted towards Met54 by 0.5 Å at the carbonyl O of Gly51, because there is more space due to the absence of CG1 atom of Ile in Met54. However, the mutation I54V introduces a smaller side chain, so the 80's loop has shifted towards Val54 by 0.6 Å and by ~ 0.1 Å at the carbonyl O of Pro79' in two subunits of PRI54V-DRV, respectively (Figure 4.6). Even with the 0.6 Å shift, no new interactions were formed between Val54 and the 80's loop. Different from PRI54M, the tip of the flap did not have significant change in PRI54V relative to the wild type PR structures.

The shift of the 80's loop caused by the mutation of 54 residue modified the interactions between inhibitor and PR clearly in PR_{I54M}-DRV, but not in the other complexes. In PR_{I54M}-DRV, residues 78-82 were further away from 54 in the flap, so the interactions between Pro81-Val82 and darunavir (the major conformation) were

weaker (the interatomic distance is 0.3-0.4 Å longer) than in the wild type as indicated in Figure 4.7. The hydrogen bond interaction between the amino group of darunavir (in the major conformation) and OD2 of Asp30 in the wild type PR was absent in PR_{I54M}-DRV, instead a water mediated the interactions between the two atoms. In the minor conformation of darunavir, however, the hydrogen bond interactions between the amino group and OD2 of Asp30 were maintained. In addition, the hydrogen bond interaction between amino group and carbonyl O of Asp30 was absent (within the interatomic distance of 4.5 Å). The loss of interactions may suggest one reason for the reduced susceptibility of virus containing PR_{I54M} to darunavir. However, no significant structural changes in the PR-inhibitor interaction were observed in PR_{I54V}-DRV, PR_{I54V}-SQV and PR_{I54M}-SQV complexes relative to the corresponding wild type PR complexes. Therefore, mutation I54M caused more obvious conformational changes than mutation I54V in the flap region and the inhibitor binding site. This is consistent with the fact that mutation I54M more commonly appears than I54V in the treatment with amprenavir and darunavir (Murphy 2004).

The Comparison of Saquinavir and Darunavir

The differences between saquinavir and darunavir interactions were investigated in the complexes of PR_{I54M} and PR_{I54M}. The major differences between PR_{I54M}-SQV and PR_{I54M}-DRV as well as between PR_{I54V}-SQV and PR_{I54V}-DRV were located in the flap and the 80's loop. Overall, the interactions of saquinavir and

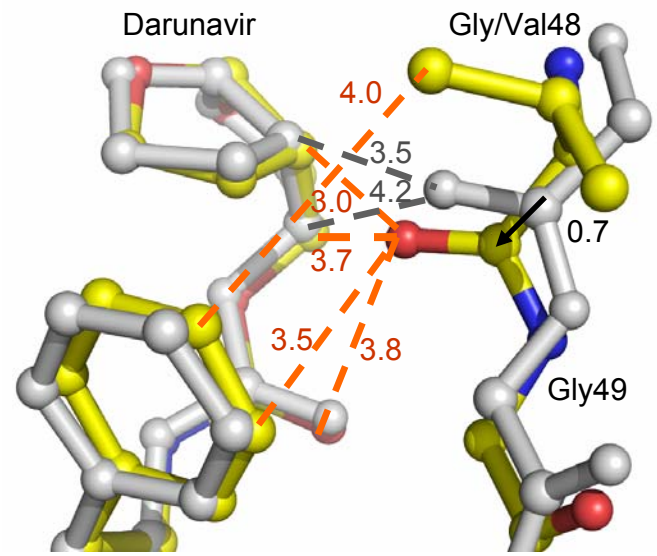

(a)

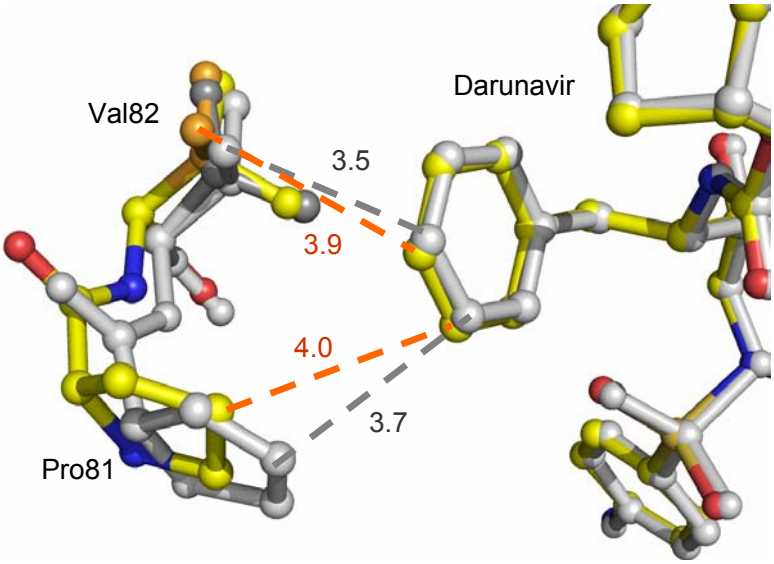

(b)

Figure 4.7: Selected PR-inhibitor interactions of (a) G48V-DRV and (b) I54M-DRV with Val82 shows alternate conformations. Darunavir is shown in minor conformations in all structures. The structures of mutants are colored by atom types and the structure of wild type PR-DRV is colored grey. Dashed lines indicate van der Waals interactions with interatomic distances shown in Å. The arrows show the shifted distances in Å between the two structures.

darunavir with PR_{I54V} were more similar than those with PR_{I54M} so the complexes with PR_{I54M} were used as examples to illustrate the differences between saquinavir and darunavir.

Saquinavir with 49 non-hydrogen atoms is larger than darunavir with 38 non-hydrogen atoms. The major PR-inhibitor interactions for saquinavir and darunavir are illustrated in Figure 4.8. Saquinavir has larger hydrophobic groups at both ends of the molecule so it forms more van der Waals interactions with numerous PR residues (Figure 4.8). However, darunavir forms 3 more direct hydrogen bonds with the main chain atoms of Asp29 and Asp30 than does saquinavir (Tie 2004; Tie 2006). The van der Waals interactions between PR and hydrophobic groups of saquinavir are possibly more vulnerable to changes due to mutations of residues in the binding site. Therefore, the binding affinity for saquinavir can be reduced more easily by mutation. On the contrary, the hydrogen bond interactions of darunavir with main-chain atoms of PR are not directly affected by mutations. Therefore, darunavir can more flexibly adapt to the changes due to mutations of the active site thus maintaining the affinity for mutated PR. Through this strategy, darunavir preserves its effectiveness to many (but not all) drug resistant mutants (Koh 2003). PR_{I54M} and PR_{I50V} showed weaker interactions with darunavir compared to the wild type PR (Figure 4.7), which is consistent with the fact that both mutants appear in HIV isolates showing resistance to darunavir but not in those resistant to saquinavir. This may suggest that saquinavir adapts to the changes caused by I54M and I50V better does than darunavir.

Another major difference between these two inhibitors was that saquinavir forms one hydrogen bond with carbonyl O of Gly48 while this interaction is

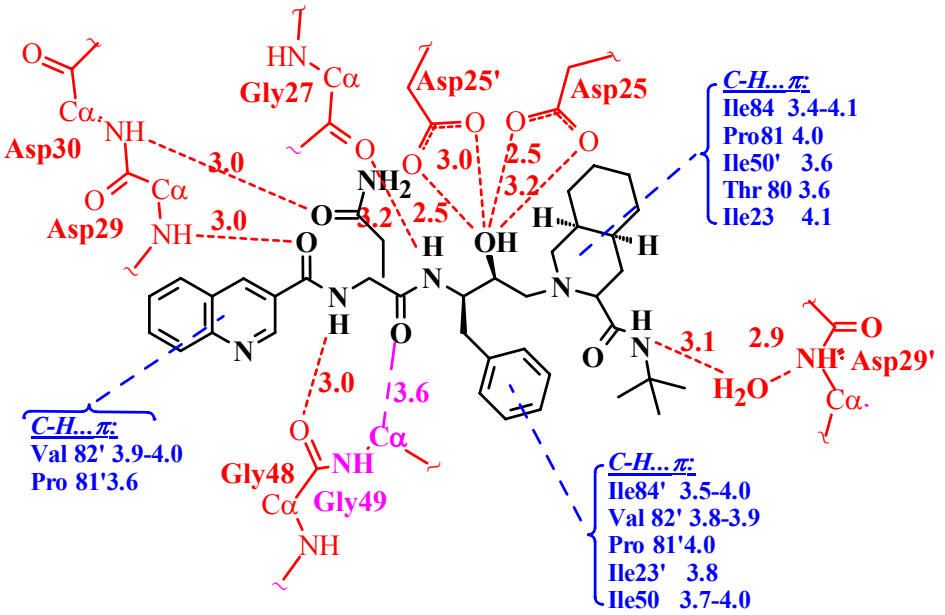

(a)

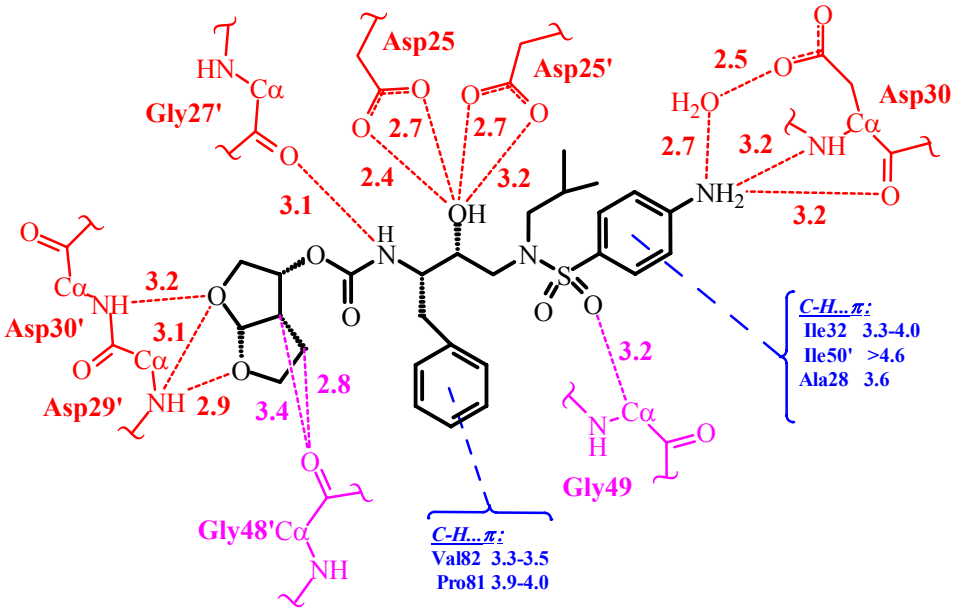

(b)

Figure 4.8: PR-inhibitor interactions in PR_{I54M}. (a) The major orientation of saquinavir. (b) The major orientation of darunavir. Hydrogen bonds are indicated in red and CH-π in blue and CH….O in purple. Interatomic distances are shown in Å.

substituted by two weaker (CH…O) interactions in darunavir complexes. The hydrogen bond between Gly48 and saquinavir can be disturbed as observed in mutant $PR_{G48V/L90M}$-SQV (Hong 2000). However, the interactions (CH…O) between Val48 and darunavir in PR_{G48V}-DRV were even tighter than in the wild type PR-DRV. This may explain why PR_{G48V} provides resistance to saquinavir but maintains susceptibility to darunavir.

Moreover, saquinavir interacts (CH…O) with Gly49 Cα atom and Gly48 carbonyl O atom in one subunit of PR, while equivalent interactions occur in two subunits of PR dimer for darunavir. In this way, darunavir may stabilize the PR dimer more than does saquinavir.

CONCLUSION

The crystal structures of flap mutants (PR_{G48V}, PR_{I50V}, PR_{I54V}, and PR_{I54M}) complexed with two clinical drugs saquinavir and darunavir have been determined to high resolutions. The inhibitor complexes of drug resistant mutants revealed conformational and interaction changes relative to their wild type PR complexes. Analysis showed that the introduction of mutations in the flap caused conformational modifications of the flap in all the complexes with the biggest deviations observed in the PR_{G48V}-DRV complex. In all the complexes, the 80's loop was flexibly adjusted to accommodate the sizes of neighboring residues. It shifted towards smaller residues Val50 and Val54, and away from longer residue Met54. Nevertheless, it shifted towards the bigger side chain of Val48 since the side chain of mutated residue was further away from the 80's loop. The 80's loop shifts did not cause the interactions

between inhibitor and PR to alter significantly in most of complexes except for PR_{G48V}-DRV and PR_{I54M}-DRV. The interactions with darunavir were enhanced in PR_{G48V}-DRV but were weakened in PR_{I54M}-DRV because of the shift of the 80's loop. The crystal structure suggests that resistance to darunavir by HIV isolates with I54M mutations may arise from the reduced binding affinity of inhibitor. This mechanism is also used by PR_{I50V} to provide resistance to darunavir and by $PR_{G48V/L90M}$ to provide resistance to saquinavir as suggested in previous studies (Hong 2000; Kovalevsky 2006). However, the reduced inhibitor interactions were not observed in the structures of PR_{I54V}-DRV, PR_{I54V}-SQV and PR_{I54M}-SQV. These structures revealed that saquinavir and darunavir differ in their interactions with different mutants. Darunavir is a better inhibitor than saquinavir for mutants with G48V, while it is the opposite for I54M. Therefore, this study has extended our understanding on the important role of residues in the flap region and the structural basis for drug resistance.

OVERALL SUMMARY

The protease inhibitors (PIs), combined with other anti-HIV drugs, have shown great success in treating HIV infection by reducing mortality and morbidity of HIV-infected individuals. However, the long-term effectiveness of treatment is undermined due to the rapid development of drug resistance. The drug resistant mutants of HIV-1 protease (PR) have been extensively studied to understand the molecular basis of the drug resistance. In many cases, mutations in the active site cavity directly disturb the interactions between the mutated residues and the inhibitor, thus the variant PR shows reduced affinity for inhibitor. In addition, mutated residues can indirectly modify the interaction of other residues with the inhibitor.

My research has focused on the drug resistant mutations in the flap (M46L, G48V, I50V, F53L, I54V and I54M) and the distal regions (L24I and G73S) of PR. These mutations have been observed in the patients treated with PIs and contribute to drug resistance to different drugs. Here, I have characterized the roles of single mutations in the development of drug resistance to indinavir, saquinavir and darunavir through crystallographic and kinetics analysis. In general, the mutated residues are observed to alter the PR properties including catalytic efficiency, conformation of the flap, dimer interface, interactions with the neighboring residues, the 80's loop and binding affinity of inhibitor/substrate (Figure 13).

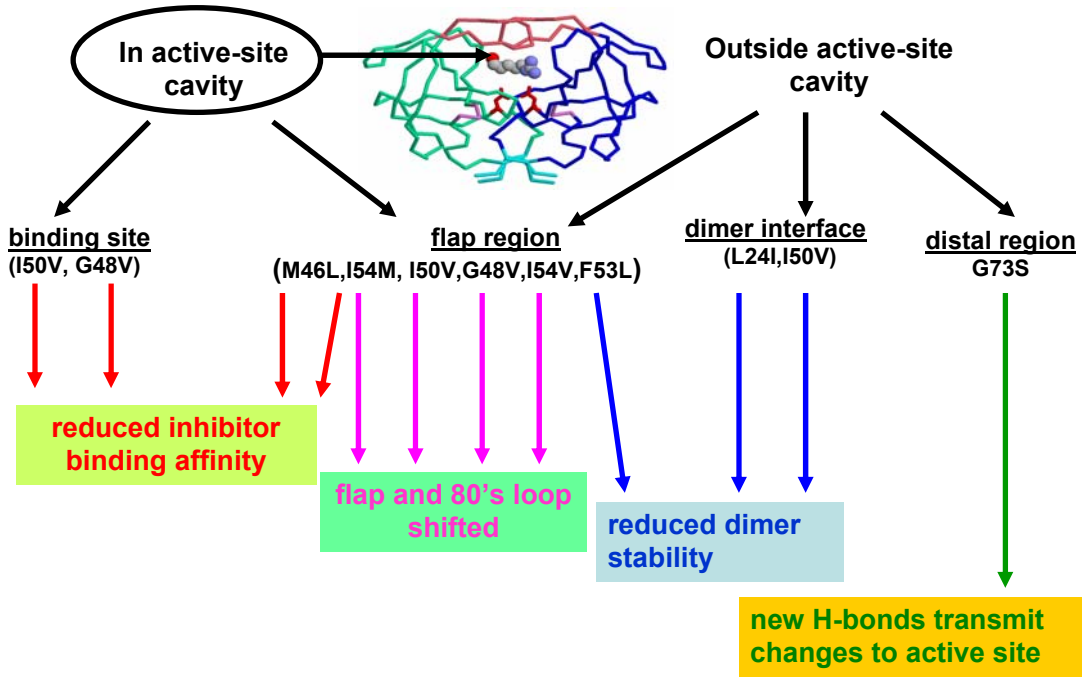

Figure 13: the summary of drug resistance mechanisms of HIV-1 protease mutants.

The mutations in the flap region

Due to the important role of the flap in substrate/inhibitor binding and intersubunit interactions, flap mutations are expected to be able to modify the PR activity, dimer stability and flap conformation. The drug resistant mutants of residues 46, 48, 50, 53 and 54 are the most commonly reported in the treatment with PIs and these mutations are frequently combined with the mutations in active site cavity. The mutations in the flap residues result in intermediate to high levels of resistance to most of the approved PIs.

Mutation F53L arises at low frequency in patients treated with multiple PIs. The PR_{F53L} dimer showed 15% of catalytic efficiency, 60% of dimer stability, 20-fold weaker inhibition by indinavir and similar inhibition by two peptide analog inhibitors relative to wild type PR. A high-resolution (1.35 Å) crystal structure of unliganded PR_{F53L} revealed that the tips of the flaps in PR_{F53L} dimer had a wider separation than in unliganded wild type PR. The mutation F53L eliminated favorable interactions between two subunits in the flap region, thus the flap in PR_{F53L} might be significantly more flexible than in the wild type PR and thus potentially reduces the binding affinity of an inhibitor. Therefore, the single mutation F53L produced substantial structural changes in the flap region in the absence of inhibitor, which suggests a new mechanism for drug resistance.

The mutation M46L provides resistance to most of the clinical PIs at intermediate to high levels, with the possible exception of saquinavir and darunavir. The main-chain atoms of Met46 can form hydrogen bonds with substrate analogs, but they do not make direct contacts with smaller PIs. Surprisingly, the crystal structure

of PR_{M46L} complexed with daruanvir (at 1.22 Å resolution) showed two inhibitor binding sites: the active site cavity as well as a new site on the flap surface. The darunavir in the active site cavity showed fewer interactions in PR_{M46L} than in wild type PR. At the second binding site, darunavir existed in a different form of diastereomer from the one in active site cavity. One half of the darunavir molecule was bound on the flap by several strong interactions with the PR, while the rest made a few hydrophobic contacts with three symmetry-related PR molecules. The conformations of residues at the second binding site were altered to accommodate the binding of darunavir. It is likely that the mutation M46L stabilized the PR flap and facilitated the binding of darunavir on the flap surface. The second inhibitor binding site may explain the significant effectiveness of darunavir on the various drug resistant mutants since other drugs probably can not bind there. Moreover, this new crystal structure with the second darunavir binding site provides a distinct model for the design of novel inhibitors targeting the flap of the HIV-1 PR.

Mutation I50V is located at the tip of the flap and makes hydrogen bond interactions with the Gly51' from the other subunit of the PR dimer. The substitution of Ile50 by Val resulted in reduced intersubunit interactions and increased dimer dissociation. Although this mutation is very rarely observed in mutants resistant to indinavir, PR_{I50V} had 50-fold higher Ki value for indinavir relative to wild type PR. The crystal structure of PR_{I50V} complexed with indinavir, which was determined at 1.1 Å resolution, revealed that Val50 had reduced van der Waals interactions with indinavir in agreement with the significantly weaker inhibition. Interestingly, the crystal structure of PR_{I50V} complexed with saquinavir did not show weaker

interactions between PR and saquinavir as observed in the complex with indinavir. Although Val is smaller in size than Ile, the mutated residueVal50 maintained good interactions with the 80's loop. The structural changes agreed with the fact that I50V is not a resistant mutation observed in the treatment with saquinavir.

Residue 48 is positioned in the flap region and makes contacts with substrates and inhibitors bound in the active site cavity. Mutation G48V is the primary drug resistant mutation selected in the treatment with saquinavir and it, alone, causes 10-fold resistance to saquinavir. The crystal structure of the double mutant $PR_{G48V/L90M}$ complexed with saquinavir shows the PR-inhibitor interactions are weakened in order to accommodate the larger side chain in G48V mutation. However, the crystal structure of PR_{G48V}-DRV showed darunavir bound to PR_{G48V} with more favorable interactions than in the wild type PR. In addition, the mutation Val48 altered the interactions with the neighboring residue Phe53 on the flap.

Mutations I54V and I54M, located on the other side of residue 48 across the flap hairpin structure, cause PR to be resistant to the new PI darunavir at intermediate and high level, respectively. The crystal structures of PR_{I54V} and PR_{I54M} complexed with saquinavir and darunavir were determined at the resolutions of 1.05-1.20 Å. Structural comparison revealed that the introduction of mutation at 54 caused the conformational changes in the flaps and the 80's loop. The 80's loop was shifted away from Met54 by 0.7 Å at the carbonyl O of Pro79 in PR_{I54M}-DRV from the position in the wild type PR-DRV, while it was shifted towards Val54 by 0.6 Å at the equivalent position in PR_{I54V}-DRV. Therefore, the conformational movement of the 80's loop was directly related to the changes in the side-chain size of the mutated

residue, independent of the bound inhibitor. A certain separation seems to be required between residue 54 and the 80's loop. However, the shift of the 80's loop did not result in the significant changes in any interactions between PR and inhibitor. Only a couple of van der Waals interactions between Pro81 and Val82 and the minor conformation of darunavir become weaker by lengthening (0.3-0.4 Å) the interatomic distances in PR_{I54M}-DRV.

The mutations in the distal regions

Mutations L24I and G73S are consistently observed at lower frequency in AIDS patients exposed to indinavir. They alter residues next to the catalytic Asp25 and on the surface of PR, respectively. The analysis of kinetics, dimer stability, and crystal structures of the HIV drug-resistant mutants PR_{L24I} and PR_{G73S} has shown distinct mechanisms used by these two mutants to resist inhibition by indinavir. The catalytic activity of PR_{L24I} dropped to less than 4% of the value for wild type PR, which is in good agreement with the sensitive location of residue 24 next to the catalytic Asp25. The relative Ki for indinavir became 2.6-fold higher in PR_{L24I}. The crystal structure of PR_{L24I} complexed with indinavir showed that mutation L24I eliminated the intersubunit interactions between Ile24 and Phe99' and consequently reduced the dimer stability of the mutant.

Residue 73 is on the protein surface and far from the active site cavity. However, G73S is reported to appear in HIV variants showing low levels of resistance in the treatment with all approved PIs, always combined with other mutations. The activity, dimer dissociation and structural properties of G73S were

very similar to those of the wild type PR. However, the relative k_{cat}/K_m of PR_{G73S} varied from 14-400% for different substrates compared to wild type PR values. Interestingly, Ser73 in PR_{G73S}-IDV formed new hydrogen bonds with Asn88, which made hydrogen bonds with Thr31 and Asp29 in the active site cavity. Therefore, the structural changes can be transmitted from residue 73 on the PR surface to the substrate binding site.

The protease inhibitors indinavir, saquinavir and darunavir

The design and modification of most of PIs are guided by the crystal structures of PR complexed with inhibitor. Saquinavir and indinavir were the initial protease inhibitors approved by FDA and are still widely used in the HAART treatment. Multiple drug resistant mutants arise with varied levels of resistance to these two inhibitors. Darunavir is a recently approved PI and it has shown excellent inhibitory profile for most of drug resistant variants, so it (boosted with ritonavir) is recommended for patients who fail in the treatment with other PIs. Saquinavir and indinavir were designed based on the structure of a natural substrate of PR, while darunavir was modified by introducing more hydrogen bonds to the main chain atoms of PR with the purpose of maintaining its potency for drug resistant mutants.

Indinavir and saquinavir are larger than darunavir because they have larger hydrophobic groups at both ends of their structures. Therefore, indinavir and saquinavir form more van der Waals interactions with PR residues. However, darunavir forms more favorable hydrogen bonds directly with the main chain atoms of PR than indinavir and saquinavir. Indinavir has more water mediated hydrogen

bond interactions than the other two inhibitors. The hydrogen bond interactions between main-chain PR and darunavir are hardly affected by mutations at the active site and other regions of PR. On the contrary, the van der Waals interactions between PR residues and hydrophobic groups of indinavir and saquinavir are more susceptible to changes thus the inhibitor binding affinity is more easily reduced in mutants. Therefore, darunavir establishes an excellent example for designing new drugs by maximizing the favorable interactions with the main chain residues to combat drug resistance of HIV.

My studies drug resistant mutants of HIV protease has confirmed that drug resistance can arise when mutations alter the PR dimer interface at the flaps or the terminal beta sheet, as well as when mutations directly alter the inhibitor binding site. Furthermore, distal mutations with relatively minor effects can transmit changes to the substrate binding site and contribute to viral resistance. PR variants with drug resistant mutations in the flap and distal regions have shown diverse changes in catalytic activity, inhibition constants, dimer stability, the flap conformation and inhibitor binding. Changes caused by mutations at distal regions can also be transmitted to the inhibitor/substrate binding site. Drug resistant mutations can cause changes in any of the above factors or combinations of those factors. In most cases, the observed structural changes in mutations were consistent with kinetic and stability changes.

Therefore, my studies of the flap mutants and distal mutants have extended our understanding of the drug resistant mechanisms of indinavir, saquinavir and darunavir in different mutants of HIV-1 protease. Atomic resolution crystal structures

will be important for the design of more effective inhibitors for resistant mutants. In particular, the structures of unliganged PR_{F53L} and of PR_{M46L} with darunavir bound in two sites provide valuable frameworks for designing novel inhibitors either to prevent the closure of flap or to target on the flap surface. In addition, these results will provide guidance for physicians to select the optimal regimens for AIDS patients who carry certain PR mutations.

REFERENCES:

Ala, P. J., DeLoskey, R.J., Huston, E.E., Jadhav, P.K., Lam, P.Y. S. , Eyermann, C.J., Hodge, C.N. Schadt, M.C., Lewandowski, F.A., Weber,P.C., McCabe, D.D., Duke,J.L. and Chang C.H. (1998). "Molecular Recognition of Cyclic Urea HIV-1 Protease Inhibitors." J. Biol. Chem. **273**: 12325 - 31.

Antonov, V. K., Ginodman, L.M., Rumsh, L.D., Kapitannikov, Y.V., Barshevskaya, T.N., Yavashev, L.P., Gurova, A.G., Volkova, LI. (1981). "Studies on the mechanisms of action of proteolytic enzymes using heavy oxygen exchange." Eur J Biochem **117**: 195-200.

Barbaro, G. (2006). "Highly active antiretroviral therapy-associated metabolic syndrome: pathogenesis and cardiovascular risk." Am J Ther **13**: 248-60.

Barre-Sinoussi, F., Chermann, J.C., Rey, F., Nugeyre, M.T., Chamaret, S., Gruest, J., Dauguet, C., Axler-Blin, C., Vezinet-Brun, F., Rouzioux, C., Rozenbaum, W., Montagnier, L. (1983). "Isolation of a T-lymphotropic retrovirus from a patient at risk for acquired immune deficiency syndrome (AIDS)." Science **220**: 868-71.

Beck, Z. Q., Morris, G.M., Elder, J.H. (2002). "Defining HIV-1 protease substrate selectivity." Curr Drug Targets Infect Disord **2**: 37-50.

Berman, H. M., Westbrook, J., Feng, Z., Gilliland, G., Bhat, T.N., Weissig, H., Shindyalov, I.N., Bourne, P.E. (2000). "The Protein Data Bank." Nucleic Acids Res **28**: 235-42.

Boden, D., Markowitz, M. (1998). "Resistance to immunodeficiency virus type 1 protease inhibitors." Antimicrobial Agents and Chemotherapy **42**: 2775-83.

Brik, A., Wong, C.H. (2003). "HIV protease: mechanism and drug discovery." Org Biochem Chem **1**: 5-14.

Brown, A. J., Korber, B.T.,Condra, J.H. (1999). "Associations between amino acids in the evolution of HIV type 1 protease sequences under indinavir therapy." AIDS Res. Hum. Retroviruses **15**: 247-253.

Brynda, J., Rezacova, P., Fabry, M., Horejsi, M., Stouracova, R., Sedlacek, J., Soucek, M., Hradilek, M., Lepsik, M., Konvalinka, J. (2004). "A phenylnorstatine inhibitor binding to HIV-1 protease: geometry, protonation, and subsite-pocket interactions analyzed at atomic resolution." J Med Chem. **47**: 2030-6.

Cairns, J., Overbaugh, J., Miller, S. (1988). "The origin of mutants." Nature **335**: 142-5.

Chen, Z., Li, Y., Schock, H.B., Hall, D., Chen, E., Kuo, L.C. (1995). "Three-dimensional structure of a mutant HIV-1 protease displaying cross-resistance to all protease inhibitors in clinical trials." J Biol Chem **270**: 433-6.

Chen, Z., Li, Y., Schock, H.B., Hall, D., Chen, E., Kuo, L.C. (1995). "Three-dimensional structure of a mutant HIV-1 protease displaying cross-resistance to all protease inhibitors in clinical trials. ." J. Biol. Chem. **270**: 433-436.

Chiu, Y. L., Greene, W.C. (2006). "APOBEC3 cytidine deaminases: distinct antiviral actions along the retroviral life cycle." J Biol Chem. **281**: 8309-12.

Chun, T. W., Stuyver, L., Mizell, S. B., Ehler, L. A., Mican, J. A., Baseler, M., Lloyd, A. L., Nowak, M. A., Fauci, A.S. (1997). "Presence of an inducible HIV-1

latent reservoir during highly active antiretroviral therapy." Proc Natl Acad Sci **94**: 13193-7.

Clavel, F., Hance, A.J. (2004). "HIV Drug Resistance." N Engl J Med **350**: 1023-35.

Clemente, J. C., Moose, R.E., Hemrajani, R., Whitford, L.R., Govindasamy, L., Reutzel, R., McKenna,R., Agbandje-McKenna, M., Goodenow, M.M., Dunn, B.M. (2004). "Comparing the accumulation of active- and nonactive-site mutations in the HIV-1 protease." Biochem. **43**: 12141-51.

Coffin, J. M., Hughes, S.H., Varmus, H.E. (1997). "Retrovirus." Cold Spring Harbor Laboratory Press (ebook).

Cohen, G. E. (1997). "ALIGN: a program to superimpose protein coordinates, accounting for insertions and deletions." J Appl Cryst **30**: 1160-1.

Collaborative Computational Project, N. (1994). "The CCP4 Suite: Programs for Protein Crystallography." Acta Cryst. D **50**: 760-3.

Collins, J. R., Burt, S.K., Erickson, J.W. (1995). "Flap opening in HIV-1 protease simulated by 'activated' molecular dynamics." Nat Struct Biol. **2**: 334-8.

Condra, J. H., Petropoulos, C.J., Ziermann, R., Schleif, W.A. , Shivaprakash, M. and Emini,E.A. (2000). "Drug resistance and predicted virologic responses to human immunodeficiency virus type 1 protease inhibitor therapy." J Infect Dis **182**: 758-765.

Condra, J. H., Schleif, W.A., Blahy, O.M., Gabryelski, L.J., Graham, D.J., Quintero, J.C., Rhodes, A., Robbins, H.L., Roth, E., Shivaprakash, M. (1995). "In vivo emergence of HIV-1 variants resistant to multiple protease inhibitors." Nature **374**: 569-71.

Croteau, G., Doyon, L., Thibeauly, D., Mckercher, G., Pilote, L., Lamarre, D. (1997). "Impaired fitness of human immunodeficiency virus type 1 variants with high-level resistance to protease inhibitor." J Virol **71**: 1089-96.

Darke, P. L., Nutt, R.F., Brady, S.F., Garsky, V.M., Ciccarone, T.M., Leu, C.T., Lumma, P.K., Freidinger, R.M., Veber, D.F., Sigal, I.S. (1988). "HIV-1 protease specificity of peptide cleavage is sufficient for processing of gag and pol polyproteins." Biochem Biophys Res Commun **156**: 297-303.

De Clercq, E. (2004). "Antivirals and antiviral strategies." Nature Rev. Microbiol **2**: 704–720.

De Mendoza, C., Gallego, O., Soriano, V. (2002). "Mechanisms of resistance to antiviral drugs - clinical implications." AIDS Rev **4**: 64-82.

De Meyer, S., Azijn, H., Surleraux, D., Jochmans, D., Tahri, A., Pauwels, R., Wigerinck, P., de Bethune, M.P. (2005). "TMC114, a novel human immunodeficiency virus type 1 protease inhibitor active against protease inhibitor-resistant viruses, including a broad range of clinical isolates." Antimicrob Agents Chemother **49**: 2314-21.

Deng, H., Liu, R., Ellmeier, W., Choe, S., Unutmaz, D., Burkhart, M., Di Marzio, P., Marmon, S., Sutton, R.E., Hill, C.M., Davis, C.B., Peiper, S.C., Schall, T.J., Littman, D.R., Landau, N.R. (1996). "Identification of a major co-receptor for primary isolates of HIV-1." Nature **381**: 661-6.

Desiraju, G., Steiner, T. (2001). "The Weak Hydrogen Bond in Structural Chemistry and Biology." Oxford University Press, Oxford, NY.

Doyon, L., Croteau, G., Thibeault, D., Poulin, F., Pilote, L., Lamarre, D. (1996). "Second locus involved in human immunodeficiency virus type 1 resistance to protease inhibitors." J. Virol **70**: 3763-9.

Drake, J. W. (1993). "Rates of spontaneous mutation among RNA viruses." PNAS **90**: 4171-4175.

Dunne, A. L., Mitchell, F.M., Coberly, S.K., Hellmann, N.S., Hoy, J., Mijch, A., Petropoulos, C.J., Mills, J., Crowe, S.M. (2001). "Comparison of genotyping and phenotyping methods for determining susceptibility of HIV-1 to antiretroviral drugs." AIDS **15**: 1471-5.

Emini, E. A. (2002). "The human Inmmunodeficiency Virus: Biology, Immunology, and Therapy." Priceton University Press **Chapter 1**(1-43).

Emini, E. A. (2002). "The human Inmmunodeficiency Virus: Biology, Immunology, and Therapy." Priceton University Press **Chapter 13**: 481-509.

Erickson, J. W., Burt, S.K. (1996). "Structural mechanisms of HIV drug resistance." Annu Rev Pharmacol Toxicol **36**: 545-71.

Erickson, J. W., Burt, S.K. (1996). "Structural mechanisms of HIV drug resistance." Ann Rev Pharmacol Toxicol **36**: 545-571.

Ermolieff, J., Lin, X., Tang, J. (1997). "Kinetic properties of saquinavir-resistant mutants of human immunodeficiency virus type 1 protease and their implications in drug resistance in vivo." Biochem. **36**: 12364-12370.

Esnouf, R. M. (1997). "An extensively modified version of MolScript that includes greatly enhanced coloring capabilities." J Mol Graph. Model **15**: 132-4.

Esnouf, R. M. (1999). "Further additions to MolScript version 1.4, including reading and contouring of electron-density maps." Acta Cryst. **D55**: 938 - 940.

Feher, A., Weber, I.T., Bagossi, P., Boross, P., Mahalingam, B., Louis, J.M., Copeland, T.D., Torshin, I.Y., Harrison, R.W., and Tozser, J. (2002). "Effect of sequence polymorphism and drug resistance on two HIV-1 Gag processing sites." Eur J Biochem. **269**(16): 4114-4120.

Finzi, D., Hermankova, M., Pierson, T., Carruth, L. M., Buck, C., Chaisson, R. E., Quinn, T. C., Chadwick, K., Margolick, J., Brookmeyer, R., Gallant, J., Markowitz, M., Ho, D. D, Richman, D.D., Siliciano, R. F. (1997). "Identification of a reservoir for HIV-1 in patients on highly active antiretroviral therapy." Science **278**: 1295-1300.

Foulkes, J. E., Prabu-Jeyabalan, M.,Cooper, D.,Henderson, G. J.,Harris, J.,Swanstrom, R.,Schiffer, C. A. (2006). "Role of invariant Thr80 in human immunodeficiency virus type 1 protease structure, function, and viral infectivity." J Virol **80**: 6906-16.

Freedberg, D. I., Ishima, R., Jacob, J., Wang, Y.X., Kustanovich, I., Louis, J.M., Torchia, D.A. (2002). "Rapid structural fluctuations of the free HIV protease flaps in solution: relationship to crystal structures and comparison with predictions of dynamics calculations." Protein Sci **11**: 221-32.

Fruton, J. S. (1987). "Hydrolytic Enzymes." Elsevier Science Pulishers: 1-37.

Gallo, R. C., Salahuddin, S.Z., Popovic, M., Shearer, G.M., Kaplan, M., Haynes, B.F., Palker, T.J., Redfield, R., Oleske, J., Safai, B., et al. (1984). "Frequent detection and isolation of cytopathic retroviruses (HTLV-III) from patients with AIDS and at risk for AIDS." Science **224**: 500-3.

Gheysen, D., Jacobs, E., de Foresta, F., Thiriart, C., Francotte, M., Thines, D., De Wilde, M. (1989). "Assembly and release of HIV-1 precursor Pr55gag virus-like particles from recombinant baculovirus-infected insect cells." Cell **59**: 103-12.

Ghosh, A. K., Kincaid, J.F., Cho, W., Walters, D.E., Krishnan, K., Hussain, K.A., Koo, Y., Cho, H., Rudall, C., Holland, L., and Buthod, J. (1998). "Potent HIV protease inhibitors incorporating high sffinity P2-ligands and (R)-hydroxyethylaminosufonamide isostere." Bioorg. Med. Chem. Lett. **8**: 979-982.

Girard, M., Habel, A., Chanel, C. (1999). "New prospects for the development of a vaccine against human immunodeficiency virus type 1." C R Acad Sci III **322**: 959-66.

Greene, W. C. (2004). "The brightening future of HIV therapeutics." Nat Immunol. **5**: 867-71.

Griffiths, J. T., Phylip, L.H., Konvalinka, J., Strop, P., Gustchina, A., Wlodawer, A., Davenport, R.J., Briggs, R., Dunn, B.M., Kay, J. (1992). "Different requirements for productive interaction between the active site of HIV-1 proteinase and substrates containing -hydrophobic*hydrophobic- or -aromatic*pro- cleavage sites." Biochemistry **31**: 5193-200.

Grinspoon, S. K. (2005). "Metabolic syndrome and cardiovascular disease in patients with human immunodeficiency virus." Am J Med **118 Suppl 2**: 23S-28S.

Gulnik, S. V., Suvorov, L.I., Liu, B., Yu, B., Anderson, B., Mitsuya, H., Erickson, J.W. (1995). "Kinetic characterization and cross-resistance patterns of HIV-1 protease mutants selected under drug pressure." Biochem **34**: 9282-9287

Gustchina, A., Kervinen, J., Powell, D.J., Zdanov, A., Kay, J., Wlodawer, A. (1996). "Structure of equine infectious anemia virus proteinase complexed with an inhibitor." Protein Sci. **5**: 1453-65.

Gustchina, A., Sansom, C., Prevost, M., Richelle, J., Wodak, S.Y., Wlodawer, A., Weber, I.T. (1994). "Energy calculations and analysis of HIV-1 protease-inhibitor crystal structures." Protein Eng. **7**: 309-317.

Gustchina, A., Weber, I.T. (1990). "Comparison of inhibitor binding in HIV-1 protease and in non-viral aspartic proteases: the role of the flap." FEBS **269**: 269-272.

Harrison, R. W., Weber, I.T. (1994). "Molecular dynamics simulations of HIV-1 protease with peptide substrate." Protein Eng **7**: 1353-63.

Hayes, J. D., Wolf, C.R. (editors) (1997). "The molecular genetic of drug resistance." Harwood Academic Publishers: 24.

Heaslet, H., Kutilek, V., Morris, G.M., Lin, Y.C., Elder, J.H., Torbett, B.E., Stout, C.D. (2006). "Structural Insights into the Mechanisms of Drug Resistance in HIV-1 Protease NL4-3." J Mol Biol **356**: 967-81.

Hertel, J., Struthers, H., Horj, C.B., Hruz, P.W. (2004). "A structural basis for the acute effects of HIV protease inhibitors on GLUT4 intrinsic activity." J Biol Chem **279**: 55147-52.

Hertogs, K., Bloor, S., Kemp, S. D., Van den Eynde, C., Alcorn, T. M., Pauwels, R., Van Houtte, M., Staszewski, S., Miller, V., Larder, B.A. (2000). "Phenotypic

and genotypic analysis of clinical HIV-1 isolates reveals extensive protease inhibitor cross-resistance: a survey of over 6000 samples." AIDS **14**: 1203-10.

Hirsch, M. S., Klibanski, A. (1998). "What price progress? Pseudo-Cushing's syndrome associated with antiretroviral therapy in patients with human immunodeficiency virus infection." Clin Infect Dis. **27**: 73-5.

Ho, D. D., Neumann, A.U., Perelson, A.S., Chen, W., Leonard, J.M., Markowitz, M. (1995). "Rapid turnover of plasma virions and CD4 lymphocytes in HIV-1 infection." Nature **373**: 123-6.

Hong, L., Zhang, X.C., Hartsuck, J.A., and Tang, J. (2000). "Crystal structure of an in vivo HIV-1 protease mutant in complex with saquinavir: insights into the mechanisms of drug resistance." Protein Sci **9**: 1898-904.

Hornak, V., Okur, A., Rizzo, R.C., Simmerling, C. (2006). "HIV-1 protease flaps spontaneously open and reclose in molecular dynamics simulations." Proc Natl Acad Sci **103**: 915-20.

Hornberger, J., Kilby, J.M., Wintfeld, N., Green, J. (2006). "Cost-effectiveness of enfuvirtide in HIV therapy for treatment-experienced patients in the United States." AIDS Res Hum Retroviruses **22**(3): 240-7.

Hruz, P. W., Murata, H., Mueckler, M. (2001). "Adverse metabolic consequences of HIV protease inhibitor therapy: the search for a central mechanism." Am J Physiol Endocrinol Metab **280**: 549-53.

Hsiou, Y., Ding, J., Das, K., Clark, A.D. Jr., Boyer, P.L., Lewi, P., Janssen, P.A., Kleim, J.P., Rosner, M., Hughes, S.H., Arnold, E. (2001). "The Lys103Asn mutation of HIV-1 RT: a novel mechanism of drug resistance." J Mol Biol **309**: 437-45.

Hyland, L. J., Tomaszek, T.A. Jr, Roberts, G.D., Carr, S.A., Magaard, V.W., Bryan, H.L., Fakhoury, S.A., Moore, M.L., Minnich, M.D., Culp. J.S. (1991). "Human immunodeficiency virus-1 protease. 1. Initial velocity studies and kinetic characterization of reaction intermediates by 18O isotope exchange." Biochemistry **30**: 8441-53.

Hyland, L. J., Tomaszek, T.A. Jr., and Meek, T.D. (1991). "Human immunodeficiency virus-1 protease. 2. Use of pH rate studies and solvent kinetic isotope effects to elucidate details of chemical mechanism." Biochemistry **30**: 8454-63.

Ishima, R., Freedberg, D. I., Wang, Y.-X., Louis, J. M., Torchia, D. A. (1999). "Flap opening and dimer-interface flexibility in the free and inhibitor-bound HIV protease." Structure **7**: 1047-55.

Jacobo-Molina, A., Ding, J., Nanni, R.G.,Clark, A.D., Jr., Lu, X. (1993). "Crystal structure of human immunodeficiency virus type 1 reverse transcriptase complexed with double-stranded DNA at 3.0 A resolution shows bent DNA." Proc. Natl. Acad. Sci. **90**: 6320-24.

James, M. N., Sielecki, A., Salituro, F., Rich, D. H., Hoffman, T. (1982). "Conformational flexibility of the active sites of aspartyl proteinases revealed by a pepstatin fragment binding penicillopepsin." Proc. Nat. Acad. Sci. **79**: 6137-41.

Jaskolski, M., Miller, M., Rao, J.K., Leis, J., Wlodawer, A. (1990). "Structure of the aspartic protease from Rous sarcoma retrovirus refined at 2-A resolution." Biochemistry **29**: 5889-98.

Jaskolski, M., Tomasselli, A.G., Sawyer, T.K., Staples, D.G., Heinrikson, R.L., Schneider, J., Kent, S.B., Wlodawer, A. (1991). "Structure at 2.5-A resolution of chemically synthesized human immunodeficiency virus type 1 protease complexed with a hydroxyethylene-based inhibitor." Biochemistry **30**: 1600-9.

Johnson, V. A., Brun-Vezinet, F., Clotet, B., Conway, B., Kuritzkes D.R., Pillay, D., Schapiro, J. M., Telenti, A., Richman, D. D. (2005). "Update of the drug resistance mutations in HIV-1: 2005." Topics in HIV Medicine **13**: 125-31.

Jones, T. A., Zou, J.Y., Cowan, S.W., and Kjeldgaard, M. (1991). "Improved methods for building protein models in electron density maps and the location of errors in these models." Acta Crystallog. **A47**: 110-119.

Jordan, S. P., Zugay, J., Darke, P. L., Kuo, L. C. (1992). "Activity and dimerization of human immunodeficiency virus protease as a function of solvent composition and enzyme concentration." J. Biol. Chem. **267**: 20028- 32.

Judd, D. A., et al. (2001). "Polyoxometalate HIV-1 Protease Inhibitors: A New Mode of Protease Inhibition." J Am Chem Soc **123**: 886-97.

Kempf, D. J., Marsh, K.C., Denissen, J.F., McDonald, E., Vasavanonda, S., Flentge, C.A., Green, B.E., Fino, L., Park, C.H., Kong, X.P. (1995). "ABT-538 is a potent inhibitor of human immunodeficiency virus protease and has high oral bioavailability in humans." Proc. Natl. Acad. Sci. **92**: 2484-8.

King, N. M., Melnick, L., Prabu-Jeyabalan, M., Nalivaika, E.A., Yang, S.S., Gao, Y., Nie, X., Zepp, C., Heefner, D.L., Schiffer, C.A. (2002). "Lack of synergy for inhibitors targeting a multi-drug-resistant HIV-1 protease. ." Protein Sci. **11**: 418-429.

King, N. M., Prabu-Jeyabalan, M., Nalivaika, E.A., Wigerinck, P., de Bethune, M.P., Schiffer, C.A. (2004). "Structural and thermodynamic basis for the binding of TMC114, a next-generation human immunodeficiency virus type 1 protease inhibitor." J Virol **78**: 12012-21.

Koh, Y., Nakata, H., Maeda, K., Ogata, H., Bilcer, G., Devasamudram, T., Kincaid, J. F., Boross, P., Wang, Y. F., Tie, Y., Volarath, P., Gaddis, L., Harrison, R. W., Weber, I. T., Ghosh, A. K., and Mitsuya, H. (2003). "A novel bis-tetrahydrofuranylurethane-containing nonpeptidic protease inhibitors (PI) UIC-94017 (TMC114) potent against multi-PI-resistant HIV in vitro." Antimicrob. Agents Chemother. **47**: 3123-3129.

Kohl, N. E., Emini, E.A., Schleif, W.A., Davis, L.J., Heimbach, J.C., Dixon, R.A., Scolnick, E.M., and Sigal, I.S. (1988). "Active human immunodeficiency virus protease is required for viral infectivity." Proc. Natl. Acac. Sci. **85**: 4686-4690.

Kohlstaedt, L. A., Wang, J., Friedman, J.M., Rice, P.A., Steitz, T.A. (1992). "Crystal structure at 3.5 Å resolution of HIV-1 reverse transcriptase complexed with an inhibitor." Science **256**: 1783-90.

Konvalinka, J., Strop, P., Velek, J., Cerna, V., Kostka, V., Phylip, L.H., Richards, A.D., Dunn,B.M., Kay, J. (1990). "Sub-site preferences of the aspartic

proteinase from the human immunodeficiency virus, HIV-1." FEBS Lett **268**: 35-8.

Kovalevsky, A. Y., Tie, Y., Liu, F., Boross, P.I., Wang, Y.F., Leshchenko, S., Ghosh, A.K., Harrison, R.W., Weber, I.T. (2006). "Effectiveness of nonpeptide clinical inhibitor TMC-114 on HIV-1 protease with highly drug resistant mutations D30N, I50V, and L90M." J Med Chem **49**: 1379-87.

Kraulis, P. J. (1991). "MOLSCRIPT: A program to produce both detailed and schematic plots of protein structures." J. Appl. Cryst. **24**: 946-950.

Kuwata, T., Miyazaki, Y., Igarashi, T., Takehisa, J., Hayami, M. (1997). "The rapid spread of recombinants during a natural in vitro infection with two human immunodeficiency virus type 1 strains." J Virol **71**: 7088-91.

Kwong, A. D., Rao, G.B., Jeang, K.T. (2005). "Viral and cellular RNA Helicase as Antiviral Targets." Nature Reviews Drug Discovery **4**: 845-853.

Lam, P. Y., Jadhav, P.K., Eyermann, C.J., Hodge, C.N., Ru, Y. (1994). "Rational design of potent, bioavailable, nonpeptide cyclic ureas as HIV protease inhibitors." Science **263**: 380-84.

Lapatto, R., Blundell, T., Hemmings, A., Overington, J., Wilderspin, A., Wood, S., Merson, J.R., Whittle, P.J., Danley, D.E., Geoghegan, K.F., et al. (1989). "X-ray analysis of HIV-1 proteinase at 2.7 A resolution confirms structural homology among retroviral enzymes." Nature **342**: 299-302.

Li, M., Laco, G.S., Jaskolski, M., Rozycki, J., Alexandratos, J., Wlodawer, A., Gustchina, A. (2005). "Crystal structure of human T cell leukemia virus protease, a novel target for anticancer drug design." Proc Natl Acad Sci **102**: 18332-7.

Liu, F., Boross, P.I., Wang, Y.F., Tozser, J., Louis, J.M., Harrison, R.W., Weber, I.T. (2005). "Kinetic, stability, and structural changes in high-resolution crystal structures of HIV-1 protease with drug-resistant mutations L24I, I50V, and G73S." J Mol Biol **354**: 789-800.

Liu, F., Kovalevsky, A.Y., Louis, J.M., Boross, P.I., Wang, Y.F., Harrison, R.W., Weber, I.T. (2006). "Mechanism of Drug Resistance Revealed by the Crystal Structure of the Unliganded HIV-1 Protease with F53L Mutation." J Mol Biol **358**: 1191-9.

Logsdon, B. C., Vickrey, J. F., Martin, P., Proteasa G., Koepke, J. I., Terlecky, S. R., Wawrzak, Z., Winters, M. A., Merigan, T. C., Kovari, L.C. (2004). "Crystal Structures of a Multidrug-Resistant Human Immunodeficiency Virus Type 1 Protease Reveal an Expanded Active-Site Cavity." J Virol **78**: 3123-32.

Logsdon, B. C., Vickrey, J.F., Martin, P., Proteasa, G., Koepke, J. I., Terlecky, S.R., Wawrzak, Z., Winters, M.A., Merigan, T.C., Kovari, L.C. (2004). "Crystal structures of a multidrug-resistant human immunodeficiency virus type 1 protease reveal an expanded active-site cavity." J. Virol. **78**: 3123-32.

Louis, J. M., Clore, G.M., Gronenborn, A.M. (1999). "Autoprocessing of HIV-1 protease is tightly coupled to protein folding." Nat. Struct. Biol. **6**: 868-875.

Louis, J. M., Ishima, R., Nesheiwat, I., Pannell, L.K., Lynch, S.M., Torchia, D.A., Gronenborn, A.M. (2003). "Revisiting monomeric HIV-1 protease. Characterization and redesign for improved properties." J Biol Chem. **278**: 6085-9.

Louis, J. M., Weber, I.T., Tozser, J., Clore, G.M., and Gronenborn, A.M. (2000). "HIV-1 protease: maturation, enzyme specificity, and drug resistance." Adv Pharmacol. **49**: 111-146.

Louis, J. M., Wondrak, E.M., Copeland, T.D., Smith, C.A., Mora, P.T., Oroszlan, S. (1989). "Chemical synthesis and expression of the HIV-1 protease gene in E. coli." Biochem Biophys Res Commun. **159**: 87-94.

Luban, J., Bossolt, K.L., Franke, E.K., Kalpana, G.V., Goff, S.P. (1993). "Human immunodeficiency virus type 1 Gag protein binds to cyclophilins A and B." Cell **73**: 1067-78.

Lyle, T. A., Wiscount, C.M., Guare, J.P., Thompson, W.J., Anderson, P.S. (1991). "Benzocycloalkyl amines as novel C-termini for HIV protease inhibitors." J Med Chem **34**: 1228-30.

Maddon, P. J., Dalgleish, A.G., McDougal, J.S., Clapham, P.R., Weiss, R.A., Axel, R. (1986). "The T4 gene encodes the AIDS virus receptor and is expressed in the immune system and the brain." Cell **47**: 333-48.

Mahalingam, B., Boross, P., Wang, Y.F., Louis, J.M., Fischer, C.C., Tozser, J., Harrison, R.W., and Weber, I.T. (2002). "Combining mutations in HIV-1 protease to understand mechanisms of resistance." Proteins: Structure, Function, and Genetics. **48**: 107-116.

Mahalingam, B., Louis, J.M., Hung, J., Harrison, R.W., and Weber, I.T. (2001). "Structural implications of drug resistant mutants of HIV-1 protease: High resolution crystal structures of the mutant protease/substrate analog complexes." Proteins: Structure, Function, and Genetics, **43**: 455-464.

Mahalingam, B., Louis, J.M., Reed, C.C., Adomat, J.M., Krouse, J., Wang, Y.F., Harrison, R.W., and Weber, I.T. (1999). "Structural and kinetic analysis of drug resistant mutants of HIV-1 protease." Eur J Biochem. **263**: 238-245.

Mahalingam, B., Wang, Y.F., Boross, P.I., Tozser, J., Louis, J.M., Harrison, R.W., and Weber, I.T. (2004). "Crystal structures of HIV protease V82A and L90M mutants reveal changes in the indinavir-binding site." Eur J Biochem. **271**((8)): 1516-1524.

Maibaum, J., Rich, D. H. (1988). "Inhibition of porcine pepsin by two substrate analogues containing statine: the effect of histidine at the P2 subsite on the inhibition of aspartic proteinases." J Med Chem **31**: 625-9.

Mansky, L. M. (1998). "Retrovirus mutation rates and their role in genetic variation." JGenVirol **79**: 1337-45.

Mansky, L. M., Temin, H.M. (1995). "Lower in vivo mutation rate of human immunodeficiency virus type 1 than that predicted from the fidelity of purified reverse transcriptase." J Virol **69**: 5087-94.

Martin, P., Vickrey, J. F., Proteasa G., Jimenez, Y.L., Wawrzak, Z., Winters, M. A., Merigan, T. C., Kovari, L.C. (2005). ""Wide-open" 1.3 Å structure of a multidrug-resistant HIV-1 protease as a drug target." Structure **13**: 1887-95.

Meagher, K. L., Carlson, H. A. (2005). "Solvation influences flap collapse in HIV-1 protease." Proteins **58**: 119-125.

Meyer, P. R., Matsuura, S.E., Schinazi, R.F., So, A.G., Scott, W.A. (2000). "Differential removal of thymidine nucleotide analogues from blocked DNA chains by HIV reverse transcriptase in the presence of physiological

concentrations of 2'-deoxynucleoside triphosphates." Antimicrob Agents Chemother **44**: 3465-72.

Meyer, P. R., Matsuura, S.E., So, A.G., Scott, W.A. (1998). "Unblocking of chain-terminated primer by HIV-1 reverse transcriptase through a nucleotide-dependent mechanism." Proc Natl Acad Sci **95**: 13471-6.

Miller, M., Jaskolski, M., Rao, J.K., Leis, J., Wlodawer, A. (1989). "Crystal structure of a retroviral protease proves relationship to aspartic protease family." Nature **337**: 576-9.

Molla, A., Korneyeva, M., Gao, Q. Vasavanonda, S., Schipper, P. J., Mo, H. M., Markowitz, M., Chernyavskiy, T., Niu,P., Lyons, N., Hsu, A., Granneman, G. R., Ho, D. D., Boucher, C. A., Leonard, J. M., Norbeck, D. W. and Kempf, D. J. (1996). "Ordered accumulation of mutations in HIV protease confers resistance to ritonavir." Nat Med **2**: 760-6.

Mulichak, A. M., Hui, J.O., Tomasselli, A.G., Heinrikson, R.L., Curry, K.A., Tomich, C.S., Thaisrivongs, S., Sawyer, T.K., Watenpaugh, K.D. (1993). "The crystallographic structure of the protease from human immunodeficiency virus type 2 with two synthetic peptidic transition state analog inhibitors." J. Biol. Chem. **268**: 13103-9.

Munshi, S., Chen, Z., Yan, Y., Li, Y., Olsen, D.B., Schock, H.B., Galvin, B.B., Dorsey, B., Kuo, L.C. (2000). "An alternate binding site for the P1-P3 group of a class of potent HIV-1 protease inhibitors as a result of concerted structural change in the 80s loop of the protease. ." Acta Crystallogr. **D56**: 381-388.

Murphy, M. D., Marousek, G.I., Chou, S. (2004). "HIV protease mutations associated with amprenavir resistance during salvage therapy: importance of I54M." J Clin Virol **30**: 62-7.

Muzammil, S., Ross, P., Freire, E. (2003). "A major role for a set of non-active site mutations in the development of HIV-1 protease drug resistance." Biochem. **42**(3): 631-638.

Naeger, L. K., Margot, N.A., Miller, M.D. (2001). "Increased drug susceptibility of HIV-1 reverse transcriptase mutants containing M184V and zidovudine-associated mutations: analysis of enzyme processivity, chain-terminator removal and viral replication." Antivir Ther **6**: 115-26.

Navaza, J. (1994). "AMoRe: An automated package for molecular replacement." Acta Cryst. **D50**: 157-163.

Navia, M. A., Fitzgerald, P.M., McKeever, B.M., Leu, C.T., Heimbach, J.C., Herber, W.K., Sigal, I.S., Darke, P.L., Springer, J.P. (1989). "Three-dimensional structure of aspartyl protease from human immunodeficiency virus HIV-1." Nature **337**: 615-20.

Nicholson, L. K., Yamazaki,T., Torchia, D.A., Grzesiek, S., Bax, A., Stahl, S.J., Kaufman, J.D., Wingfield, P.T., Lam, P.Y., Jadhav, P.K. (1995). "Flexibility and function in HIV-1 protease." Nat Struct Biol **2**: 274-80.

Nishio, M., Hirota, M., Umezawa, Y. (1998). "The C-H/pie Interaction. Evidence, Nature, and Consequences." Wiley-VCH, New York, NY

Nivesanond, K., Peeters, A., Lamoen, D., van Alsenoy, C. (2005). "Ab Initio Calculation of the Interaction Energy in the P2 Binding Pocket of HIV-1 Protease." Int J Quant Chem **105**: 292-9.

Noble, S., Foulds, D. (1996). "Saquinavir: a review of its pharmacology and clinical potential in the management of HIV infection." Drugs **52**: 93-112.

Ohtaka, H., Freire, E. (2005). "Adaptive inhibitors of the HIV-1 protease." Prog Biophys Mol Biol **88**: 193-208.

Okimoto, N., Tsukui, T., Hata, M, Hoshino, M., Tsuda, M (1999). "Hydrolysis Mechanism of the Phenylalanine-Proline Peptide Bond Specific to HIV-1 Protease: Investigation by the ab Initio Molecular Orbital Method." J Am Chem Soc **121**: 7349-54.

Otwinowski, Z., Minor, W. (1997). "Processing of X-ray diffraction data in oscillation mode." Methods in Enzymology **276**: 307-326.

Ozer, N., Haliloglu, T., Schiffer, C.A. (2006). "Substrate specificity in HIV-1 protease by a biased sequence search method." Proteins **64**: 444-56.

Palella, F. J. J., Delaney, K.M., Moorman, A.C., Loveless, M.O., Fuhrer, J., Satten, G.A., Aschman, D.J., Holmberg, S.D. (1998). "Declining morbidity and mortality among patients with advanced human immunodeficiency virus infection. HIV Outpatient Study Investigators." N Engl J Med **338**: 853-60.

Partaleis, J. A., Yamaguchi, K., Tisdale, M., Vlair, E.E., Falcione, C., Maschera, B., Myers, R.E., Pazhanisamy, S., Futer, O., Cullinan, A.B., Stuver, C.M., Byrn, R.A., Livingston, D.J. (1995). "In vitro selection and characteization of human immunodeficiency virus type 1 (HIV-1) isolates with reduced sensitivity to hydroxyethylamino sulfonamide inhibitors." J Virol **69**: 5228-35.

Pearl, L., Blundell, T. (1984). "The active site of aspartic proteinases." FEBS Lett **174**: 96-101.

Perelson, A. S., Neumann, A.U., Markowitz, M. etal (1996). "HIV-1 dynamics in vivo: virion clearance rate, infected cell life-span, and viral generation time. ." Science **271**: 1582-1586.

Perryman, A. L., Lin, J.H., McCammon, J.A. (2004). "HIV-1 protease molecular dynamics of a wild-type and of the V82F/I84V mutant: possible contributions to drug resistance and a potential new target site for drugs." Protein Sci. **13**: 1108-23.

Pettit, S. C., Simsic, J., Loeb, D.D., Everitt, L., Hutchison, C.A. 3rd, Swanstrom, R. (1991). "Analysis of retroviral protease cleavage sites reveals two types of cleavage sites and the structural requirements of the P1 amino acid." J Biol Chem **266**: 14539-47.

Piana, S., Carloni, P., Parrinello, M. (2002). "Role of conformational fluctuations in the enzymatic reaction of HIV-1 protease." J Mol Biol **319**: 567-83.

Poorman, R. A., Tomasselli, A.G., Heinrikson, R.L., Kezdy, F.J. (1991). "A cumulative specificity model for proteases from human immunodeficiency virus types 1 and 2, inferred from statistical analysis of an extended substrate data base." J Biol Chem **266**: 14554-61.

Popovic, M., Sarngadharan, M.G., Read, E., Gallo, R.C. (1984). "Detection, isolation, and continuous production of cytopathic retroviruses (HTLV-III) from patients with AIDS and pre-AIDS." Science **224**: 497-500.

Potterton, E., Briggs, P., Turkenburg, M., Dodson, E. A. (2003). "Graphical user interface to the CCP4 program suite." Acta. Cryst. D **59**: 1131-7.

Prabu-Jeyabalan, M., Nalivaika, E., and Schiffer, C.A. (2002). "Substrate shape determines specificity of recognition for HIV-1 protease: analysis of crystal structures of six substrate complexes." Structure **10**(369-81).

Prabu-Jeyabalan, M., Nalivaika, E., Schiffer, C.A. (2002). "Substrate shape determines specificity of recognition for HIV-1 protease: analysis of crystal structures of six substrate complexes. ." Structure **10**: 369-81.

Prabu-Jeyabalan, M., Nalivaika, E.A., King, N.M., and Schiffer, C.A. (2003). "Viability of a drug-resistant human immunodeficiency virus type 1 protease variant: structural insights for better antiviral therapy." J Virol. **77**: 1306-1315.

Preston, B. D., Poiesz, B.J., Loeb, L.A. (1988). "Fidelity of HIV-1 reverse transcriptase." Science **242**: 1168-71.

Rao, J. K., Erickson, J.W., Wlodawer, A. (1991). "Structural and evolutionary relationships between retroviral and eucaryotic aspartic proteinases." Biochemistry **30**: 4663-71.

Ridky, T. W., Kikonyogo, A., Leis, J., Gulnik, S., Copeland, T., Erickson, J., Wlodawer, A., Kurinov, I., Harrison, R.W., and Weber, I.T. (1998). "Drug-resistant HIV-1 proteases identify enzyme residues important for substrate selection and catalytic rate." Biochemistry **37**: 13835-45.

Riviere, Y., Blank, V., Kourilsky, P., Israel, A. (1991). "Processing of the precursor of NF-kappa B by the HIV-1 protease during acute infection." Nature **350**: 625-6.

Roberts, N. A., Martin, J.A., Kinchington, D., Broadhurst, A.V., Craig, J.C., Duncan, I.B., Galpin, S.A., Handa, B.K., Kay, J., Krohn, A., et al (1990). "Rational design of peptide-based HIV proteinase inhibitors." Science **248**: 358-61.

Robertson, D. L., Sharp, P.M., McCutchan, F.E., Hahn, B.H. (1995). "Recombination in HIV-1." Nature **374**: 124-6.

Robinson, L. H., Myers, R.E., Snowden, B.W., Tisdale, M., and Blair, E.D. (2000). "HIV type 1 protease cleavage site mutations and viral fitness: implications for drug susceptibility phenotyping assays." AIDS Res. Hum. Retrovir. **16**: 1149-1156.

Rodriguez-Barrios, F., Gago, F. (2004). "HIV protease inhibition: limited recent progress and advances in understanding current pitfalls." Curr Topics in Med Chem **4**: 991-1007.

Romanelli, F., Pomeroy, C. (2000). "Human immunodeficiency virus drug resistance testing: state of the art in genotypic and pheno typic testing of antiretrovirals." Pharmacotherapy **20**: 151-7.

Rose, R. B., Craik, C.S., and Stroud, R.M. (1998). "Domain flexibility in retroviral proteases: Structural implications for drug resistance mutations." Biochemistry **37**: 2607-21.

Rose, R. B., Rose, J.R., Salto, R., Craik, C.S., Stroud, R.M. (1993). "Structure of the protease from simian immunodeficiency virus: Complex with an irreversible nonpeptide inhibitor." Biochemistry **32**: 12498-507.

Rowley, R. L., Pakkanen, T. (1999). "Determination of a Methane Intermolecular Potential Model for Use in Molecular Simulations from ab initio Calculations." J Chem Phys **110**: 3368-77.

Sarkhel, S., Desiraju, G. R. (2004). "N-H…O, O-H…O, and C-H…O Hydrogen Bonds in Protein-Ligand Complexes: Strong and Weak Interactions in Molecular Recognition." Prot Struct Funct. Bioinf **54**: 246-59.

Sayle, R. A., Milner-White, E.J. (1995). "RasMol: Biomolecular graphics for all." Trends Biochem Sci **20**: 374-6.

Schechter, I., Berger, A. (1967). "On the size of the active site in proteases. I. Papain." Biochem Biophys Res Commun **27**: 157-62.

Schinazi, R. F., Larder, B.A., Mellors, J.W. (1997). "Mutations in retroviral genes associated with drug resistance." Antivir. News **5**: 129-42.

Schramm, H. J., Billich, A., Jaeger, E., Rucknagel, K.P., Arnold, G., Schramm, W. (1993). "The inhibition of HIV-1 protease by interface peptides." Biochem Biophys Res Commun **194**: 595-600.

Seelmeier, S., Schmidt, H., Turk, V., von der Helm, K. (1988). "Human immunodeficiency virus has an aspartic-type protease that can be inhibited by pepstatin A." Proc Natl Acad Sci **85**: 6612-6.

Shafer, R. W. (2002). "Genotypic testing for human immunodeficiency virus type 1 drug resistance." Clin Microbiol Rev **15**: 247-77.

Shao, W., Everitt, L., Manchester, M., Loeb, D.D., Hutchison, C.A. 3rd, Swanstrom, R. (1997). "Sequence requirements of the HIV-1 protease flap region determined by saturation mutagenesis and kinetic analysis of flap mutants." Proc Natl Acad Sci **94**: 2243-8.

Shapiro, J. M., Winters, M.A., Lawrence, J., Merigan,T.C. (1999). "Clinical cross-resistance between the HIV-1 protease inhibitors saquinavir and indinavir and correlations with genotypic mutations." AIDS **13**: 359-65.

Sheldrick, G. M., Schneider, T.R. (1997). "High resolution refinement." Methods in Enzymology **277**: 319-343.

Shoeman, R. L., Sachse, C., Honer, B., Mothes, E., Kaufmann, M., Traub, P. (1993). "Cleavage of human and mouse cytoskeletal and sarcomeric proteins by human immunodeficiency virus type 1 protease. Actin, desmin, myosin, and tropomyosin." Am J Pathol **142**: 221-30.

Silva, A. M., Cachau, R.E., Sham, H.L., and Erickson, J.W. (1996). "Inhibition and Catalytic Mechanism of HIV-1 Aspartic Protease." J. Mol. Bio. **255**(2): 321-346.

Smith, K. A. (2003). "The HIV vaccine saga." Med Immunol **2**: 1-7.

Sperka, T., Pitlik, J., Bagossi, P., Tözser, J. (2005). "Beta-lactam Compounds as Apparently Uncompetitive Inhibitors of HIV-1 Protease." Bioorg Med Chem Lett **15**: 3086-90.

Suguna, K., Padlan, E.A., Smith, C.W., Carlson, W.D., Davies, D.R. (1987). "Binding of a reduced peptide inhibitor to the aspartic proteinase from Rhizopus chinensis: implications for a mechanism of action." Proc Natl Acad Sci **84**: 7009-13.

Surleraux, D. L., Tahri, A., Verschueren, W.G., Pille, G.M., de Kock, H.A., Jonckers, T.H., Peeters, A., De Meyer, S., Azijn, H., Pauwels, R., de Bethune, M.P.,

King, N.M., Prabu-Jeyabalan, M., Schiffer, C.A., Wigerinck, P.B. (2005). "Discovery and Selection of TMC114, a Next Generation HIV-1 Protease Inhibitor." J Med Chem **48**: 1813-22

Swairjo, M. A., Towler, E.M., Debouck, C., Abdel-Meguid, S.S. (1998). "Structural role of the 30's loop in determining the ligand specificity of the human immunodeficiency virus protease." Biochemistry **37**: 10928-36.

Tian, G., Ghanekar, S.V., Aharony, D., Shenvi, A.B., Jacobs, R.T., Liu, X., Greenberg, B.D. (2003). "The mechanism of gamma-secretase: multiple inhibitor binding sites for transition state analogs and small molecule inhibitors." J Biol Chem **278**: 28968-75.

Tie, Y., Boross, P.I., Wang, Y.F., Gaddis, L., Hussain, A.K., Leshchenko, S., Ghosh, A.K., Louis, J.M., Harrison, R.W., and Weber, I.T. (2004). "High resolution crystal structures of HIV-1 protease with a potent non-peptide inhibitor (UIC-94017) active against multi-drug-resistant clinical strains." J Mol Biol. **338**(2): 341-52.

Tie, Y., Boross, P.I., Wang, Y.F., Gaddis, L., Liu, F., Chen, X., Tozser, J., Harrison, R.W., Weber, I.T. (2005). "Molecular basis for substrate recognition and drug resistance from 1.1 to 1.6 angstroms resolution crystal structures of HIV-1 protease mutants with substrate analogs." FEBS J **272**: 5265-77.

Tie, Y., Kovalevsky, A. Y, Boross, P.I., Wang, Y.F., Ghosh, A.K., Tozser, J., Harrison, R.W., and Weber, I.T. (2006). "High Resolution Crystal Structures of HIV-1 Protease and Mutants V82A and I84V with Saquinavir " Proteins: Structure, Function, and Bioinformatics: in press.

Tomasselli, A. G., Heinrikson, R.L. (1994). "Specificity of retroviral proteases: an analysis of viral and nonviral protein substrates." Methods Enzymol **241**: 279-301.

Tomasselli, A. G., Heinrikson, R.L. (2000). "Targeting the HIV-protease in AIDS therapy: a current clinical perspective." Biochim Biophys Acta **1477**: 189-214.

Tong, L., Pav, S., Pargellis, C., Do, F., Lamarre, D., Anderson, P.C. (1993). "Crystal structure of human immunodeficiency virus (HIV) type 2 protease in complex with a reduced amide inhibitor and comparison with HIV-1 protease structures." Proc. Natl. Acad. Sci. **90**: 8387-91.

Tozser, J., Blaha, I., Copeland, T.D., Wondrak, E.M., Oroszlan, S. (1991). "Comparison of the HIV-1 and HIV-2 proteinases using oligopeptide substrates representing cleavage sites in Gag and Gag-Pol polyproteins." FEBS Lett. **281**(1-2): 77-80.

Tozser, J., Gustchina, A., Weber, I.T., Blaha, I., Wondrak, E.M., Oroszlan, S. (1991). "Studies on the role of the S4 substrate binding site of HIV proteinases." FEBS Lett **279**: 356-60.

Tozser, J., Weber, I.T., Gustchina, A., Blaha, I., Copeland, T.D., Louis, J.M., Oroszlan, S. (1992). "Kinetic and modeling studies of S3-S3' subsites of HIV proteinases." Biochemistry **31**: 4793-800.

UNAIDS/WHO (2005). " UNAIDS/WHO "AIDS Epidemic Update." http://www.unaids.org/epi/2005/doc/report_pdf.asp.

Vacca, J. P., Fitzgerald, P.M., Holloway, M.K., Hungate, R.W., Starbuck, K.E. (1994). "Conformationally constrained HIV-1 protease inhibitors." Bioorg Medic Chem Lett **4**: 499-504.

Velazquez-Campoy, A., Todd, M. J., Vega, S., and Freire, E. (2001). "Catalytic efficiency and vitality of HIV-1 proteases from African viral subtypes." Proc Natl Acad Sci **98**: 6062-67.

Vickrey, J. F., Logsdon, B. C., Proteasa, G., Palmer, S., Winters, M. A., Merigan, T. C., Kovari, L. C. (2003). "HIV-1 protease variants from 100-fold drug resistant clinical isolates: expression, purification, and crystallization." Protein Exp. Purif. **28**: 165-172.

Vondrasek, J., van Buskirk, C.P., Wlodawer, A. (1997). " Database of three-dimensional structures of HIV proteinases." Nat. Struct. Biol. **4**: 8.

Wainberg, M. A., Friedland, G. (1998). "Public health implications of antiretroviral therapy and HIV drug resistance." JAMA **279**: 1977-83.

Wartha, F., Horn, A. H. C., Meiselbach, H., Sticht, H. (2005). "Molecular Dynamics Simulations of HIV-1 Protease Suggest Different Mechanisms Contributing to Drug Resistance." J. Chem. Theory Comput. **1**: 315-24.

Weber, I. T. (1990). "Comparison of the crystal structures and intersubunit interactions of human immunodeficiency and Rous sarcoma virus proteases. ." J Biol Chem. **265**: 10492-10496.

Wei, X., Ghosh, S.K., Taylor, M.E., Johnson, V.A., Emini, E.A., Deutsch, P., Lifson, J.D., Bonhoeffer, S., Nowak, M.A., Hahn, B.H.,et al. (1995). "Viral dynamics in human immunodeficiency virus type 1 infection." Nature **373**: 117-22.

Wlodawer, A., Erickson, J.W. (1993). "Structure-based inhibitors of HIV-1 protease." Annu. Rev. Biochem., **62**: 543-585.

Wlodawer, A., Gustchina, A., Reshetnikova, L., Lubkowski, J., Zdanov, A., Hui, K.Y., Angleton, E.L., Farmerie, W.G., Goodenow, M.M., Bhatt, D., et al. (1995). "Structure of an inhibitor complex of the proteinase from feline immunodeficiency virus." Nat. Struct. Biol. **2**: 480-488.

Wlodawer, A., Miller, M., Jaskolski, M., Sathyanarayana, B.K., Baldwin, E., Weber, I.T., Selk, L.M., Clawson, L., Schneider, J., Kent, S.B. (1989). "Conserved folding in retroviral proteases: Crystal structure of a synthetic HIV-1 protease." Science **245**: 616-621.

Wlodawer, A., Vondrasek, J. (1998). "Inhibitors of HIV-1 protease: a major success of structure-assisted drug design. ." Annu. Rev. Biophys. Biomol. Struct. **27**: 249-284.

Wondrak, E. M., Louis, J.M. (1996). "Influence of flanking sequences on the dimer stability of human immunodeficiency virus type 1 protease." Biochemistry. **35**: 12957-12962.

Wu, L., Gerard, N.P., Wyatt, R., Choe, H., Parolin, C., Ruffing, N., Borsetti, A., Cardoso, A.A., Desjardin, E., Newman, W., Gerard, C., Sodroski, J. (1996). "CD4-induced interaction of primary HIV-1 gp120 glycoproteins with the chemokine receptor CCR-5." Nature **384**: 179-83.

Wu, T. D., Schiffer, C.A., Gonzales, M.J., Taylor, J., Kantor, R., Chou, S., Israelski, D., Zolopa, A.R., Fessel, W.J., and Shafer, R.W. (2003). "Mutation patterns

and structural correlates in human immunodeficiency virus type 1 protease following different protease inhibitor treatments." J Virol. **77**: 4836-4847.

Xie, D., Gulnik, S., Gustchina, E., Yu, B., Shao, W., Qoronfleh, W., Nathan, A., and Erickson, J. W. (1999). "Drug resistance mutations can effect dimer stability of HIV-1 protease at neutral pH." Protein Sci. **8**: 1702-7.

York, D. M., Darden, T. A.,Pedersen, L. G.,Anderson, M. W. (1993). "Molecular modeling studies suggest that zinc ions inhibit HIV-1 protease by binding at catalytic aspartates." Environ Health Perspect **101**: 246-50.

Yotsuji, A., Mitsuyama, J., Hori, R., Yasuda, T., Saikawa, I., Inoue, M., Mitsuhashi, S. (1988). "Mechanism of action of cephalosporins and resistance caused by decreased affinity for penicillin-binding proteins in Bacteroides fragilis." Antimicrob Agents Chemother **32**: 1848-53.

Yu, D., Wild, C.T., Martin, D.E., Morris-Natschke, S.L., Chen, C.H., Allaway, G.P., Lee, K.H. (2005). "The discovery of a class of novel HIV-1 maturation inhibitors and their potential in the therapy of HIV." Expert Opin Investig Drugs **14**: 681-93.

Zhang, Y. M., Imamichi, H., Imamichi, T., Lane, H.C., Falloon, J., Vasudevachari, M.B., and Salzman, N.P. (1997). "Drug resistance during indinavir therapy is caused by mutations in the protease gene and its Gag substrate cleavage sites." J. Virol **71**: 6662-70.

Zhang, Z.-Y., Poorman, R.A., Maggiora, L.L., Heinrikson, R.L., Kezdy, F.J. (1991). "Dissociative inhibition of dimeric enzymes: kinetic characterization of HIV-1 protease by its COOH-terminal tetrapeptide." J Biol Chem **266**: 15591-4.

Zhao, B., Winborne, E., Minnich, M.D., Culp, J.S., Debouck, C., Abdel-Meguid, S.S. (1993). "Three-dimensional structure of a simian immunodeficiency virus protease/inhibitor complex. Implications for the design of human immunodeficiency virus type 1 and 2 protease inhibitors." Biochemistry **32**: 13054-60.

APPENDICES I: The list of HIV protease structures determined by Liu F.

NO.	PR	Inhibitor	Space Group	Reso	Rwork	Rfree	PDB Code	Status
1	WT	p2-NC	P21212	1.40	0.15	0.19	2AOD	published
2	L24I		P21212	1.10	0.11	0.13	2AVM	published
3	I50V		P21212	1.30	0.11	0.14	2AVQ	published
4	D25N		P21212	1.05	0.14	0.17		done
5	L24I	IDV	P212121	1.10	0.11	0.14	2AVO	published
6	I50V		P212121	1.10	0.11	0.14	2AVS	published
7	G73S		P21	1.50	0.14	0.22	2AVV	published
8	F53L	None	P41212	1.35	0.15	0.22	2G69	published
9	L90M	DRV	P21212	1.25	0.14	0.19	2F81	published
10	M46L		P212121	1.22	0.14	0.20	2HS2	done
11	G48V		P21212	1.40	0.16	0.22		done
12	I54M		P21212	1.30	0.15	0.20		done
13	I54V		P21212	1.18	0.15	0.19		done
14	D25N		P21212	1.30	0.15	0.20		done
15	I50V	SQV	P21212	1.20	0.16	0.21		done
16	I54M		P212121	1.05	0.14	0.16		done
17	F53L		P212121	1.65	0.25	0.35		In process

APPENDICES II: The activity, stability and structural changes in drug resistant mutants of HIV protease.

PR	Location	Resistance level	Activity and stability changes	Structural changes
L24I	Next to Asp25/ dimer interface	Low to IDV	k_{cat}/K_m: dropped to 4 % **IDV**:relative Ki =3 **p2-NC**:relative Ki=2.6 **CA-p2:** relative Ki=0.05	**IDV:** reduced dimer interactions **p2-NC:** reduced dimer interactions
D25N	catalytic residue	N/A	increased dimer dissociation	**DRV:** reduced PR-inhibitor interactions
M46L	Flap	Intermediate to NFV, low to others except DRV	k_{cat}/K_m: dropped to 50 % **DRV:** relative Ki=10	**DRV:** two binding sites Reduced PR- inhibitor interactions at the active site
G48V	Flap/inhibitor and substrate binding	SQV, NFV: high, ATV, IDV, LPV: low	**SQV:** relative Ki=10	**DRV:** flap conformation and 80's loop shift, tighter PR-inhibitor interaction
I50V	Flap/inhibitor and substrate binding/dimer interface	Very high to APV, high to DRV and LPV	k_{cat}/K_m:18% lower **IDV:** relative Ki=50 **P2-NC:** relative Ki=19 **CA-p2:** relative Ki=3	**IDV:** reduced dimer interactions and PR-inhibitor interactions **SQV:** flap and 80's loop shift, not reduce PR-inhibitor contacts **p2-NC:** reduced dimer interactions, reduced PR-inhibitor interactions
F53L	Flap/dimer interface	Low to all PIs	k_{cat}/K_m: 15% lower **IDV:** relative Ki=20	Reduce dimer stability, flap wider open
I54V	Flap	Low to all PIs		**DRV:** 80's loop shift towards Val54. **SQV:** 80's loop shift towards Val54
I54M	Flap	High to DRV, APV intermediate to LPV		**DRV:** 80's loop shift away from Met54, reduced PR-DRV interactions. **SQV:** 80's loop shift away from Met54
G73S	Protein surface	Low to all PIs	k_{cat}/K_m:14-400% for different substrates	**IDV:** new hydrogen bonds transmitting changes to the substrate binding site

APPENDICES III: The publications and presentations by Liu F.

Peers Reviewed Papers

1. Kovalevsky A.Y., Liu F., Leshchenko, S., Ghosh A.K., Louis J.M., Harrison R.W., Weber I.T. (2006) Ultra-high Resolution Crystal Structure of HIV-1Protease Mutant Reveals Two Binding Sites for Clinical Inhibitor TMC114. *J Mol Biol*. 363:161-173.

2. Liu F., Kovalevsky A.Y., Boross P.I., Louis J.M., Harrison R.W., Weber I.T. (2006) Mechanism of Drug Resistance Revealed by the Crystal Structure of the Unliganded HIV-1 Protease with F53L Mutation. *J Mol Biol*. 358(5):1191-9.

3. Kovalevsky A.Y., Tie Y., Liu F., Boross P.I., Wang Y.F., Leshchenko S., Ghosh A.K., Harrison R.W., Weber I.T. (2006) Effectiveness of Nonpeptidic Clinical Inhibitor TMC114 to Highly Drug Resistant Mutations D30N, I50V and L90M of HIV-1 Protease. *J Med Chem.* 49(4):1379-1387.

4. Liu F., Boross P.I., Wang Y.-F., Tozser J., Louis J.M., Harrison R.W., Weber I.T. (2005) Kinetic, Stability, and Structural Changes in High-resolution Crystal Structures of HIV-1 Protease with Drug-resistant Mutations L24I, I50V, and G73S. *J Mol Biol.* 354(4):789-800.

5. Tie Y, Boross P.I., Wang Y.-F, Gaddis L., Liu F., Chen X., Tozser J., Harrison R.W., Weber I.T. (2005) Molecular basis for substrate recognition and drug resistance from 1.1 to 1.6 angstroms resolution crystal structures of HIV-1 protease mutants with substrate analogs. *FEBS J.* 272(20):5265-5277.

Conference Abstracts

6. Liu F., Mahalingam B., Boross P.I., Wang Y.-F., Louis J.M., Tozser J., Harrison R.W. and Weber I.T. (2003) Analysis of HIV-1 Protease Mutants to Understand Mechanisms of Resistance. Retroviruses International Meeting Cold Spring Harbor Lab, NY.

7. Liu F., Mahalingam B., Boross P.I., Wang Y.-F., Louis J.M., Tozser J., Harrison R.W. and Weber I.T. (2003) Analysis of HIV-1 Protease Mutants to Understand Mechanisms of Resistance. Georgia State Biotech Symposium: From Bacterial Physiology to Molecular Genetics to Biotechnology, Georgia State University, Atlanta, GA.

8. Liu F., Mahalingam B., Boross P.I., Wang Y.-F., Louis J.M., Tozser J., Harrison R.W. and Weber I.T. (2004) Analysis of HIV-1 Protease Mutants to Understand Mechanisms of Resistance. SECABC Biotech/Biocomputing Symposium, Georgia State University, Atlanta, GA.

9. Liu F., Boross P.I., Tozser J., Louis J.M., Harrison R.W. and Weber I.T. (2005) Analysis of HIV-1 Protease Mutants to Understand Mechanisms of Resistance. *FEBS J.* 272 (supplement1):12.

10. Liu F., Boross P.I., Louis J.M., Tozser J., Harrison R.W. and Weber I.T. (2006). Distinct Structural Changes in High Resolution Crystal Structures of HIV-1 Protease with Drug Resistant Mutations L24I, I50V, and G73S. The Third Annual Ser-Cat Symposium, Georgia State University, Atlanta, GA.

Poster Presentations at Scientific Conferences

1. **Liu, F**., Tie, Y., Iro, A., Wang, Y-F., Gaddis, L., Mahalingam, B., Boross, PI., A. Ghosh, Harrison, RW., Weber, IT. "High Resolution Crystal Structures of HIV Protease Mutants with Inhibitors." 11th Annual Suddath Symposium and Annual Georgia Cancer Coalition Spring Symposium, Georgia Institute of Technology, Atlanta, GA, March 27-29, 2003.

3. **Fengling Liu,** Bhuvaneshwari Mahalingam, Yunfeng Tie, Peter Boross, Yuan-Fang Wang, John M. Louis, Jozsef Tozser, Robert W. Harrison, Irene T. Weber. Analysis of HIV-1 Protease Mutants to Understand Mechanism of Resistance. Retroviruses International Meeting Cold Spring Harbor Lab, New York, May 19-23, 2003

4. **Fengling Liu**, Bhuvaneshwari Mahalingam, Yunfeng Tie, Peter Boross, Yuan-Fang Wang, X. Chen, John M. Louis, Jozsef Tozser, Robert W. Harrison, Irene T. Weber. "Analysis of HIV-1 Protease Mutants to Understand Mechanisms of Resistance." Georgia State Biotech Symposium 2003: From Bacterial Physiology to Molecular Genetics to Biotechnology, Georgia State University, Atlanta, GA, June 16-17, 2003.

6. **F. Liu**, Boross, P., Mahalingam, B., Wang, Y-F., Gaddis, L., Louis, JM., Harrison, R.W., Weber, I.T. "Crystallographic and kinetic analysis of drug-resistant mutants of HIV protease." 12th Annual Suddath Symposium, Georgia Institute of Technology, Atlanta, GA, March 19-20, 2004.

7. **Fengling Liu**, Bhuvaneshwari Mahalingam, Peter Boross, Yuan-Fang Wang, John M. Louis, Jozsef Tozser, Robert W. Harrison, Irene T. Weber. "Analysis of HIV-1 Protease Mutants to Understand Mechanisms of Resistance." SECABC Biotech/Biocomputing Symposium, Georgia State University, Atlanta, GA, May 24-25, 2004.

8. **Fengling Liu**, Bhuvaneshwari Mahalingam, Peter Boross, Yuan-Fang Wang, John M. Louis, Jozsef Tozser, Robert W. Harrison, Irene T. Weber. "Analysis of HIV-1 Protease Mutants to Understand Mechanisms of Resistance." Gordon

Research Conference "Diffraction Methods in Structural Biology", Bates College, Lewiston, Maine, July 11-16, 2004.

10. **Fengling Liu**, Peter Boross, John M. Louis, Jozsef Tozser, Robert W. Harrison, Irene T. Weber. "Analysis of HIV-1 Protease Mutants to Understand Mechanisms of Resistance." The Protein World Proteins and Peptides: Structure, Function and Organization: 30th FEBS Congress, 9th IUBMB Conference, Budapest, Hungary, July 2-7, 2005.

11. **Fengling Liu**, Peter Boross, John M. Louis, Jozsef Tozser, Robert W. Harrison, Irene T. Weber Distinct Structural Changes in High Resolution Crystal Structures of HIV-1 Protease with Drug Resistant Mutations L24I, I50V, and G73S. SECABC Biotech/Biocomputing Symposium, Georgia State University, Atlanta, GA, Nov 24-25, 2005.

12. **Fengling Liu**, Peter Boross, John M. Louis, Jozsef Tozser, Robert W. Harrison, Irene T. Weber Distinct Structural Changes in High Resolution Crystal Structures of HIV-1 Protease with Drug Resistant Mutations L24I, I50V, and G73S. The Third Annual Ser-Cat Symposium, Georgia State University, Atlanta, GA, March 10, 2006.

Contributions to other posters presentations

13. Mahalingam, B., Tie, Y., **Liu, F.,** Iro, A., Wang, Y-F., Boross, P., Harrison, R.W., Weber, I.T. "High Resolution Crystal Structures of HIV Protease Mutants and the Implications for Drug Resistance." University System of Georgia Symposium, Applying Bioinformatics: From Genes to Systems, Georgia State University, Atlanta GA, Oct.4, 2002.

14. Wang Y.-F., Mahalingam B, Tie Y., Boross P., **Liu F.,** Louis J.M., Tozser J., Harrison R. W. and Weber I. T. "Analysis of HIV-1 Protease Mutants To Understand Mechanisms of Resistance." AIDS Structural Biology Meeting, Bethesda, MD, June 18-20, 2003.

15. Yuan-Fang Wang, Yunfeng Tie, Peter I. Boross, **Fengling Liu**, Laquasha Gaddis, Arun K. Ghosh, John M. Louis, Robert W. Harrison, Irene T. Weber. "What Can We Learn From Crystal Structures At Atomic Resolution?" AIDS Structural Biology Meeting, Bethesda, MD, June 9-11, 2004.

16. Andrey Yu. Kovalevsky, Yunfeng Tie, **Fengling Liu,** Peter I. Boross, Yuan-Fang Wang, Arun K. Ghosh, Robert W. Harrison, Irene T. Weber. "Crystal Structures At Near-Atomic Resolution of Drug Resistant HIV-1 Protease Mutants with the Potent Inhibitor UIC94017 (TMC114)" AIDS Structural Biology Meeting, Bethesda, MD, June 23-24, 2005.

17. Yunfeng Tie, Andrey Y. Kovalevsky, **Fengling Liu,** Peter Boross, Yuan-Fang Wang, Arun K. Ghosh, Robert W. Harrison, Irene T. Weber. "High Resolution Crystal Structures of HIV-1 Protease Mutants With Potent New Clinical Inhibitor TMC-114." 2nd SECABC Fall Workshop on Biocomputing, Georgia State University, Atlanta GA, Oct 27, 2005.

18. Andrey Y. Kovalevsky, Yunfeng Tie, **Fengling Liu,** Peter I. Boross, Yuan-Fang Wang, Arun K. Ghosh, Robert W. Harrison, Irene T. Weber. Effectiveness of Nonpeptidic Clinical Inhibitor TMC114 to Highly Drug Resistant Mutations D30N, I50V and L90M of HIV-1 Protease. The Third Annual Ser-Cat Symposium, Georgia State University, Atlanta, GA, March 10, 2006.

19. Andrey Y. Kovalevsky, Yunfeng Tie, **Fengling Liu**, Peter I. Boross, Yuan-Fang Wang, Sofiya Leshchenko, Arun K. Ghosh, John M. Louis, Robert W. Harrison, Irene T. Weber. Understanding Mechanisms of HIV-1 Protease Drug Resistance: Insights from Unliganded and Darunavir-complexed crystal structures. The 36th Mid-Atlantic Macromolecular Crystallography Meeting, Wake Forest University, NC, June 1-3, 2006.